

Estimating natural mortality rates for northern shrimp (*Pandalus borealis*) from a wide range of its latitudinal distribution in the  
Northeast Atlantic

Thea Båtevik



A thesis submitted in partial fulfilment of the requirement for the degree

Master of Science in Marine Biology

Supervisors:

Guldborg Søvik

Mikaela Bergenius

Jeppe Kolding

UNIVERSITY OF BERGEN

Department of Biological Science (BIO)

June, 2020

# ACKNOWLEDGEMENTS

First of all, I would like to express my sincere gratitude to my supervisors Dr. Guldborg Søvik (Institute of Marine Research), Dr. Mikaela Bergenius (Swedish University of Agricultural Science) and prof. Jeppe Kolding (University of Bergen) who have shown great interest in my thesis. Thank you for all your help and guidance. Especially I would like to highlight Guldborg, who has put countless hours into seeing me through, answering questions after hours and being uttermost supportive. Thank you to the Institute of Marine Research for allowing me to participate on research cruises both in the Porsanger Fjord in May and October 2019, and in the Norwegian Deep and Skagerrak in January 2020 (and thank you to sea sickness tablets), and to the Swedish University of Agricultural Science for having me at a research stay in September 2019. Thank you to Massimiliano Cardinale and Mats Ulmestrand at the Swedish University of Agriculture who have answered questions about statistics and the biology of the Gullmars Fjord shrimp stock. Thank you to Fabian Zimmerman, Trude Thangstad and Jon Albretsen who have provided me with maps and figures.

I would also like to thank the Department of Biological Science at the University of Bergen, for five wonderful years, both during my bachelor's degree and my master's degree. I am also very grateful to my fellow students, for all the pep-talks and long lunch breaks (until Corona). I also have to thank my family for your patience and support.

Bergen, 26. June 2020

Thea Båtevik

# ABSTRACT

Natural mortality ( $M$ ) is one of the most important parameters in stock assessment and management.  $M$  is, however, notoriously difficult to estimate. Natural mortality of the northern shrimp, *Pandalus borealis*, in the Northeast Atlantic is poorly studied. In lack of better options, the assessment on the Norwegian Deep and Skagerrak (NDSK) shrimp stock applies a value estimated for the Barents Sea shrimp stock, even though the dynamics of these differ in terms of e.g. longevity and growth. As the total mortality ( $Z$ ) of a fish stock equals the natural mortality ( $M$ ) when the fishing pressure ( $F$ ) is absent ( $Z = M$ ), samples from three unfished populations of *P. borealis* in the Northeast Atlantic, the Tana and Porsanger Fjords of northern Norway and the Gullmars Fjord of Sweden, provided an opportunity to derive direct estimates of  $M$  for *P. borealis* in this area. Given the lack of calcareous hard parts from which age can be read in crustaceans, length-based methods were applied. For such length-based methods, stock specific growth parameters are important. As such, it was aimed to estimate stock (fjord) specific growth parameters and natural mortality rates from all study sites. Stock specific growth parameters were estimated for each fjord site using a bootstrapped electronic length frequency analysis with simulated annealing (TropFishR library in R). Estimated growth parameters were used in a linearized length converted catch curve analysis to estimate  $Z$ . Separate estimates of fishing pressure were calculated for the Kvænangen Fjord of northern Norway (fished reference fjord) as well as for the Gullmars Fjord, as the high level of experimental trawling during the study period was assumed to influence the mortality of the stock. For these study sites natural mortality was estimated as  $M = Z - F$  ( $y^{-1}$ ). As all the fjord sites revealed a descending instantaneous mortality rate with increasing age, mortality was split into two intervals, representing younger ( $M_Y$ ) and older ( $M_O$ ) shrimp.  $M_Y$  ranged from 0.42 to 0.94  $y^{-1}$  whereas  $M_O$  ranged from 0.38 to 0.81  $y^{-1}$ . Latitudinal trends did not predict expected patterns in growth and mortality, where the slowest growth and lowest natural mortality were estimated for the Gullmars Fjord, the southernmost and warmest study site. Estimated growth and mortality in the fjord sites of northern Norway followed the expected temperature trend, where the warmer Tana Fjord, relative to that of the Outer Porsanger Fjord, gave a faster growth and higher natural mortality. Temperature, shrimp density, re-oxygenation of water masses and predation pressure were discussed as possible factors influencing growth and mortality at each fjord site.

# TABLE OF CONTENT

Acknowledgements.....	2
Abstract .....	3
Table of content.....	4
1 Introduction.....	6
1.1 General introduction .....	6
1.2 The biology of <i>Pandalus borealis</i> .....	8
1.3 Objectives.....	10
2 materials and Methods.....	11
2.1 Study sites.....	11
2.1.1 Gullmars Fjord .....	11
2.1.2 Troms and Finnmark County .....	13
2.2 Trawling experiments .....	16
2.2.1 The Gullmars Fjord .....	16
2.2.2 Porsanger, Tana and Kvænangen Fjords .....	18
2.3 Bottom temperature.....	20
2.4 Shrimp density.....	20
2.5 Fishing pressure .....	21
2.6 Statistical analyses.....	21
2.6.1 Software .....	21
2.6.2 Estimating growth.....	22
2.6.3 Estimating total mortality .....	26
3 Results .....	27
3.1 Length frequency distributions .....	27
3.2 Growth.....	29
3.2.1 Approach 1: Varying Loo .....	29
3.2.2 Approach 2: Fixed Loo.....	34
3.2.3 Comparing growth between Approach 1 and 2.....	40
3.2.4 Most plausible growth parameters .....	41
3.3 Mortality .....	42
3.4 Bottom temperature.....	47
3.5 Shrimp density.....	49
4 Discussion .....	50
4.1 Length frequency distributions .....	50
4.2 Growth.....	52

4.3 Mortality .....	54
4.4 Limitations of study .....	56
4.5 Further implications of results .....	59
4.5.1 ECOPATH model in northern Norway.....	59
4.5.2 NDSK stock assessment.....	59
5 Conclusions.....	60
6 References .....	61
7 Appendices.....	68
Appendix 1 Catch data .....	68
A).....	68
B).....	69
C).....	70
D).....	71
E).....	72
Appendix 2 Scenario 1 .....	73
A).....	73
B).....	74
C).....	75
D).....	76
Appendix 3 Scenario 4.....	77
A).....	77
B).....	78
C).....	79

# 1 INTRODUCTION

## 1.1 GENERAL INTRODUCTION

Life history parameters related to longevity, growth and mortality play a crucial role in fisheries stock assessment (Sparre and Venema, 1998). These can vary significantly between stocks of the same species, where slower growth and longer lifespans normally are seen in northern, colder areas and the opposite for southern, warmer areas (Pauly, 1980; Nilssen and Hopkins, 1991; Brander, 1995). Mortality is essential in understanding the dynamics of any fish stock, where the total mortality ( $Z$ ) of a stock is the combination of natural mortality ( $M$ ) and fishing mortality ( $F$ ). When expressed as the instantaneous rate per year ( $y^{-1}$ ), the total mortality can be calculated as  $Z = M + F$  (Pauly, 1982; Simpfendorfer, Bonfil and Latour, 2005). Natural mortality constitutes mortality due to natural causes, including predation, starvation, disease and old age, among others (Vetter, 1988). It is one of the most important parameters in stock assessment and management, as it influences the productivity of a stock (Clark, 1999; Aanes *et al.*, 2007; Williams, 2011).  $M$  is, however, notoriously difficult to estimate (Vetter, 1988). Direct methods where information strictly pertaining to the species or stock of interest are often time consuming and expensive (Vetter, 1988), and indirect methods related to life history information are often inaccurate (Francis, 2012; Hoenig, 2017). In all analytic models currently applied in fisheries stock assessment, knowledge of  $M$  is necessary in order to determine the sustainable exploitation level of a stock (ICES, 2016). While many stock assessment applications have to assume a single, constant value for  $M$  to represent natural mortality for the exploitable lifespan of a stock,  $M$  is believed to vary over a species life span, with a decline of  $M$  with age (Vetter, 1988; Caddy, 1991; Gislason *et al.*, 2010). Additionally,  $M$  can be highly variable between or within years, due to variability in e.g. population density and predation pressure (Nilssen and Hopkins, 1991; Jørgensen *et al.*, 2014).

Northern shrimp, *Pandalus borealis*, is by far the most abundant and commercially important species of shrimp in the Northeast Atlantic (Shumway *et al.*, 1985; Garcia, 2007). The Barents Sea and the Norwegian Deep/Skagerrak (NDSK) stocks are the two commercially most important (Garcia, 2007). The species is also found in fjords and coastal areas from the Swedish west coast and along the entire Norwegian coast, sustaining coastal shrimp fisheries with local importance (Havforskningsinstituttet, 2019). Still, natural mortality is poorly understood for the NDSK stock and smaller stocks along the coasts, and no direct estimates of  $M$  for these stocks exist today (ICES, 2016). Consequently, even though the dynamics of the shrimp populations in the NDSK and the Barents Sea differ in terms of e.g. longevity and growth (Nilssen and

Hopkins, 1991), the present length-based assessment model for the shrimp stock in the NDSK is using an  $M$  of  $0.75\text{yr}^{-1}$  (ICES, 2016), estimated for the Barents Sea population in the 1970s (Berenboim et al., 1991), in lack of better options.

The most reliable direct methods for estimating  $M$  are likely telemetry and tagging studies, following tagged individuals through their life span (Hampton, 2000; Hightower, Jackson and Pollock, 2001; Pollock, Jiang and Hightower, 2004). Some successful estimates of natural mortality using tagging are recorded for other species of shrimp (Siddeek, 1991; Xiao and McShane, 2000). However, for *P. borealis*, tagging experiments have been problematic (Skúladóttir, 1985), and are not commonly applied. Though rare, unexploited stocks where  $F$  is close or equal to zero provide opportunities for estimating  $M$  directly. As the total mortality then will equal the natural mortality ( $Z = M$ ), a direct estimate of  $M$  can be derived by estimating  $Z$ . A commonly applied method for estimating  $Z$  is a catch curve analysis (Pajuelo and Lorenzo, 1996; Tserpes and Tsimenides, 2001), studying the exponentially decreasing abundance of a stock by age (Chapman and Robson, 1960). Length-based versions of this method, such as the linearized length converted catch curve have for a long time been used for organisms such as crustaceans for which hard calcareous parts from which age can be read are lacking (Sparre and Venema, 1998).

Various circumstances present us with two unfished areas of *P. borealis* in the Northeast Atlantic. The Gullmars Fjord on the west coast of Sweden, located in the southernmost part of the distributional area of northern shrimp in the Northeast Atlantic, was between 1990 and 1997 closed for all commercial bottom trawling. In northern Norway, the Tana and Porsanger Fjords were in 1972, and to this date still are, closed for commercial bottom trawling. These three unfished fjords provide a unique opportunity to derive estimates of  $M$  from a large part of the distributional range of northern shrimp in the Northeast Atlantic. Data on northern shrimp from these fjord sites exist from two different research projects in respectively Sweden and Norway. After six years of commercial shrimp trawling being prohibited in the Gullmars Fjord, an experimental research project was carried out in order to investigate impacts of trawling on the bottom habitat. Shrimp data were sampled from some of the trawl hauls conducted during the one-year long experimental survey (Hansson *et al.*, 1997, 2000). In the unfished fjords of northern Norway, as well as in the fished Kvænangen Fjord (reference fjord), three research cruises were in 2018 and 2019 conducted by the Norwegian Institute of Marine Research (IMR) (Søvik, Strand and Nedreaas, 2019). The surveys were part of a detailed mapping and investigation of the fjord ecosystems before a possible re-opening of the shrimp trawl fishery,

presently considered by the Norwegian Directorate of Fisheries. Shrimp data were collected for estimating  $M$ , alongside many other objectives. Length data (length frequency distributions) exist from both research projects conducted in the fjords of Sweden and Norway. As mortality estimations based on length frequency (LFQ) distributions are highly dependent on life history parameters related to growth, applying stock specific growth parameters is recommended (Sparre and Venema, 1998). Stock specific growth parameters and natural mortality rates will be estimated from sets of LFQ distributions by applying the electronic length frequency analysis (ELEFAN) (Pauly and Sparre, 1991) and the linearized length converted catch curve (Sparre and Venema, 1998) in the TropFishR library in R (R-Core-Team, 2013; Mildenerger, Taylor and Wolff, 2017). For comparison, a separate estimate of the fishing pressure in the fished Kvænangen Fjord can be estimated, so that  $M = Z - F$  (Vetter, 1988).

*P. borealis* have a wide geographical distribution, with varying life history traits related to growth and mortality depending on latitude and environmental factors (Shumway *et al.*, 1985; Nilssen and Hopkins, 1991). A summary of the biology of northern shrimp is given below. Objectives of the study and hypotheses are thereafter presented.

## 1.2 THE BIOLOGY OF *PANDALUS BOREALIS*

Northern shrimp (*Pandalus borealis*) (Fig. 1.1) are generally found in areas with discrete muddy grounds at depths of 50-500 meters (Shumway *et al.*, 1985). Its geographical distribution ranges from southern, warmer areas to northern, colder areas (with temperatures between -1 and 12°C), at latitudes ranging from 40 to 82 °N (Nilssen and Hopkins, 1991). Substratum, temperature, salinity and depth are all important influencers of the species' distributional pattern (Shumway *et al.*, 1985).



**Figure 1.1.** *Pandalus borealis* from the Norwegian Deep. Picture taken by Thea Båtevik (2020) on the annual shrimp survey conducted by the Norwegian Institute of Marine Research.

*P. borealis* is a protandric hermaphrodite, where each individual first matures and reproduces as male, followed by a transitional or intersexual phase before becoming a female (Shumway *et al.*, 1985). The female shrimps spawn once a year, extruding the eggs in late summer to early autumn before carrying them on the pleopods until hatching commences in spring the following year. The spawning and hatching period vary from July to December, and February to June, respectively, where higher temperatures prompt a shorter spawning and earlier hatching period, and lower temperatures prompt the opposite (Shumway *et al.*, 1985).

*P. borealis* is a schooling species, often observed in groups of similar sized individuals (Shumway *et al.*, 1985). Aggregations of female shrimps on inshore, shallow grounds can be observed as hatching commences in spring (Shumway *et al.*, 1985). The pelagic larvae have a potential for extensive dispersal in the presence of oceanic currents (Drengstig *et al.*, 2000). Juveniles normally settle and remain on inshore, shallow grounds, before joining the adult population at the end of their first year (Hjort and Ruud, 1938; Shumway *et al.*, 1985). Some authors have reported on juveniles remaining separate from the adult stock for up to 1.2 years (Rasmussen, 1953; Nilssen and Hopkins, 1991).

*P. borealis* are opportunistic omnivores acting both as scavengers and predators (Shumway *et al.*, 1985), feeding on among others polychaetes, porifera, copepods, foraminifera, excretory pellets, sand and shrimp belonging to their own or other species (Hjort and Ruud, 1938; Shumway *et al.*, 1985). Shrimp also feed on plankton in the water column during vertical diurnal migrations (Hudon, Parsons and Crawford, 1992). *P. borealis* are itself an important food source for demersal fish (Parsons, 2005), thereby linking trophic levels. Cod, roundnose grenadier, velvet belly and blue whiting have been identified as the key predators of northern shrimp in the NDSK by Jørgensen *et al.* (2014), but also other species feed on them (Shumway *et al.*, 1985; Skorda, 2018).

The maximum measured carapace length (CL) of *P. borealis* is around 37 mm (Shumway *et al.*, 1985). Shrimp have seasonal growth, where a period of rapid growth between spring and early autumn is followed by a stagnant growth period during late autumn and winter (Shumway *et al.*, 1985). As shrimp moult as they grow, they consequently lack hard parts from which age can be read. However, as shrimp hatch only once a year, distinct modal peaks in size distributions for the first 2-3 year classes enable ageing through modal progression analysis (Sparre and Venema, 1998). There is a positive correlation between growth in *P. borealis* and temperature, where the fastest growth rates and shortest life spans are seen in southern and warmer areas, and opposite (Shumway *et al.*, 1985; Nilssen and Hopkins, 1991). However,

authors have reported on deviations from this relationship (Hopkins and Nilssen, 1990), and other factors such as resource availability and population density are considered important as well (Nilssen and Hopkins, 1991). Variability in growth between year-classes have also been reported (Bergström, 1992a; Savard, Parsons and Carlsson, 1994; Skúladóttir, 1999), likely influenced by variations in temperature, population density and recruitment (Nilssen and Hopkins, 1991). Individual growth variability within year-classes is also common. Larger males are known to undergo the transformation into females first, followed by an accelerated rate of growth in the subsequent months, while shrimp with a delayed sex transformation may be restricted in their growth (Rasmussen, 1953; Shumway *et al.*, 1985).

Estimated values of total ( $Z$ ) and natural ( $M$ ) mortality for northern shrimp are highly variable. Nilssen and Hopkins (1991) (review article) reported on ranges of  $M$  from 0.1 to 0.8  $y^{-1}$ , and ranges in  $Z$  from 0.5 to about 2  $y^{-1}$  (mean =  $1.2 \pm 0.3$  95% confidence interval). The highest estimated values of  $Z$  were those determined from semi-enclosed fjord populations with both high fishing intensity and predation by cod (Nilssen and Hopkins, 1991). A negative relationship has been recorded between  $Z$  and longevity, as well as a weak positive relationship between  $Z$  and temperature (Nilssen and Hopkins, 1991).

### 1.3 OBJECTIVES

The main aim of this study is to derive estimates of natural mortality for stocks from different parts of the large latitudinal gradient of *Pandalus borealis* in the Northeast Atlantic, applying length-based methods. As mortality estimations based on length data are dependent on growth parameters which can vary greatly along latitudinal and environmental gradients, stock specific growth parameters will be estimated as well.

The main objectives of the study are thus to:

- i) estimate stock specific growth parameters for the Gullmars, Porsanger, Tana and Kvænangen Fjords,
- ii) estimate stock specific natural mortality rates for the Gullmars, Porsanger, Tana and Kvænangen Fjords,
- iii) compare growth and natural mortality between the southern and northern study sites, as well as between fjords of northern Norway.

The Gullmars Fjord in Sweden is likely to have more similar life history traits to the NDSK shrimp stock compared to that of the Barents Sea (Nilssen and Hopkins, 1991), and may offer a more accurate  $M$ -value than the one used presently. As Jørgensen *et al.* (2014) suggest that

the current assumption of  $M = 0.75 \text{ y}^{-1}$  in the assessment model for northern shrimp in the NDSK is too low, it is expected that the direct estimate of  $M$  for the Gullmars Fjord stock will be higher. Given the positive relationship between growth and warmer, boreal areas at lower latitudes, and opposite (see section 1.2) (Shumway *et al.*, 1985; Nilssen and Hopkins, 1991), it is hypothesised that growth will be higher in the Gullmars Fjord compared to that of the fjords in northern Norway. As faster growth implies a shorter life span and thus a higher mortality (Shumway *et al.*, 1985; Nilssen and Hopkins, 1991), shrimp natural mortality is therefore expected to be higher in the Gullmars Fjord compared to the fjords in northern Norway.

## 2 MATERIALS AND METHODS

### 2.1 STUDY SITES

#### 2.1.1 GULLMARS FJORD

The Gullmars Fjord, located on the western coast of Sweden (58.2-58.5°N and 11.3-11.7°E) (Fig. 2.1), is a 35 km long fjord, with an area of approximately 50 km<sup>2</sup> (Svanesson, 1984). The fjord has a maximum depth of 120 m in the deeper basin in the middle of the fjord, and is separated from the deeper parts of Skagerrak by a sill with a depth of about 42 m in the fjord mouth (Svanesson, 1984). Temperature measurements from 1969-70 (most recent published temperature data from this fjord) reveal year-around temperatures of 4-6 °C at depths of 70-110 m, where stagnant bottom water was normally renewed and oxygenated each spring (Svanesson, 1984). Hansson *et al.* (1997) reported on no renewal of water masses during the survey period in 1997, resulting in oxygen levels remaining low for the duration of the year (Fig. 2.2). There has been a shrimp fishery in the Gullmars Fjord since 1902. In 1983, the fjord was defined as a protected marine area, and on January 1, 1990, all commercial shrimp trawling was stopped (Hansson *et al.*, 1997).

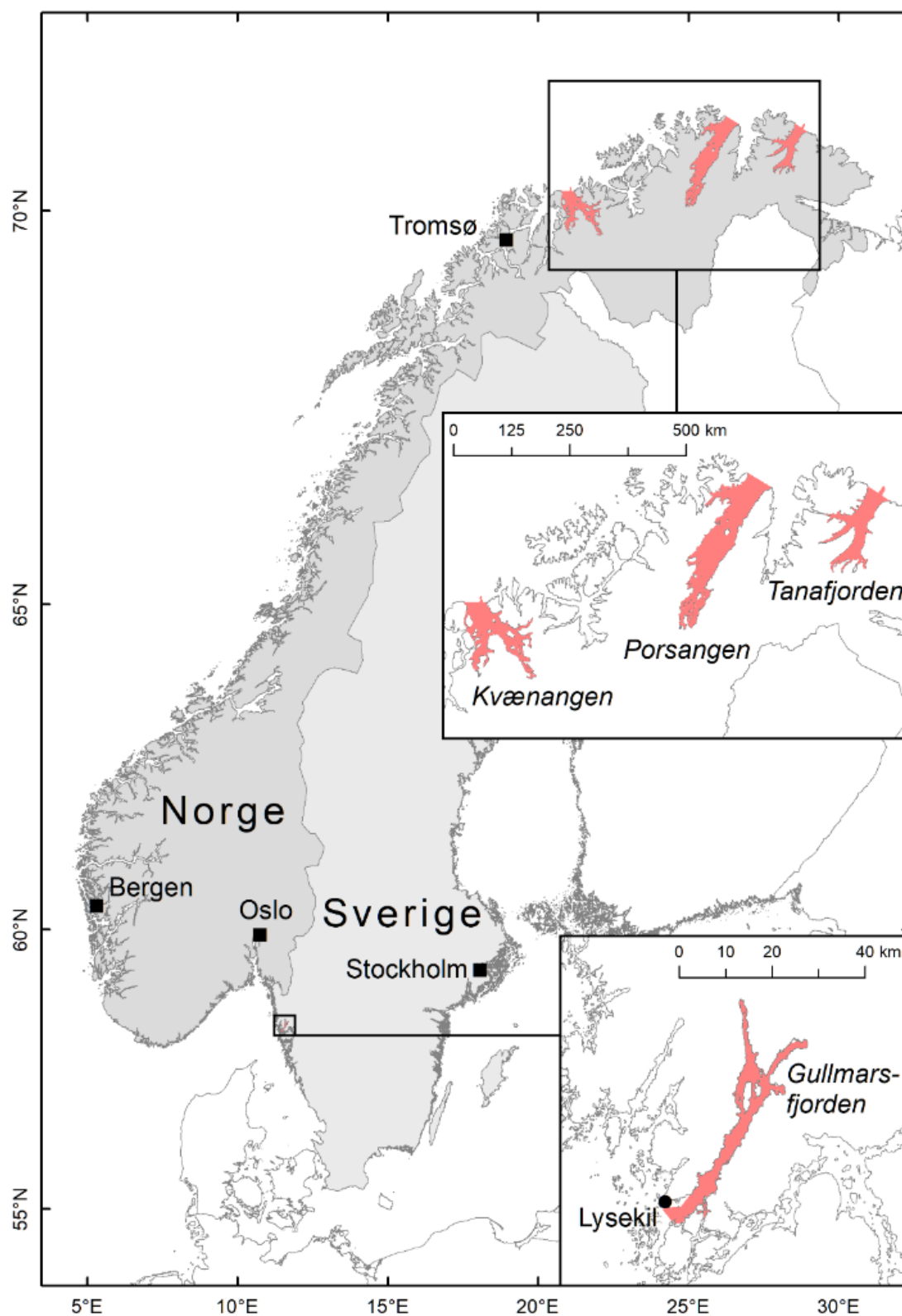


**Figure 2.1.** The Gullmars Fjord in Sweden and the Porsanger, Tana, Kvænangen and Reisa Fjords in Norway. In this thesis “Kvænangen” denotes the combined area of the Kvænangen and Reisa Fjords. Map by Trude Hauge Thangstad, Norwegian Institute of Marine Research, 2020.

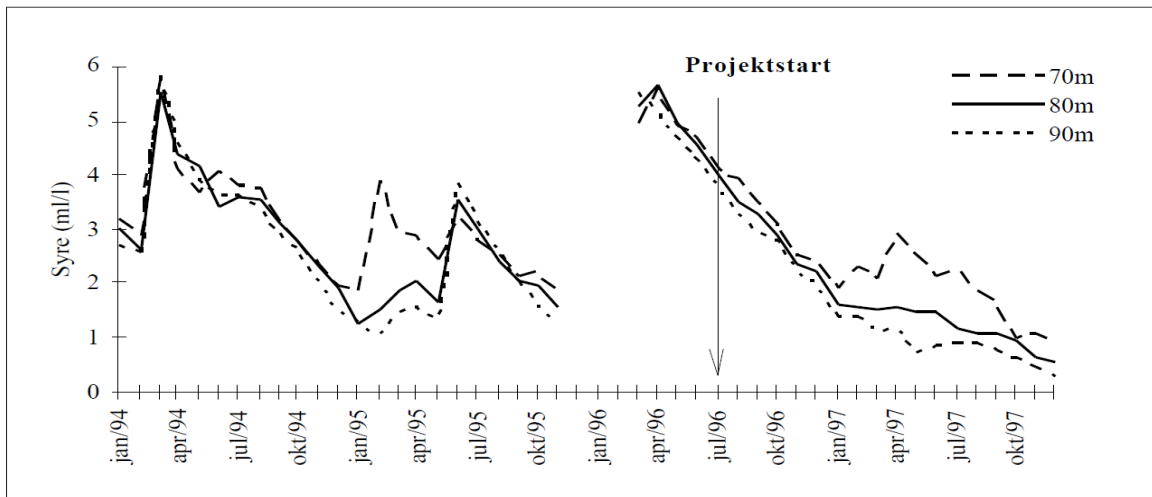


**Figure 2.2.** Oxygen levels (“Syre”) (ml/l) in the Gullmars Fjord in 1994-1997. “Projektstart” denotes the beginning of the study period from which the length data applied in the current study and Hansson *et al.* (1997) are gathered from. Figure borrowed from Hansson *et al.* (1997).

## 2.1.2 TROMS AND FINNMARK COUNTY

Porsanger Fjord, Tana Fjord and Kvænangen Fjord are located in Troms and Finnmark County, in the northern part of Norway (Fig. 2.1). The three fjords are treated as separate study sites for which growth and mortality are estimated.

### 2.1.2.1 PORSANGER FJORD

The Porsanger Fjord (70-71°N and 25-26.5°E) is one of the largest fjords in northern Norway, being 120 km long and covering an area of approximately 1877 km<sup>2</sup> (Fiskeridirektoratet, 2020b). The fjord opens into the Barents Sea in the north, with its maximum depth of approximately 300 m in the fjord mouth (no sill) (Fiskeridirektoratet, 2020b). Approximately 50 km into the fjord, just north of the island Lille-Tamsøya, there is a sill with a depth of 160 m, separating the outer and middle part of the fjord, with a deep basin of 280 m just inside the sill. The fjord has strong outward flowing bottom and surface currents on the eastern side of the fjord, and opposite for the western side (Fig. 2.3). The innermost part of the Porsanger Fjord, separated from the middle part by a sill with a depth of 60 m northeast of the island Reinøya, has a maximum depth of 110 m (Fiskeridirektoratet, 2020b). Bottom temperatures range from an annual average of 5 °C in the outer fjord, to arctic conditions in the innermost basin, varying from sub-zero in spring/summer to about 2 °C in autumn (Christiansen and Fevolden, 2000; Mankettikkara, 2013). The fjord had an active shrimp trawl fishery from 1931 (Hjort and Ruud, 1938) until 1972 when the fjord was closed for all commercial bottom trawling (Sætra, 2019).

Preliminary analyses of the fjord ecosystem show that the density of shrimp in the eastern innermost part of the Porsanger Fjord is much higher than in the rest of the fjord, with densities of 11-15 tons/km<sup>2</sup> in the innermost part compared to 2-3 tonnes/km<sup>2</sup> in the middle and outer

parts (Søvik, Strand and Nedreaas, 2019). There was hardly any shrimp caught in the western part of the innermost part of the fjord. Even though recent genetic studies reveal no significant spatial genetic structure among shrimp in the different parts of the Porsanger Fjord (Hansen, 2020), the difference in temperature and the likely presence of high intraspecific competition in the inner eastern basin may influence growth and thus mortality. Thus, it was decided to handle the innermost eastern part of the Porsanger Fjord as a separate study site in the analyses, enabling to estimate growth and mortality from an arctic shrimp stock as well. The eastern innermost part and the middle and outermost parts of the Porsanger Fjord will be addressed as the Inner Porsanger Fjord and the Outer Porsanger Fjord, respectively (the few shrimps found in the western inner part were included in the Inner Porsanger Fjord study site).

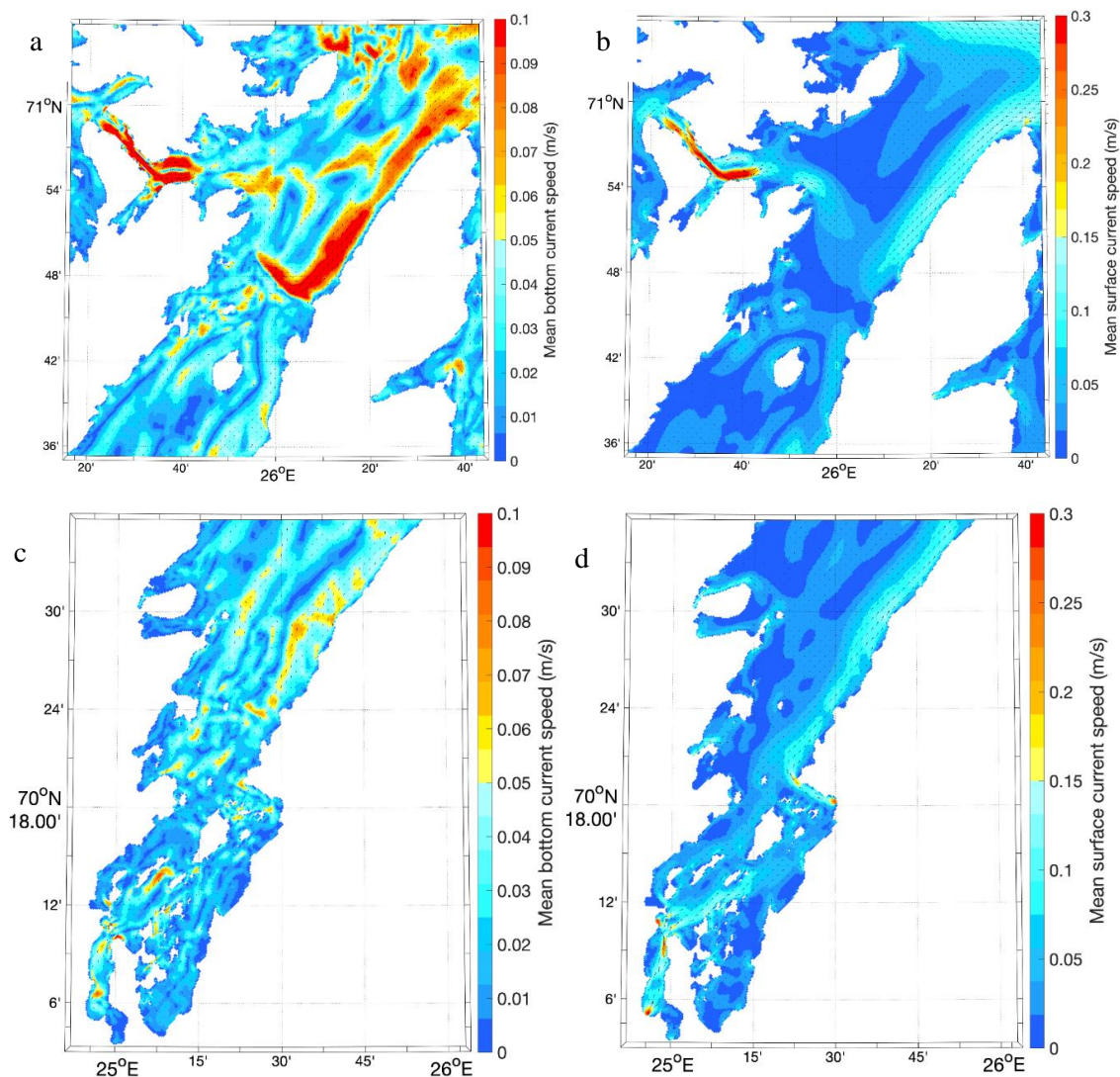


**Figure 2.3.** Mean annual bottom (a, c) and surface (b, d) current speed (m/s) for the northern (a, b) and southern (c, d) parts of the Porsanger Fjord from April 2017-March 2019 based on results from a hydrodynamical model using ROMS (<http://myroms.org>) with a horizontal resolution of 160m x 160m. The coastal model providing input along the open boundaries, NorKyst800, is explained in detail in Asplin et al. (2020). Map by Jon Albretsen, Norwegian Institute of Marine Research, 2020.

### 2.1.2.2 TANA FJORD

The Tana Fjord (70.5-71 °N and 28-28.5 °E) is located approximately 80 km east of the Porsanger Fjord (Fiskeridirektoratet, 2020b). It opens into the Barents Sea in the north and reaches 65 km southwards into the country, with a deep basin of approximately 300 m depth in the outer part (no sill) (Fiskeridirektoratet, 2020b). It has strong outward flowing bottom and surface currents on the eastern side of the fjord, and inflowing bottom and surface currents on the western side (Fig. 2.4). Temperatures range seasonally between 2 and 8 °C (Nordgård *et al.*, 1982, cited in Corner, Steinsund and Aspeli (1996). The fjord had an active shrimp trawl fishery from 1931 (Hjort and Ruud, 1938) until 1972 when the fjord was closed for all commercial bottom trawling (Sætra, 2019).

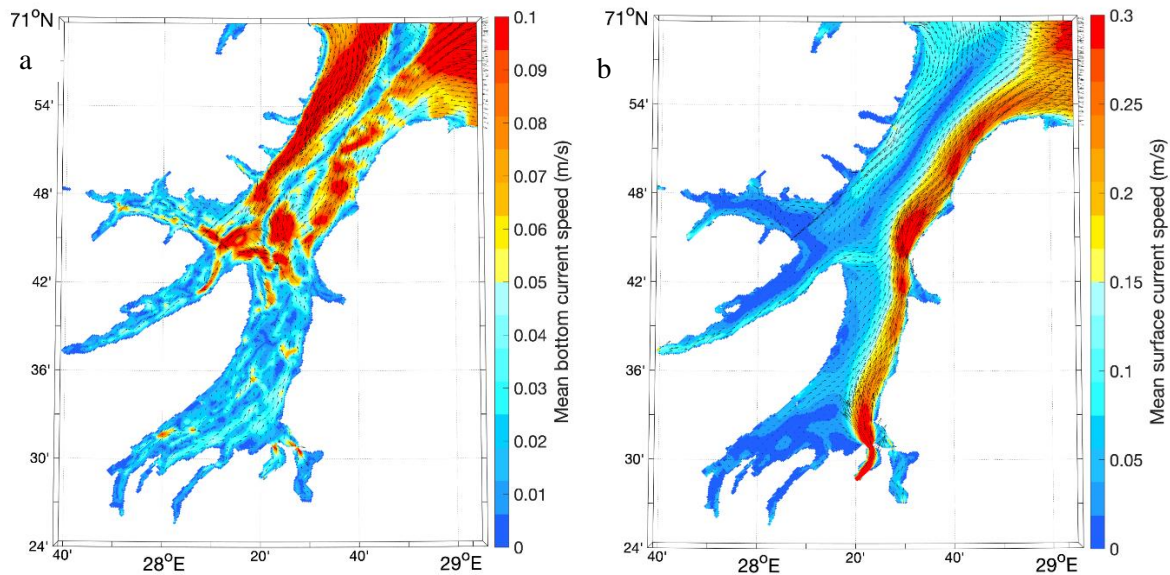


**Figure 2.4.** Mean annual bottom (a) and surface (b) current speed (m/s) for the Tana Fjord from April 2017-March 2019 based on results from a hydrodynamical model using ROMS (<http://myroms.org>) with a horizontal resolution of 160m x 160m. The coastal model providing input along the open boundaries, NorKyst800, is explained in detail in Asplin *et al.* (2020). Map by Jon Albretsen, Norwegian Institute of Marine Research, 2020.

### 2.1.2.3 KVÆNANGEN FJORD

The Kvænangen Fjord (69.5-70.2 °N and 20.5-22 °E), located 165 km south-west of the Porsanger Fjord, is approximately 74 km long (Fig. 2.1). The fjord has its maximum depth at 400 m, and no sill in the fjord mouth (Fiskeridirektoratet, 2020b). It has outward flowing surface currents on the eastern side of the fjord, but no clear patterns in bottom current (Fig. 2.5). The fjord has had an active shrimp trawl fishery since 1931 (Hjort and Ruud, 1938), with annual commercial landings of 180 tons the last 10 years (2009-2019) (Fiskeridirektoratet, 2020a). All shrimp trawls used north of 62 °N need to be equipped with a fish sorting grid. Having

geographical and climatic conditions similar to both the Porsanger and Tana Fjords, as stated by Nedreaas (Sætra, 2019), the Kvænangen Fjord was selected as the reference fjord when exploring the impact of absence of trawling on the closed fjord ecosystems of the Tana and Porsanger Fjords. Given the smaller area of the Kvænangen Fjord compared to the Tana and Porsanger Fjords, it was decided to include also the adjacent Reisa Fjord, such that the Kvænangen Fjord in this thesis will be synonymous with the combined area of the Kvænangen and Reisa Fjords.

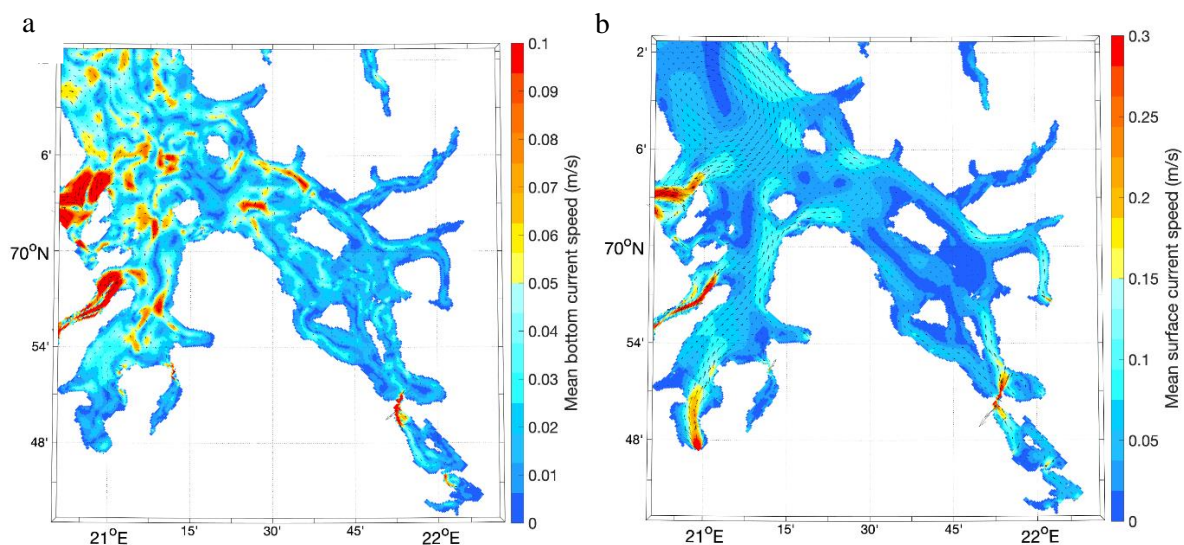


**Figure 2.5.** Mean annual bottom (a) and surface (b) current speed (m/s) for the Kvænangen Fjord from April 2017-March 2019 based on results from a hydrodynamical model using ROMS (<http://myroms.org>) with a horizontal resolution of 160m x 160m. The coastal model providing input along the open boundaries, NorKyst800, is explained in detail in Asplin et al. (2020). Map by Jon Albretsen, Norwegian Institute of Marine Research, 2020.

## 2.2 TRAWLING EXPERIMENTS

### 2.2.1 THE GULLMARS FJORD

After six years of commercial bottom trawling being prohibited in the Gullmars Fjord, an experimental research project was carried out in order to investigate the composition of the benthic community on the un-trawled fjord bottom and impacts of trawling on the bottom habitat (Hansson *et al.*, 1997, 2000). Six areas in the middle part of the fjord, the maximum number fitting in the deeper basin relevant for a shrimp fishery, were selected for the experimental bottom trawl survey. The bottom substrate in all the sites was pure clay (Höglund, 1947, cited in Hansson *et al.*, 2000). Each site was defined as a transect (1.5 km long) (Hansson *et al.*, 1997). Three of the transects were trawled (T1-T3), while three remained un-trawled (K1-

K3), serving as control areas for the trawl impact investigation (Fig. 2.6, Table 2.1). The commercial fishing boat “Littorina” (LL784) was hired for the experimental surveys, conducting trawl hauls along the assigned trawling transects. All three transects were trawled in one trawling event. The trawl used was of the “Gullmarstrål” kind, equal to the commercial trawls used before the closure of the fjord. The trawl consisted of 38 mm stretched meshes (20 mm bar length), whereas the square and wings were made up of larger meshes (70 mm stretched). Trawling speed was 1.5-2.0 knots. The overall trawling of the hired vessel was intended to be equal to the total annual fishing effort in the fjord in the years before the closure, when four boats were trawling approximately 90 to 120 days a year. Data were collected every month between December 1996 and November 1997, except from mid-December until mid-February when the fjord was ice bound (Hansson *et al.*, 1997). A total of 104 trawl hauls were conducted on the site (covering T1, T2 and T3) during the 1-year long experiment. The total catch was analysed, but only the shrimp samples were of interest for this master thesis. A subsample of 2 kg (on average 400 individuals) was randomly taken from the total catch from each of 3 to 4 trawl hauls (covering all three transects) each month, resulting in LFQ data from 27 of the 104 trawl hauls over the course of the experiment (Table 2.2). For each shrimp, sex and stage were determined, and length measured. CL was measured to the closest 0.1 mm using an electronic sliding calliper.

**Table 2.1.** Start and stop positions and depth interval of the three trawled transects in the experimental bottom trawl survey in the Gullmars Fjord in December 1996 to November 1997 (Hansson *et al.*, 1997).

Area	Start position	Stop position	Depth interval
T1	58°20.30'N, 11°33.30'E	58°20.90'N, 11°34.11'E	79-90 m
T2	58°21.30'N, 11°35.35'E	58°21.90'N, 11°35.85'E	88-93 m
T3	58°22.40'N, 11°36.67'E	58°23.00'N, 11°37.22'E	76-81 m

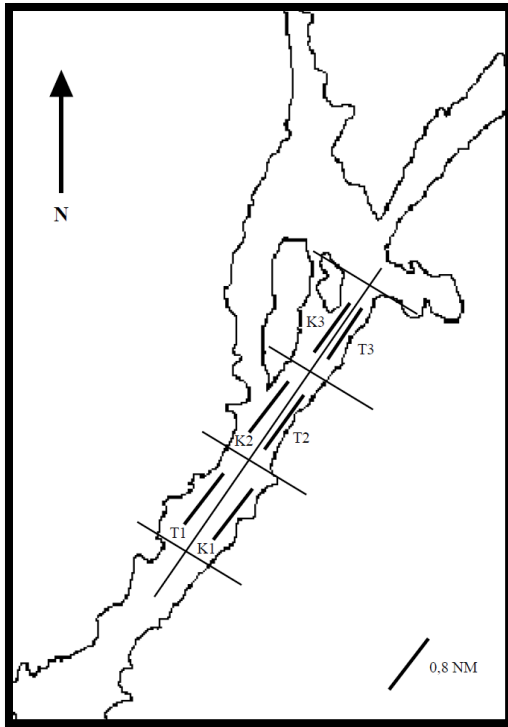


**Figure 2.6.** The six sites of the experimental bottom trawl survey in the Gullmars Fjord in December 1996 to November 1997. T1-T3 were trawled, while K1-K3 were control areas. The black lines indicate trawl hauling transects with a length of 0.8 nautical miles (1.5 km). Map borrowed from Hansson *et al.* (1997).

**Table 2.2.** Number of trawl hauls (samples) from which shrimp were collected in the Gullmars Fjord, and number of shrimp in samples per month.

	December 1996	February 1997	March 1997	April 1997	May 1997	June 1997	August 1997	September 1997	October 1997	November 1997
n/ samples	3	3	3	5	3	1	1	3	3	2
n/ shrimp	1334	1269	1412	2194	1236	445	404	1148	1249	992

### 2.2.2 PORSANGER, TANA AND KVÆNANGEN FJORDS

The Porsanger, Tana and Kvænangen Fjords were extensively mapped by the Norwegian Institute of Marine Research in 2018 and 2019. The mapping was done as part of the on-going investigation of the fjord ecosystems in the un-trawled fjords, carried out before a possible re-opening of the shrimp trawl fishery in the Porsanger and Tana Fjords. Three research cruises were conducted with the hired commercial shrimp trawler “Katla” (LK7560, 14.95m) (Søvik, Strand and Nedreaas 2019). The trawl used was a shrimp trawl 1600 ma with no fish sorting grid, 15 mm meshes in the cod end and 35 m sweeps. The gear used was a bobbins chain with rolling elements with a diameter of 15 cm. The cruises were carried out in autumn 2018 (01.10-01.11), spring 2019 (18.03-10.04) and autumn 2019 (30.09-23.10). Each cruise lasted about 3 weeks, with approximately one week of trawling in each of the fjords. Each fjord was divided into four areas (strata) based on depth (above and below 170 m (the present trawling border)), as well as trawlable soft bottom areas and non-trawlable rocky bottom areas. The exception was

the Porsanger Fjord that was divided into five areas due to the inner eastern basin being defined as a separate study site. In contrary to the trawling experiment in the Gullmars Fjord, where three fixed experimental transects were trawled, trawling stations in the Troms and Finnmark County were randomly selected for each cruise. The number of trawl stations per stratum for trawable ground deeper and shallower than 170 m were proportional to the area of the respective strata. Trawling speed was 1.2-1.7 knots, with approximately 15 minutes of bottom time. Three to five trawl stations were conducted each day between 08:00-20:00. In the Tana, Outer and Inner Porsanger, and Kvænangen Fjords, a total of 69, 72, 9 and 83 trawl hauls were conducted during the three cruises, respectively (Fig. 2.7). The total catch was analysed, but only the shrimp data were of interest for this master thesis. A random subsample of approximately 300 specimens was taken from each trawl haul containing shrimp. For each shrimp, sex and stage were determined, and length measured to the closest 0.1mm using an electronic sliding calliper. This resulted in length frequency data from 68, 57, 7 and 61 trawl hauls from the Tana, the Outer and Inner Porsanger, and Kvænangen Fjords, respectively (Table 2.3).

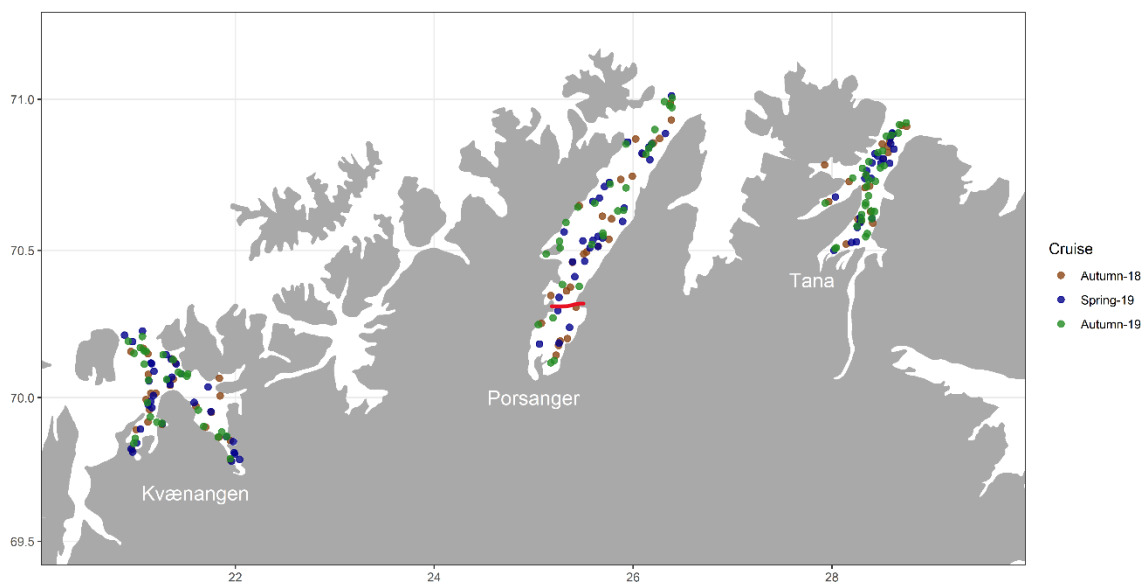


**Figure 2.7.** Trawling stations from the three cruises in autumn 2018 (brown), spring 2019 (blue) and autumn 2019 (green) in the Kvænangen, Porsanger and Tana Fjord. The red line in the Porsanger Fjord represents the separation of the Outer and Inner Porsanger Fjord. Map by Fabian Zimmerman, Norwegian Institute of Marine Research, 2020.

**Table 2.3.** Number of trawl hauls (samples) containing shrimp, and number of shrimp in samples for each research cruise for all fjord sites in northern Norway.

Fjord site	Autumn 2018		Spring 2019		Autumn 2019	
	Samples	n/ shrimp	Samples	n/ shrimp	Samples	n/ shrimp
Outer Porsanger Fjord	18	4628	19	3621	20	4745
Inner Porsanger Fjord	3	906	2	592	2	558
Tana Fjord	18	4442	22	5256	28	6032
Kvænangen Fjord	20	5537	20	5262	21	5945

## 2.3 BOTTOM TEMPERATURE

In the Gullmars Fjord, unpublished hydrographic data exist from the year after the experiment was conducted. Temperature was measured in the middle of the fjord (N58°19.40, E11°32.80), at 10 m intervals from 50 to 110 m depth, from one to three times a month between January and December 1998, except for July. Mean monthly bottom temperature (110 m) with standard deviation was calculated for all months and as an annual mean.

For the Norwegian fjord sites, bottom temperatures were measured during the trawling surveys in spring and autumn 2019. Temperature was measured during each trawl haul, with a HOBO temperature logger (<https://www.onsetcomp.com/hoboware-free-download>) attached to the headline of the trawl. Additional temperature measurements were conducted using the same kind of temperature loggers attached to shrimp traps in autumn 2018 and spring 2019, during parallel trap surveys at the same time as the trawling surveys. Mean bottom temperature with standard deviation was calculated for each of the fjord sites for autumn 2018 and spring and autumn 2019 using data from both the trawl hauls and the shrimp trap surveys. Bottom temperature maps were made by Trude Thangstad at the Norwegian Institute of Marine Research for each of the fjord sites for autumn 2018, spring 2019 and autumn 2019.

## 2.4 SHRIMP DENSITY

For the Gullmars Fjord, shrimp density as estimated by a trawl haul,  $D_i$  (tonnes/km<sup>2</sup>), was calculated as total biomass of shrimp in the trawl divided by the bottom area covered by the trawl during the haul, i.e. the swept area,  $A_{swept}$ :

$$A_{swept} = w \cdot s \cdot t \quad (1)$$

$w$  = width of trawl

$s$  = speed

$t$  = time trawling at bottom

Shrimp density in the fjord site,  $D_{ave}$ , was calculated as the average of the shrimp densities from all 104 experimental trawl hauls in the fjord from December 1996 to November 1997.

For the Outer and Inner Porsanger, Kvænangen and Tana Fjords, shrimp density (tonnes/km<sup>2</sup>) was estimated for each fjord site based on preliminary biomass estimates (Søvik, Strand and Nedreaas, 2019) made in StoX (Johnsen et al., 2019). Density in a fjord was calculated as the total biomass in the particular fjord divided by the area of shrimp grounds in the same fjord (the

trawlable strata),  $A_{shrimp}$  (see below, section 2.5). Delimitations of the shrimp ground areas are still work in progress and all estimates are thus preliminary.

## 2.5 FISHING PRESSURE

Fishing pressure,  $F$ , was calculated for the fished Kvænangen Fjord in order to compare natural mortality between the fished and unfished fjords. Furthermore,  $F$  was calculated for the Gullmars Fjord, as it can be questioned whether this fjord was truly unfished, as the trawling experiment from which the shrimp data were collected attempted to resemble the high fishing pressure in the fjord before the closure of the fisheries (Hansson *et al.*, 1997, 2000).

The total average shrimp biomass in a fjord,  $B$ , was estimated as the mean density multiplied by the total area of the shrimp distribution in the fjord:

$$B = D_{ave} \cdot A_{shrimp} \quad (2)$$

$D_{ave}$  = average shrimp density in fjord

$A_{shrimp}$  = total area with known distribution of shrimp in fjord

Whereas the area ( $A_{shrimp}$ ) in the Kvænangen Fjord was based on areas of soft bottom, read from bathymetric maps and registered shrimp grounds, it was for the Gullmars Fjord roughly estimated as the total area of the fjord bottom deeper than 60 m.

A proxy for the fishing mortality,  $F$ , was calculated by equation 3:

$$F = C/B \quad (3)$$

$C$  = total catch

For the Kvænangen Fjord,  $C$  was set equal to the official commercial landings in 2019 as no discard estimates were available for estimating the total catch, whereas for the Gullmars Fjord,  $C$  was set equal to the total shrimp catch from all 104 trawl hauls conducted over the study period.

## 2.6 STATISTICAL ANALYSES

### 2.6.1 SOFTWARE

All statistical analyses were conducted using the statistical computing software “R”, version 3.3.2 (R-Core-Team, 2013). For the growth and total mortality estimates, a series of functions in the TropFishR library (Mildenberger, Taylor and Wolff, 2017) were applied. The package contains a wide range of stock assessment methods specifically designed for data-limited stocks with length frequency (LFQ) data, adding updated features and optimisation techniques to

methods such as ELEFAN (Pauly and David, 1981) and the linearized length converted catch curve (Sparre and Venema, 1998), traditionally run in FISAT (Pauly and Sparre, 1991).

## 2.6.2 ESTIMATING GROWTH

### 2.6.2.1 DATA PREPARATION

Raw length measurements with corresponding sampling dates for each fjord site were imported into R. The length data were aggregated into length classes with bin sizes of 0.5 mm, creating LFQ data sets with abundance per length class. For the Gullmars Fjord, data were aggregated by month, whereas data from the three research cruises in northern Norway were aggregated by cruise and fjord site. Mean catch per length per month/cruise was calculated and assigned a mean date. Data were multiplied by 100 in order to avoid values below one. This resulted in 10 aggregated sampling dates for the Gullmars Fjord, and three for each of the Inner and Outer Porsanger, Tana and Kvænangen Fjords (Appendix 1, Tables A1-A5).

### 2.6.2.2 ELECTRONIC LENGTH FREQUENCY ANALYSIS

A bootstrapped ELEFAN with simulated annealing (SA) was applied for the growth analyses. The method is an optimized version of the original electronic length frequency analysis (ELEFAN) (Pauly and David, 1981). The SA-function allows for an unconstrained simultaneous search for optimal combinations of von Bertalanffy growth parameters (von Bertalanffy, 1938; Mildenerger, Taylor and Wolff, 2017). The bootstrap-function, available in the “fishboot” library in R (Schwamborn, Mildenerger and Taylor, 2018b), estimates uncertainties around the estimated growth parameters. Regardless of the known seasonal growth pattern for northern shrimp (Shumway *et al.*, 1985), it was decided to run the non-seasonalized version of the ELEFAN\_SA analysis, as the aim of the study was to estimate the average growth over a year. Preliminary model runs accounting for seasonalized growth revealed no significant improvements in the fit. In these cases the simpler model is also recommended (Taylor, 2020).

ELEFAN is based on the principles of modal progression analysis (Sparre and Venema, 1998), where each mode in a length distribution represents a separate age group (cohort). All cohorts are assumed to follow the same recruitment and growth pattern and can thus be allocated the same set of growth parameters, derived from the von Bertalanffy growth function (VBGF) (equation 4), (von Bertalanffy, 1938; Pauly and David, 1981), where length at age  $t$ ,  $L(t)$  is given by:

$$L(t) = L_{\infty} \cdot (1 - e^{(-K(t-t_0))}) \quad (4)$$

$t = \text{age (y)}$

$K = \text{the curvature parameter (y}^{-1}\text{)}$

$L_{\infty}$  (“L-infinity”) = the asymptotic length (mm)

$t_0 = \text{the theoretical age when length equals zero in a length-age coordinate system}$

The length data applied in the analysis represent a pseudo-cohort, which means that the data sampled over one year are assumed to resemble those of a cohort during its life span (Sparre and Venema, 1998). In the ELEFAN analysis in TropFishR,  $t_0$  is replaced by  $t_{\text{anchor}}$ , the time point anchoring growth curves in a length-time coordinate system, instead of a length-age coordinate system (Schwamborn, Mildenerger and Taylor, 2018a).

The first steps of the ELEFAN\_SA analysis were run according to the description by Pauly and David (1981). As a first step, the LFQ data were plotted (LFQ distributions). The LFQ data were thereafter restructured using the “lfqRestructure” function, where a “moving average”-value (MA) is assigned. This value decides the range of the subset of length classes in the “moving average frequency” (Box 1) (Pauly and David, 1981). Whereas the traditional analysis run in FISAT has an MA set to 5, TropfishR allows for selecting an MA, where Taylor and Mildenerger (2017) suggest that the MA should be based on the number of length classes in the smallest cohort. For the Gullmars Fjord the LFQ distributions (Fig. 3.1) revealed 8-10 length classes for the smallest modal peaks (assumed to represent cohorts). As the MA must be an odd number the value was thus set to 9. The Outer and Inner Porsanger, Tana and Kvænangen Fjords had 10-12 length classes in the smallest modal peaks (Fig. 3.1). Thus, the MA was set to 11.

The bootstrapped ELEFAN\_SA analysis was run using the “ELEFAN\_SA\_boot” function. The best fitted growth parameters and the corresponding VBGF with 95% confidence intervals (CI), were visualized using the “vbgfCI\_time” function. Variance around the parameters were visualized using the “univariate\_density” function, where the mean and the 95% CI of the distribution of  $L_{\infty}$ ,  $K$ ,  $t_{\text{anchor}}$  and  $\phi$ , the growth performance index, where  $\phi = \ln(K) + 2 \cdot \ln(L_{\infty})$  (Pauly and Munro, 1984; Moreau, Bambino and Pauly, 2014), are plotted in a univariate density estimate plot. A von Bertalanffy growth curve was superimposed on the LFQ distributions, using the “LfqFitCurves function”.

As the objective *Rn*-value (Box 1) should not be the only criteria for fitting the von Bertalanffy growth curve (Taylor, 2020; Wang *et al.*, 2020), the subjective interpretation of how well the superimposed von Bertalanffy growth curve traced through the modal peaks in the LFQ distributions, as well as the biological reasonableness of the growth parameters, were the main determinants of evaluating the best fit.

To explore the trends in the data two approaches were conducted (see below, 2.6.2.2.1, 2.6.2.2.2). A trial-error method for each approach resulted in four different scenarios (Table 2.4) with varying initial values (seed values) and upper and lower limits for *L<sub>oo</sub>*, *K* and *t<sub>anchor</sub>*.

Box 1 – running the bootstrapped ELEFAN with simulated annealing

Identifiable peaks in the dataset are attributed scores based on its deviation from the moving average frequency. These scores make up the available sum of peaks (ASP), constituting the maximum available points which can possibly be accumulated by a single growth curve. Each iteration in the analysis is given a score by calculating the accumulated points obtained by each growth curve when passing through the peaks (positive points) or through the troughs separating peaks (negative points), making up the “explained sum of peaks” (ESP). The model tests different values for *L<sub>oo</sub>*, *K* and *t<sub>anchor</sub>*, until the ESP/ASP ratio reaches a maximum (*Rn*-value,  $\leq 1$ ), and yields the growth parameters corresponding to this optimum ratio (“best fitted growth parameters”) (Pauly and David, 1981).

**Table 2.4.** Scenarios resulting from a trial-error method for approaches 1 and 2.

	<b>L<sub>oo</sub></b>	<b>K</b>	<b>t<sub>anchor</sub></b>
<b>Approach 1</b>			
Scenario 1	Varying L <sub>oo</sub>	Large range	Free range
Scenario 2	Varying L <sub>oo</sub>	Large range	Restricted
<b>Approach 2</b>			
Scenario 3	Fixed L <sub>oo</sub>	Large range	Restricted
Scenario 4	Fixed L <sub>oo</sub>	Lower bound of 0.4	Restricted

Due to a negative relationship between *L<sub>oo</sub>* and *K*, an initial input estimate for *L<sub>oo</sub>* with upper and lower bounds is recommended (Taylor and Mildenerger, 2017). The initial value for *L<sub>oo</sub>* was, for each fjord site, estimated using the *L<sub>max</sub>* approach, where *L<sub>oo</sub>* is derived from the largest measured individual in the sample, *L<sub>max</sub>* (equation 5) (Gayanilo, Sparre and Pauly, 1996).

$$L_{oo} = L_{max} \cdot 0.95 \quad (5)$$

The upper and lower bounds for *L<sub>oo</sub>* (95 % CI) were calculated based on the standard deviation (SD) of *L<sub>oo</sub>* from the assessment model (Stock Synthesis (SS3)) for the NDSK shrimp stock, using the SD (1.47 mm) estimated during a benchmark for the stock in 2016 (ICES, 2016). Given the varying number of samples between the fjord sites, the SD was used instead of the

standard error (SE = SD/sqrt(n)) when calculating the 95 % CI for *Loo* (pers. com. Massimiliano Cardinale, 2019) (equation 6).

$$CI = Loo \pm SD \cdot 1.96 \quad (6)$$

*SD* = the standard deviation of *Loo* from the 2016 NDSK benchmark

*1.96* = the standard constant approximation for a 95 % CI

In order to not restrict the model search, the *K*- and *t\_anchor*-values were set to search through a larger range of values. Based on the knowledge on *K*-values for shrimp (Shumway *et al.*, 1985; Nilssen and Hopkins, 1991), the *K*-value was set to search between 0.1 and 0.9 with a seed value of 0.5. The *t\_anchor*-value, interpreted as the peak hatching time, was set to search the whole range of possible values (0-1), with a seed value of 0.5, where a value represents a fraction of the year (e.g. 0.7068 = 15<sup>th</sup> of September). As the NDSK shrimp stock larvae hatch between February and April (pers. com. Guldborg Søvik), and lower temperatures result in a prolonged hatching time (Rasmussen, 1953; Thomassen, 1976; Nilssen and Hopkins, 1991) the outputs for the *t\_anchor* values were for all fjord sites expected to fall within the range of 1<sup>st</sup> of February (0.09) and 30<sup>th</sup> of May (0.41).

#### 2.6.2.2.1 APPROACH 1: VARYING LOO BETWEEN FJORD SITES

In Approach 1, the bootstrapped ELEFAN\_SA analysis was run with a varying *Loo* aiming to estimate stock (fjord) specific growth parameters. In order to visually compare growth between fjord sites from a scenario run, the estimated *Loo*- and *K*-values were plotted using equation 4. Growth curves from the VBGFs were plotted for ages 0-7 (y) with  $t_0 = 0$  (origo). As most of the growth appear in the first few years of a species' life span (Sparre and Venema, 1998), the slope of the curves were visually compared for ages 0-4 (y). The  $\phi$ -values yielded by a bootstrapped ELEFAN\_SA run, representing the growth performance based on the yielded *Loo*- and *K*-values (see above, section 2.6.2.2) were also used for comparing growth, where a higher value represent a faster growth, and opposite.

#### 2.6.2.2.2 APPROACH 2: FIXED LOO

Analyses were run with a fixed *Loo*-value. When *Loo* is kept constant over all study sites, the *K*-values can be used for a direct comparison of the site-specific growth rates (pers. com. Jeppe Kolding, 2020). This approach was introduced mainly to compare growth between fjord sites, where a higher *K*-value implies a faster growth, and opposite. The fixed *Loo*-value was determined based on the median of the output values yielded in Approach 1.

### 2.6.3 ESTIMATING TOTAL MORTALITY

The linearized length converted catch curve analysis was run in TropfishR based on the description in (Sparre and Venema, 1998).

The length data were, per study site, pooled into one frequency distribution with average catch data (abundance per length class). In order to convert from length to age, a linearized length converted catch curve analysis was applied with the estimated  $K$ - and  $L_{\infty}$ -values. The length data are transformed into an age-based catch-curve, a graphical representation of the logarithmic number of survivors plotted against relative age, where the descending side represents losses due to mortality (Sparre and Venema, 1998). If the abundance of a stock decrease exponentially with size (or age), the slope of the log-transformed data should form a linear pattern. From this, a linear regression line can be fitted, where the total mortality,  $Z$ , can be estimated as the slope of the line (Ricker, 1975). As such, only data points following a linear pattern are selected. The relationship between length and exact age becomes uncertain as one approaches  $L_{\infty}$ , as the largest individuals may be bigger due to faster growth, not because they are older (Sparre and Venema, 1998). Additionally, there are often few large specimens in the samples. The last 1-2 age groups were therefore not included in the regression lines, unless they did not impact the slope of the fitted linear regression line. The estimated  $Z$  with 95% CI was displayed in a catch curve plot window using the “catchCurve” function.

## 3 RESULTS

### 3.1 LENGTH FREQUENCY DISTRIBUTIONS

The LFQ distributions revealed from two to three modal peaks (assumed to represent separate cohorts) at all fjord sites (Fig. 3.1). The only exception was the Inner Porsanger Fjord, where the 2019 samples revealed no clear modal peaks (Fig. 3.1), likely due to the few samples collected from this specific study site (Table. 2.3). Consequently, no further emphasis will be put in the results from this specific fjord site. Estimated growth parameters and corresponding growth curves will be included in tables and figures for the interest of readers but will not be addressed in the text.

Whereas the 2018 autumn LFQ distributions from the Outer Porsanger Fjord revealed four modal peaks, only three were visible in the spring and autumn LFQ distributions the following year (Fig. 3.1). As younger shrimp normally join the adult stock after approximately one year (Rasmussen, 1953; Shumway *et al.*, 1985; Nilssen and Hopkins, 1991), the first modal peaks (approximately 10-15 mm mean CL) were interpreted as one-year olds (1-goup) (Fig 3.1). Whereas a distinct 1-group was evident already during spring in the Kvænangen Fjord, very few specimens belonging to the 1-group were caught during early spring in the Outer Porsanger and Tana Fjords (Fig. 3.1). In the Gullmars Fjord, some 1-group specimens were caught in early spring (February), developing into a more distinct cohort in the LFQ distribution comes summer and late autumn. During autumn, the assumed 1-group formed a distinct modal peak for all fjord sites. The 1-group specimens were somewhat smaller in the Outer Porsanger and Gullmars Fjords than in the Tana and Kvænangen Fjords during autumn, with mean CL of approximately 14-15 mm and 16-18 mm, respectively. All the fjord populations had large specimens of shrimp in the 3+ group, with CL ranging from 29 to 35 mm. The 3+ group shrimp in the Kvænangen Fjord were larger than the shrimp in the +-groups in the other fjord sites. For the Gullmars Fjord, large specimens of shrimp disappeared from the LFQ distributions from March-June 1997, compared to that of December 1996 and February 1997.

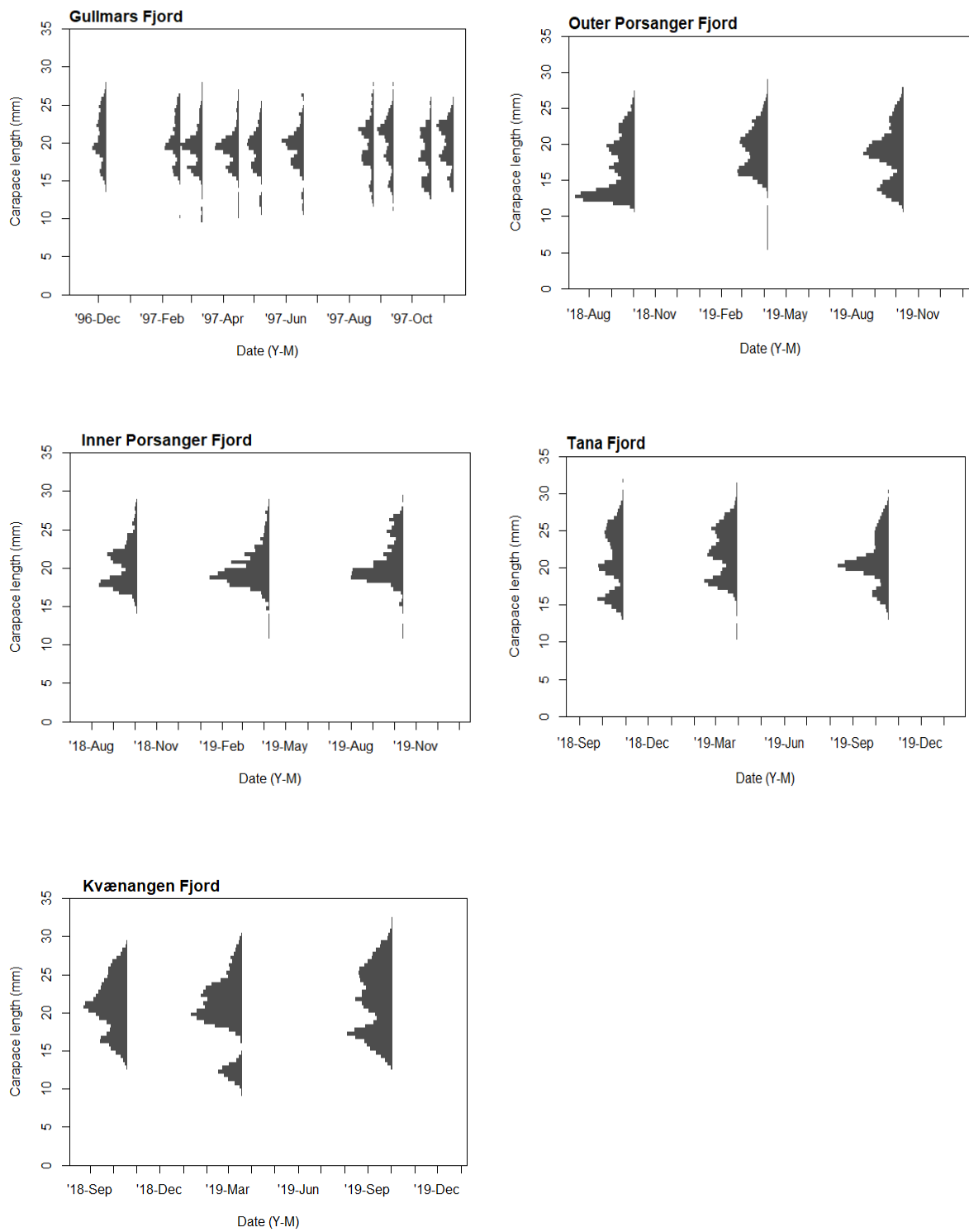


**Figure 3.1.** Length frequency distributions of shrimp per average date for all fjord sites (Appendix 1, Tables. A1-5). The Gullmars Fjord data are aggregated by month, while the data from the Norwegian fjord sites are aggregated by research cruise.

## 3.2 GROWTH

### 3.2.1 APPROACH 1: VARYING LOO

The analyses run with a varying *Loo* and large search ranges for *K* and *t\_anchor* (Scenario 1) gave *t\_anchor*-values (hatching time) deviating from biologically reasonable expectation in the Gullmars and Outer Porsanger Fjords (Table 3.1). The results are presented in more detail in Appendix 2, but are not used further in this thesis. Consequently, values of *t\_anchor* were restricted to a biological reasonable range (1<sup>st</sup> of February – 30<sup>th</sup> of May, see above, section 2.6.2.2), for all further scenario runs. An additional Approach 1 scenario (Scenario 2) was conducted, where *t\_anchor* was restricted while *Loo* and *K* were allowed to vary as in Scenario 1.

The estimated values for *Loo*, *K*, and *t\_anchor* yielded by Scenario 2 varied between the five fjord sites (Fig. 3.2, Table 3.1). CI around the growth curves for the Gullmars Fjord were wider than for the other fjord sites (Fig. 3.2). The wide CI was likely due to the bimodal distribution for both *Loo* and *K* in the univariate density estimate plot (Fig. 3.3). This implies that an alternative set of growth parameters than the “best fitted growth parameters” from the ELEFAN\_SA analysis (Fig. 3.2) may be equally possible for the sampled data from the Gullmars Fjord. The univariate distributions were unimodal for the other fjord sites, except for the Outer Porsanger, with a small second mode for some of the parameters (Fig. 3.3). The growth curves tracing through the modal peaks revealed from five to seven age groups (including the 0-group) in the different fjord sites (Fig. 3.4). The second and third line of the growth curve (from the bottom of the plot), representing the 1- and 2-groups, respectively, hit all the 1- and 2-group modal peaks in the LFQ distributions from all sampling events for the Gullmars, Tana and Kvænangen Fjords (Fig. 3.4). For the Outer Porsanger Fjord, the growth curve did not trace well through the modal peaks, as the third and fourth lines were skewed towards the lower part of the 2- and 3- group modal peaks for both 2019 samples (Fig. 3.4). This was likely because the growth curve aimed to trace through both the second and third modal peak in the autumn 2018 sample, that likely belong to the same cohort (see below, section 4.1).

When visually comparing the slope of the plotted growth curves for ages 0-4, growth appears higher in the Kvænangen Fjord, compared with the Tana, Gullmars and Outer Porsanger Fjords (Fig. 3.5). This is supported by the  $\phi$ -values, where the highest value was estimated for the Kvænangen Fjord, and the lowest for the Outer Porsanger Fjord (Table. 3.1).

**Table 3.1.** Estimated growth parameters from four scenarios from the bootstrapped ELEFAN\_SA analyses, with 95 % confidence intervals from the univariate density estimate plots ( , ). Scenario 1: Varying *Loo* between fjord sites and large search range for *K* and *t\_anchor*. Scenario 2: Varying *Loo* and restricted *t\_anchor*. Scenario 3: Fixed *Loo* and restricted *t\_anchor*. Scenario 4: Fixed *Loo*, restricted *t\_anchor* and *K*.

	<b>Loo</b>	<b>K</b>	<b>t_anchor</b>	<b>φ</b>	<b>Rn-value</b>
<b>Approach 1</b>					
<b>Scenario 1</b>					
Gullmars Fjord	25.7 (25.06, 36.89)	0.45 (0.37, 0.48)	0.91 (0.61, 1.01)	2.46 (2.42, 2.49)	0.68
Outer Porsanger Fjord	25.7 (24.93, 25.92)	0.64 (0.41, 0.70)	0.66 (0.00, 0.99)	2.63 (2.42, 2.67)	0.82
Inner Porsanger Fjord	27.1 (23.91, 27.84)	0.67 (0.34, 0.84)	0.13 (-0.01, 0.99)	2.70 (2.42, 2.72)	0.50
Tana Fjord	27.8 (27.2, 29.59)	0.49 (0.42, 0.52)	0.13 (-0.06, 1.02)	2.57 (2.53, 2.6)	0.93
Kvæningen Fjord	30.1 (29.93, 30.28)	0.52 (0.38, 0.55)	0.20 (0.00, 1.08)	2.67 (2.55, 2.71)	0.88
<b>Scenario 2</b>					
Gullmars Fjord	24.8 (24.50, 26.17)	0.53 (0.32, 0.55)	0.09 (0.06, 0.43)	2.51 (2.35, 2.52)	0.57
Outer Porsanger Fjord	25.3 (25.02, 25.89)	0.45 (0.43, 0.53)	0.20 (0.09, 0.39)	2.47 (2.44, 2.56)	0.78
Inner Porsanger Fjord	26.7 (25.07, 27.49)	0.72 (0.45, 0.86)	0.21 (0.09, 0.31)	2.71 (2.47, 2.75)	0.55
Tana Fjord	27.5 (27.15, 28.51)	0.50 (0.47, 0.53)	0.13 (0.08, 0.20)	2.58 (2.57, 2.60)	0.88
Kvæningen Fjord	30.1 (29.96, 30.28)	0.53 (0.50, 0.54)	0.23 (0.14, 0.26)	2.66 (2.65, 2.69)	0.89
<b>Approach 2</b>					
<b>Scenario 3</b>					
Gullmars Fjord	27.0 (26.99, 27.01)	0.34 (0.30, 0.34)	0.40 (0.18, 0.43)	2.39 (2.34, 2.39)	0.52
Outer Porsanger Fjord	27.0 (26.99, 27.01)	0.50 (0.51, 0.50)	0.38 (0.37, 0.41)	2.56 (2.56, 2.57)	0.78
Inner Porsanger Fjord	27.0 (26.99, 27.01)	0.70 (0.68, 0.71)	0.21 (0.14, 0.23)	2.71 (2.70, 2.71)	0.55
Tana Fjord	27.0 (26.99, 27.01)	0.53 (0.52, 0.55)	0.18 (0.10, 0.26)	2.59 (2.58, 2.61)	0.93
Kvæningen Fjord	27.0 (26.99, 27.01)	0.68 (0.67, 0.75)	0.34 (0.33, 0.40)	2.69 (2.69, 2.74)	0.86
<b>Scenario 4</b>					
Gullmars Fjord	27.0 (26.99, 27.01)	0.45 (0.44, 0.65)	0.10 (0.09, 0.11)	2.52 (2.51, 2.53)	0.47
Outer Porsanger Fjord	27.0 (26.99, 27.01)	0.50 (0.50, 0.51)	0.40 (0.38, 0.41)	2.56 (2.56, 2.57)	0.74
Inner Porsanger Fjord	27.0 (26.99, 27.01)	0.70 (0.68, 0.71)	0.21 (0.14, 0.22)	2.71 (2.70, 2.71)	0.55
Tana Fjord	27.0 (26.99, 27.01)	0.55 (0.52, 0.56)	0.24 (0.11, 0.27)	2.60 (2.58, 2.61)	0.95
Kvæningen Fjord	27.0 (26.99, 27.01)	0.68 (0.67, 0.69)	0.34 (0.32, 0.36)	2.69 (2.69, 2.70)	0.86

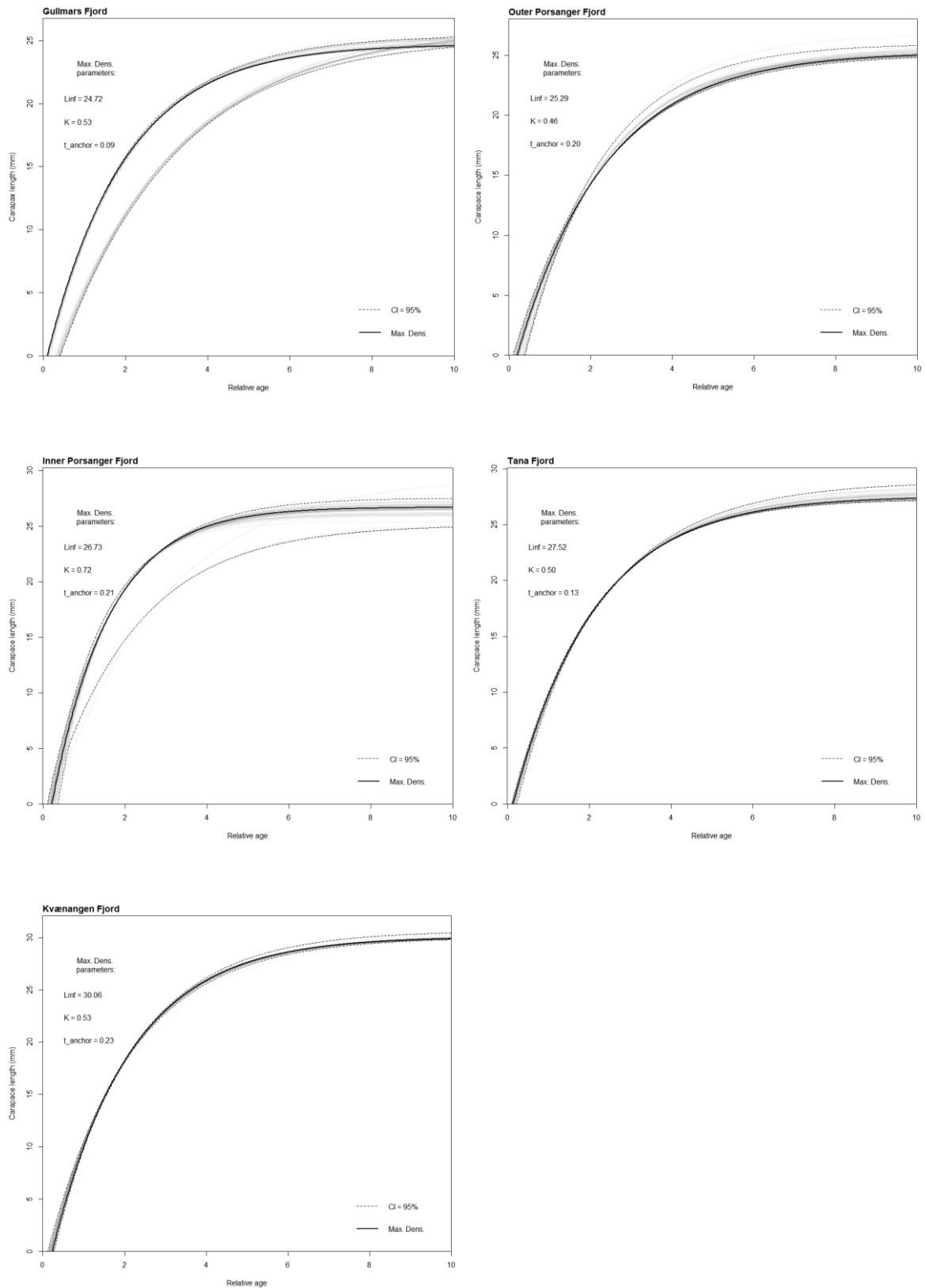


**Figure 3.2.** Scenario 2: Output from the bootstrapped ELEFAN analyses with simulated annealing from all fjord sites. The von Bertalanffy growth curve (Max. Dens) from the best fitted growth parameters are plotted with confidence intervals (CI=0.95 %) (dotted lines). Grey lines indicate other iterations from the same run in the analyses.

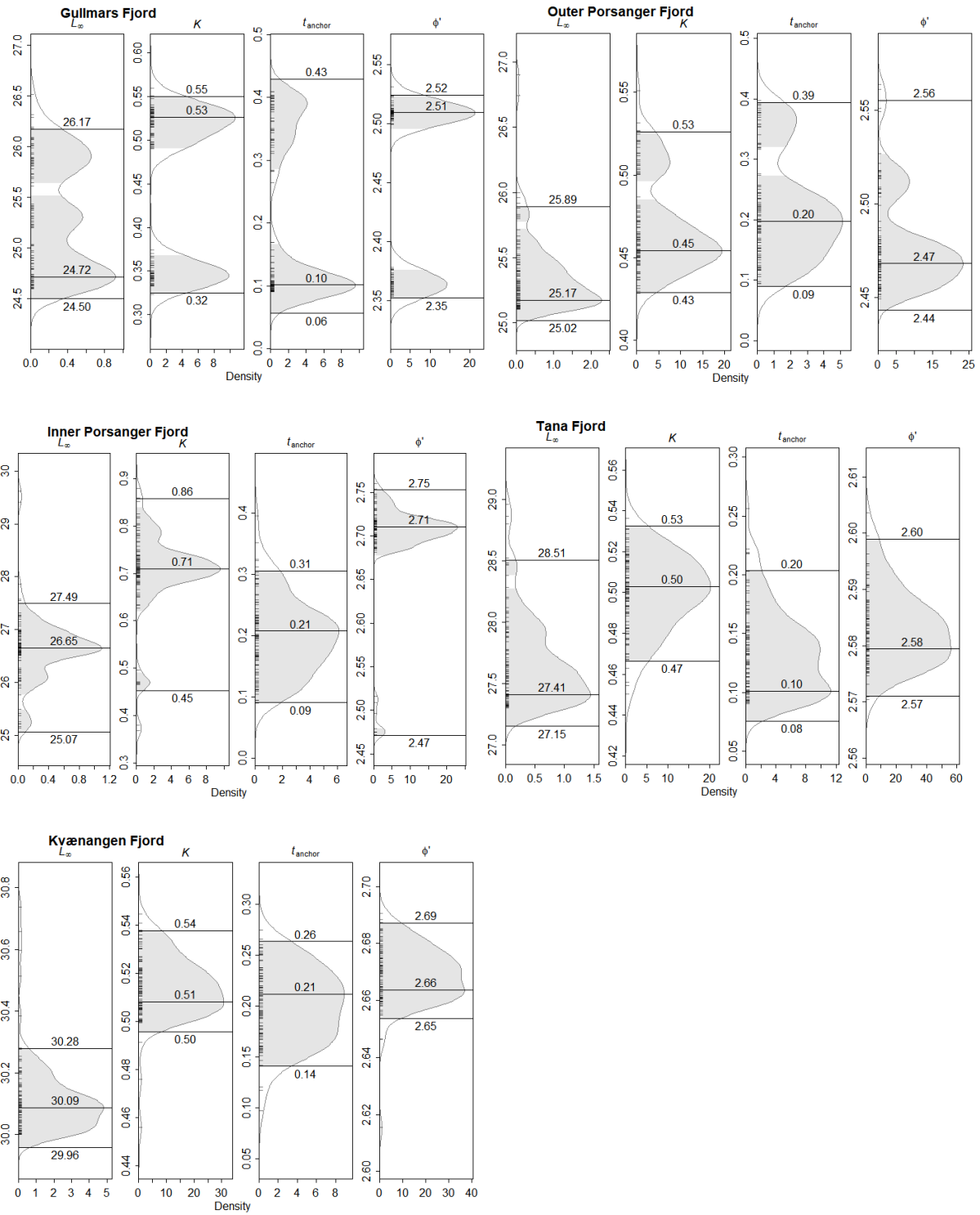


**Figure 3.3.** Scenario 2: Univariate density estimate plots for the von Bertalanffy growth parameters from the bootstrapped ELEFAN analysis with simulated annealing, for all fjord sites.

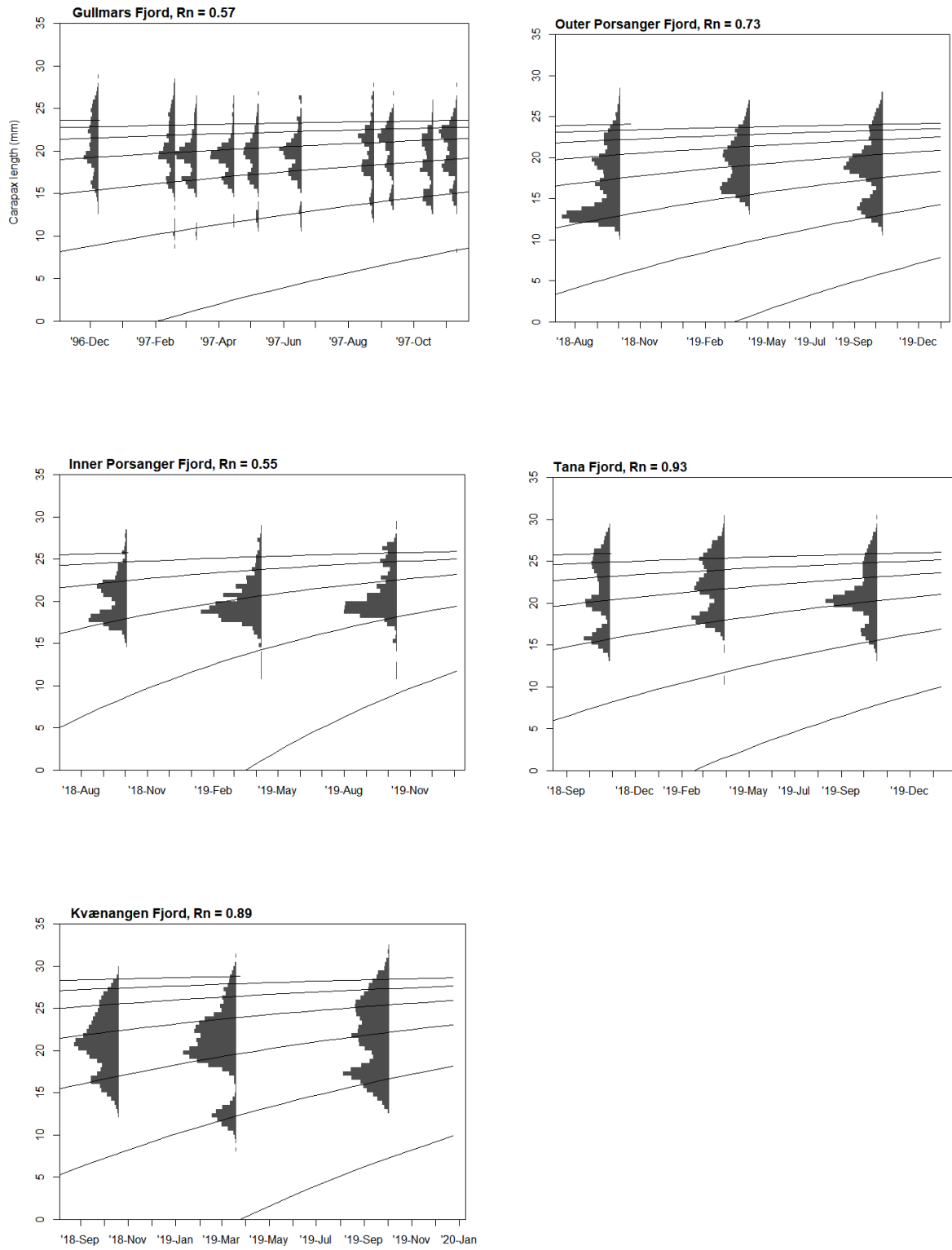


**Figure 3.4.** Scenario 2: The estimated von Bertalanffy growth curves from the bootstrapped ELEFAN analyses with simulated annealing superimposed on length frequency distributions for all fjord sites.

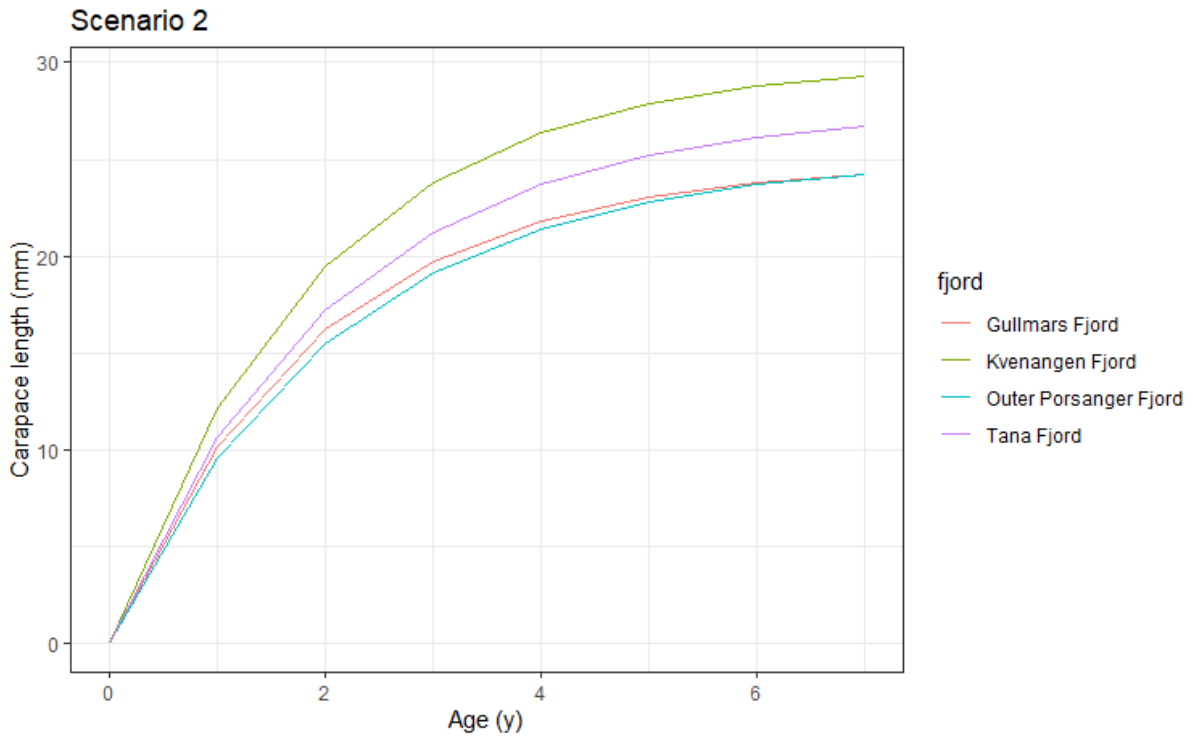


**Figure 3.5.** Scenario 2: von Bertalanffy growth curves from each fjord site given by the “best fitted growth parameters” from the bootstrapped ELEFAN analyses with simulated annealing (Table 3.1).

### 3.2.2 APPROACH 2: FIXED LOO

The median of the *Loo*-values yielded from the Scenario 2 runs equalled 26.88 ( $\pm$  2.10) mm. Based on this, it was decided to fix *Loo* at 27 mm when fitting the VBGF curves. The analyses run with a fixed *Loo* of 27 mm and a restricted *t\_anchor* (1<sup>st</sup> of February-30<sup>th</sup> of May) constitute Scenario 3.

Scenario 3 gave a higher relative growth rate (*K*-value) in the Kvænangen Fjord (0.68) compared to that of the Tana (0.53), Outer Porsanger (0.50) and Gullmars Fjords (0.34) (Fig. 3.6, Table 3.1). These findings are consistent with what was found in the Scenario 2 run (Fig. 3.5), except for the remarkably lower growth found in the Gullmars Fjord. These findings are also supported by the estimated  $\phi$ -values (Table 3.1). The CIs for both the growth curves and the variance in the analyses were narrower than for the Scenario 2 runs (Figs. 3.6, 3.7). The growth curves tracing through the modal peaks revealed from five (Kvænangen Fjord) to nine year-classes (Gullmars Fjord) (Fig. 3.8). The second and third line of the growth curves traced well through the 1- and 2-group modal peaks for the Tana, Kvænangen and Outer Porsanger Fjords (Fig. 3.8). However, for the autumn 2018 sample in the Outer Porsanger Fjord, the fourth line traced through the third modal peak instead of the second, appearing to ignore the extra

modal peak present (see below, section 4.1). For the Gullmars Fjord, an extra line was added to the growth curve, such that the third and fourth lines, and not the second and third lines, traced through the 1- and 2-group modal peaks, respectively (Fig. 3.8). This means the shrimp would be two years when they first appear in the catches, which contradicts the assumption that the first modal peaks in the LFQ distributions are 1-year olds (see above, section 3.1).

It was thus decided to run a new scenario where the  $K$ -value was forced to search among higher values. Thus, a lower bound of 0.4 for  $K$  was added to the model settings, constituting Scenario 4. These analyses yielded  $K$ -values identical to those from Scenario 3 for the Outer Porsanger and Kvænangen Fjords, and a slightly higher value for the Tana Fjord (0.55) (Table 3.1, Appendix 3A, Fig. A3). Growth was still lowest in the Gullmars Fjord (0.45) (Fig. 3.9) when compared with the other study sites. This result was also supported by the estimated  $\phi$ -values (Table 3.1). The univariate distributions were unimodal, with a narrow CI around the growth curve (Figs. 3.10, 3.9). The growth curve tracing through the modal peaks revealed seven year-classes for the Gullmars Fjord (Fig. 3.11). The second, third and fourth lines in the growth curve traced well through the 1-, 2- and 3-group modal peaks.

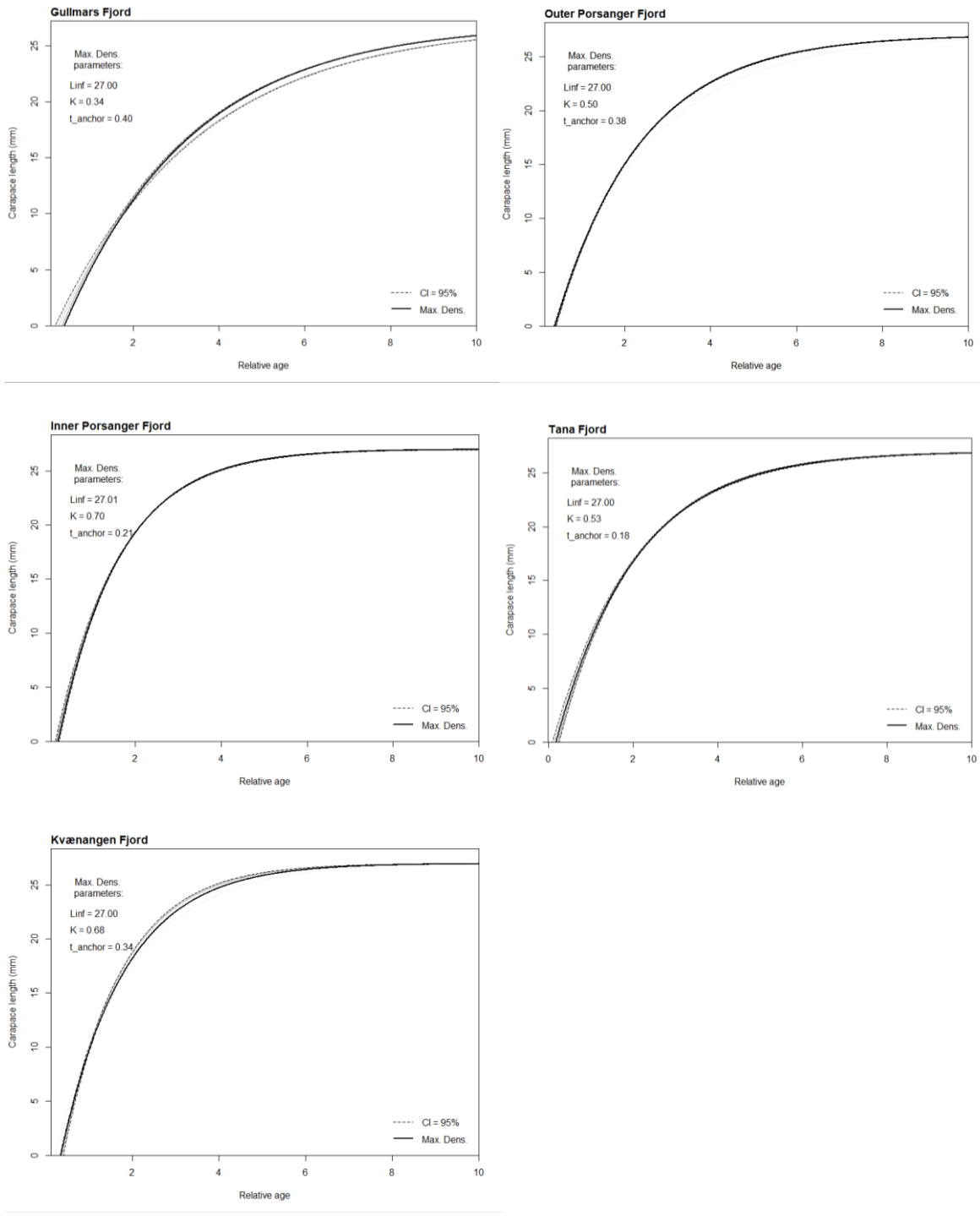


**Figure 3.6.** Scenario 3: Output from the bootstrapped ELEFAN analyses with simulated annealing from all fjord sites. The von Bertalanffy growth curve (Max. Dens.) from the best fitted growth parameters are plotted with confidence intervals (CI=0.95 %). Grey lines indicate other iterations from the same run in the analyses.

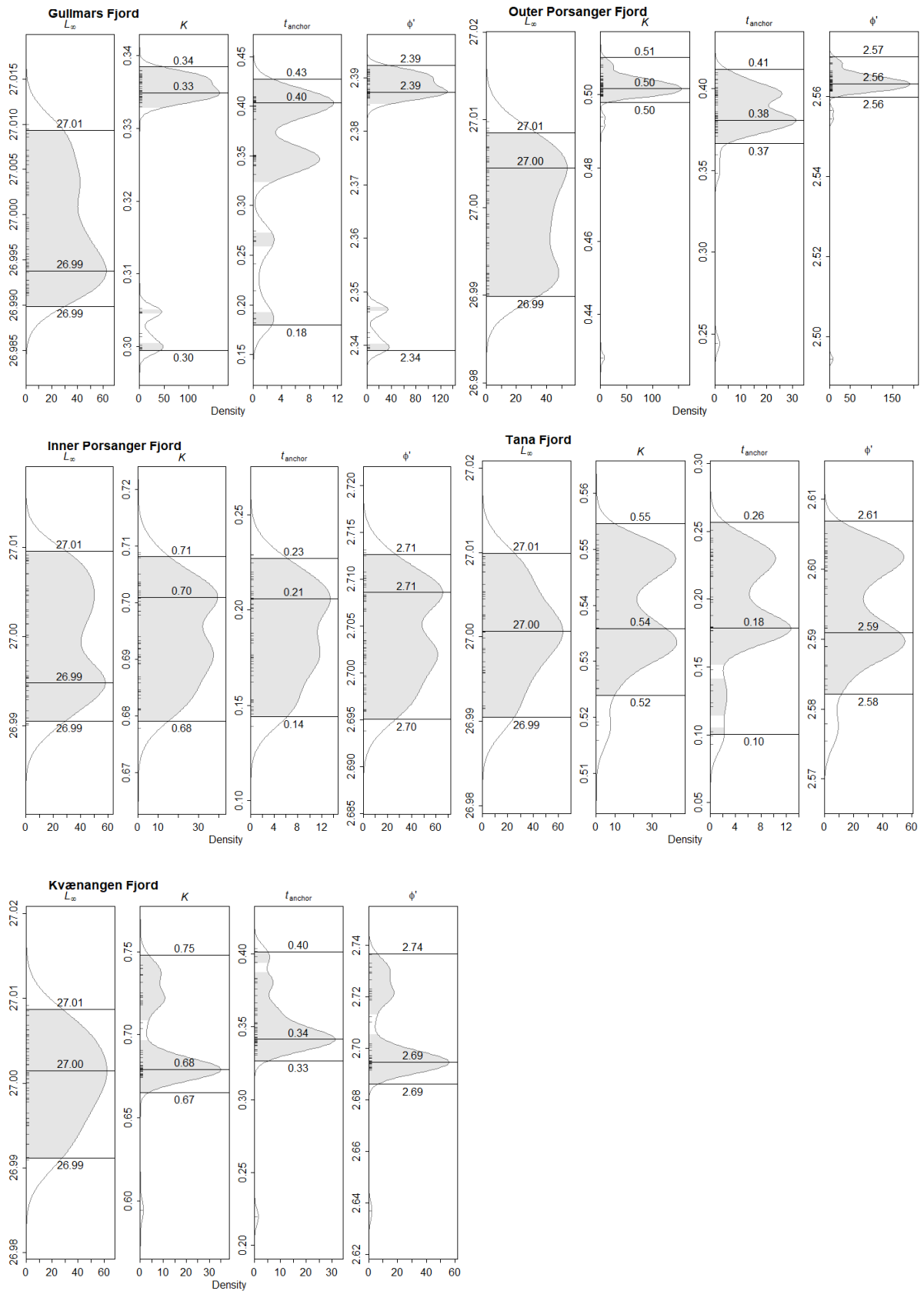


**Figure 3.7.** Scenario 3: Univariate density estimate plots for the von Bertalanffy growth parameters from the bootstrapped ELEFAN analysis with simulated annealing, for all fjord sites.

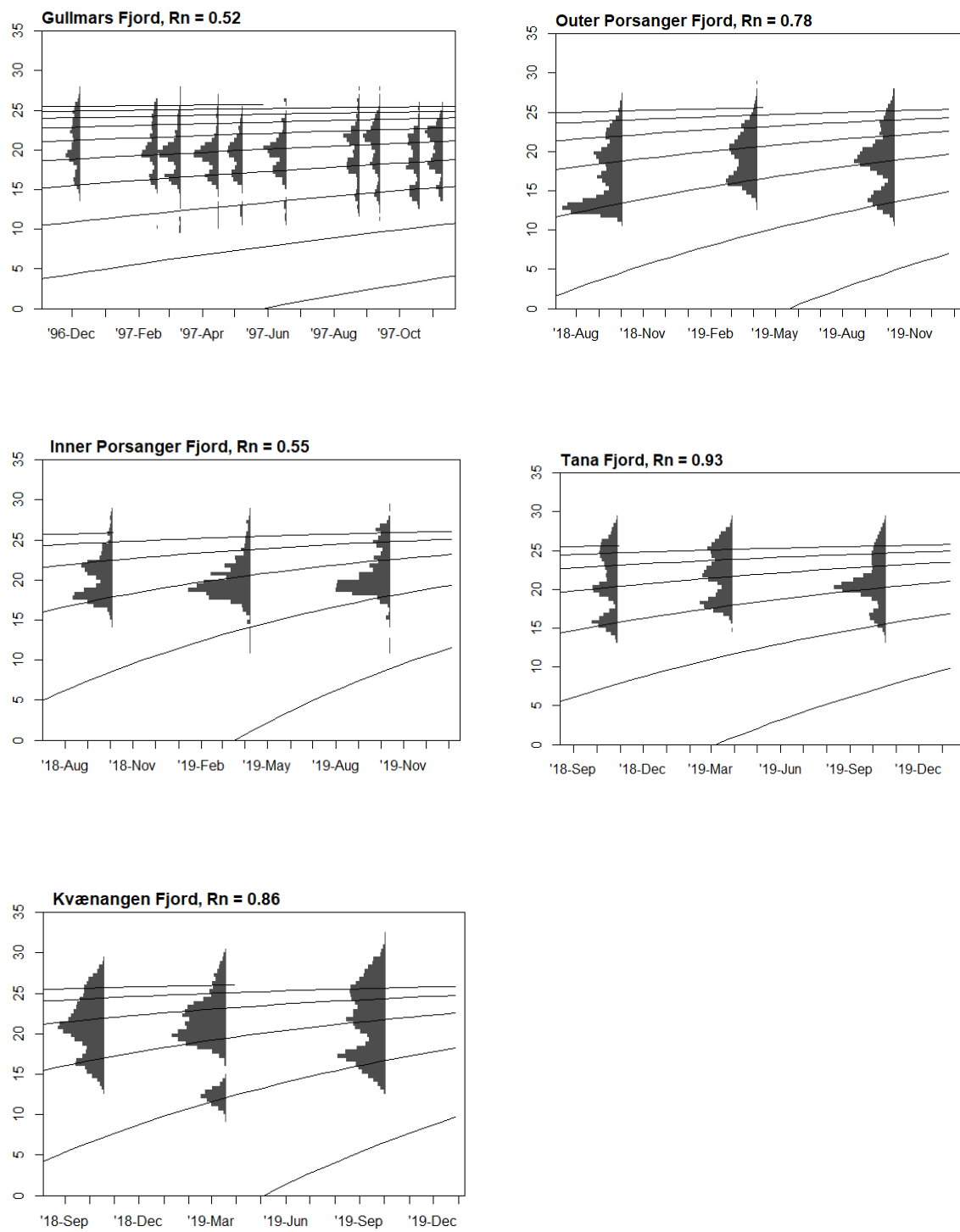


**Figure 3.8.** Scenario 3: The estimated von Bertalanffy growth curves from the bootstrapped ELEFAN analyses with simulated annealing superimposed on length frequency distributions for all fjord sites.

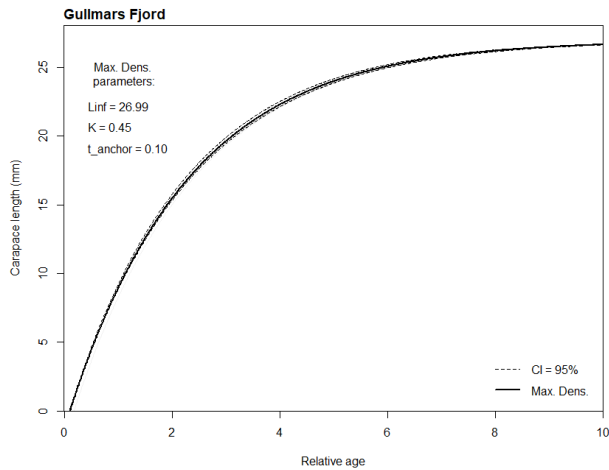


**Figure 3.9.** Scenario 4: Output from the bootstrapped ELEFAN analysis with simulated annealing from the Gullmars Fjord. The von Bertalanffy growth curve (Max. Dens) from the best fitted growth parameters is plotted with confidence intervals (CI=0.95 %). Grey lines indicate other iterations from the same run in the analyses.

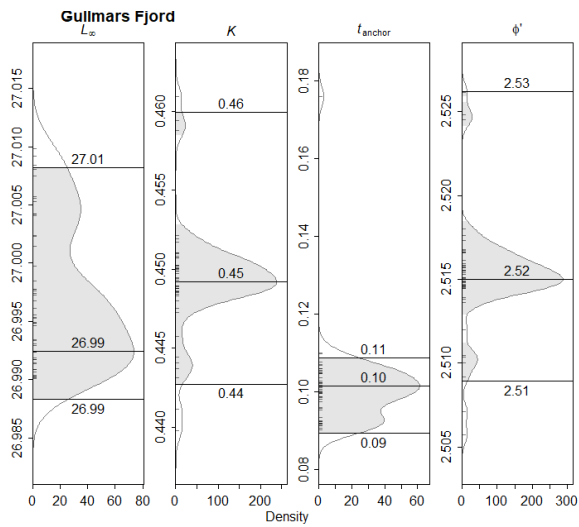


**Figure 3.10.** Scenario 4: Univariate density estimate plot for the von Bertalanffy growth parameters from the bootstrapped ELEFAN analysis with simulated annealing from the Gullmars Fjord.

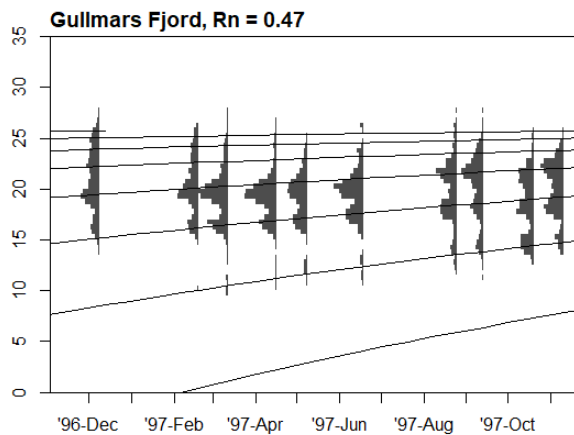


**Figure 3.11.** Scenario 4: The estimated von Bertalanffy growth curve from the bootstrapped ELEFAN analysis with simulated annealing superimposed on length frequency distributions from the Gullmars Fjord.

### 3.2.3 COMPARING GROWTH BETWEEN APPROACH 1 AND 2

Growth patterns of Approaches 1 and 2 were compared by plotting the growth curves given by values of  $L_{oo}$  and  $K$  for each scenario run (2-4). The Scenario 4 growth curves appear identical to those of Scenario 3 for all fjord sites as they are overlapping, except for the Gullmars Fjord (Fig. 3.12). For the Gullmars Fjord, scenarios 2 and 4 present us with similar growth patterns for ages 0-3 y, whereas Scenario 3 yielded a lower growth (Fig. 3.12). Scenarios 2 and 3 had similar growth patterns for the Tana Fjord for all ages, whereas for the Kvænangen Fjord growth appear similar only for ages 0-3 (Fig. 3.12). For the Outer Porsanger Fjord Scenario 2 yielded a lower growth than Scenario 3.

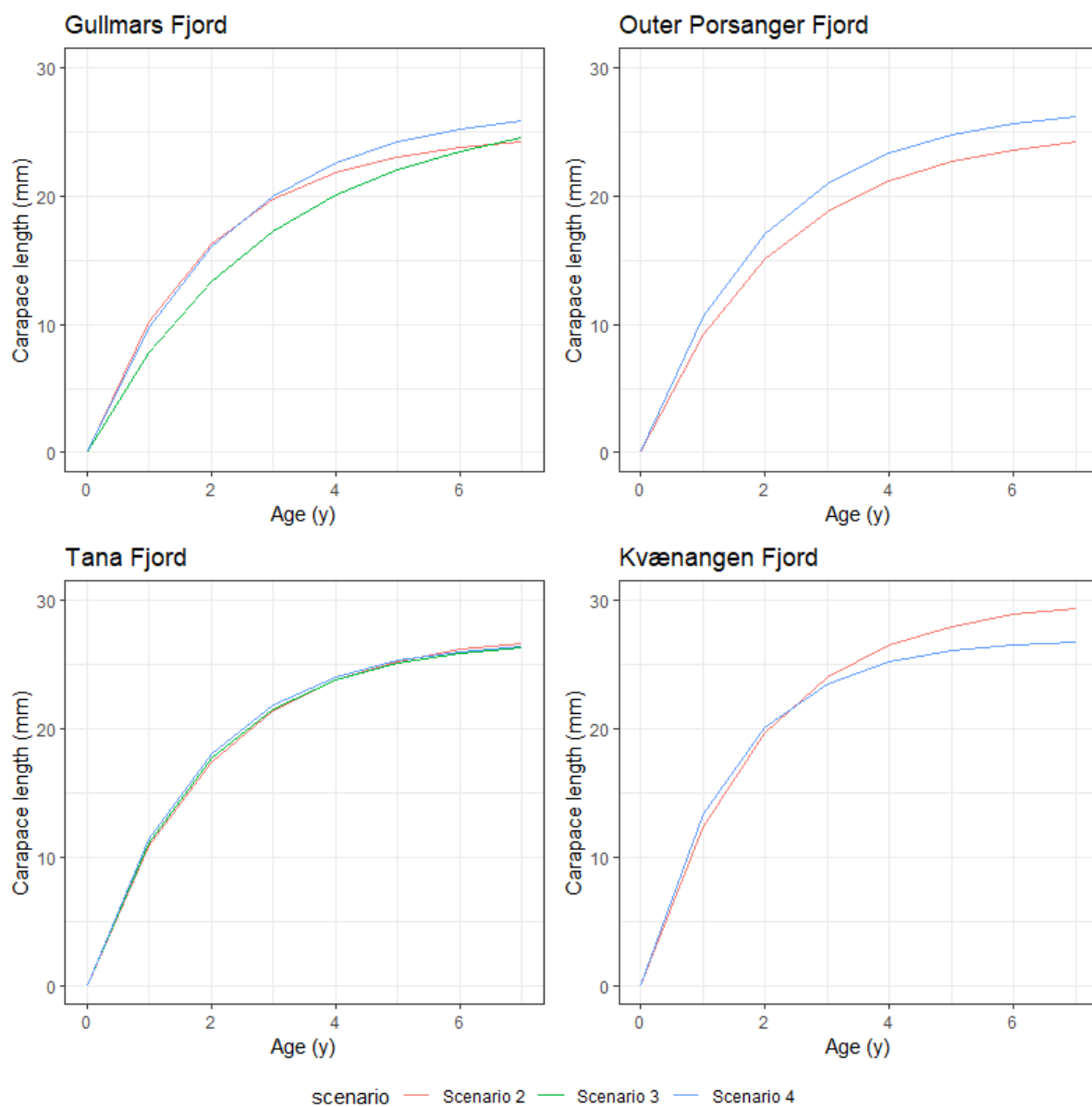


**Figure 3.12.** The von Bertalanffy growth curves resulting from the best fitted growth parameters from the bootstrapped ELEFAN analyses from scenarios 2, 3 and 4 for each fjord site (Table 3.1). Note that growth curves yielded from Scenario 3 and 4 are overlapping for all fjord sites but the Gullmars Fjord.

### 3.2.4 MOST PLAUSIBLE GROWTH PARAMETERS

For the Kvænangen and Tana Fjords, the unimodal parameter distributions (Fig. 3.3) and the well-fitted growth curves tracing through the LFQ distributions (Fig. 3.2) give strength to the credibility of the “best fitted growth parameters” yielded in Scenario 2 for these specific fjord sites (Table 3.1). Regarding the Gullmars Fjord, as the “best fitted growth parameters” yielded a well-fitted growth curve (Fig. 3.2) that traced through the 1-, 2- and 3- group modal peaks, they are considered suitable for the sampled data, despite the bimodal distributions in the univariate density plots (Fig. 3.3). For the Outer Porsanger Fjord the growth parameters from Scenario 2 are considered little plausible, as they yielded a poorly fitted growth curve (Fig. 3.4). As the Scenario 3 growth curve traced well through the LFQ distributions (Fig. 3.8), Scenario 3 growth parameters are considered the “most plausible growth parameters” for the Outer Porsanger Fjord (Table 3.1), despite that Approach 2 (Scenario 3) growth parameters initially were used only for comparing growth between the fjord sites.

When visually comparing the slope of the plotted growth curves from the “most plausible growth parameters” (Table 3.2), growth appear highest in the Kvænangen Fjord, lowest in the Gullmars Fjord, and similar in the Tana and Porsanger Fjords (Fig. 3.13). This is supported by the  $\phi$ -values, where the highest value was estimated for the Kvænangen Fjord, and the lowest for the Gullmars Fjord, and a slightly higher value for the Tana Fjord compared to that of the Outer Porsanger Fjord (Table. 3.2).

**Table 3.2.** Most plausible estimated growth parameters from the bootstrapped ELEFAN\_SA analyses, with 95 % confidence intervals from the univariate density estimate plots. Scenario 2: Varying *Loo* and restricted *t\_anchor*. Scenario 3: Fixed *Loo* and restricted *t\_anchor*.

Fjord site	Scenario	Loo	K	t_anchor	$\phi$
Gullmars Fjord	2	24.8 (24.50, 26.17)	0.53 (0.32, 0.55)	0.09 (0.06, 0.43)	2.51 (2.35, 2.52)
Outer Porsanger Fjord	3	27.0 (26.99, 27.01)	0.50 (0.51, 0.50)	0.38 (0.37, 0.41)	2.56 (2.56, 2.57)
Tana Fjord	2	27.5 (27.15, 28.51)	0.50 (0.47, 0.53)	0.13 (0.08, 0.20)	2.58 (2.57, 2.60)
Kvænangen Fjord	2	30.1 (29.96, 30.28)	0.53 (0.50, 0.54)	0.23 (0.14, 0.26)	2.66 (2.65, 2.69)

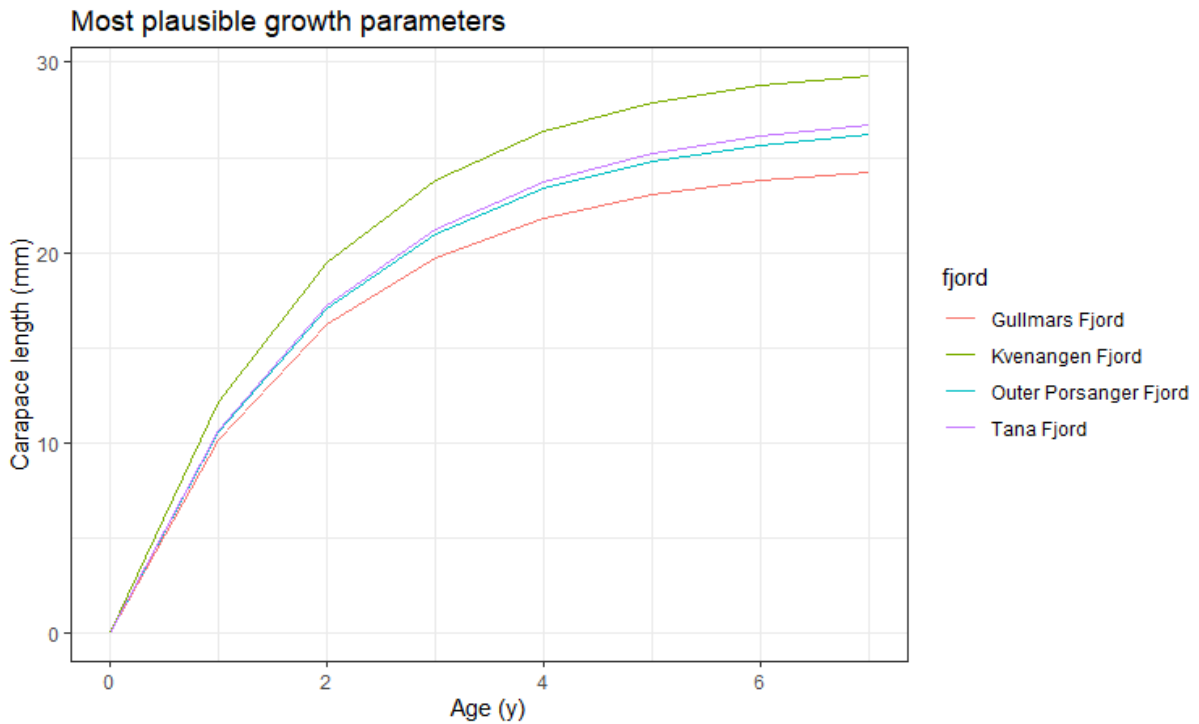


**Figure 3.13.** von Bertalanffy growth curves (equation 4) from each fjord site resulting from the “most plausible growth parameters” (Table 3.2).

### 3.3 MORTALITY

As the missing modal peaks in the LFQ distributions in the Inner Porsanger Fjord led to difficulties when estimating growth parameters, and the results were considered unreliable, mortality was not estimated for this specific fjord site. The estimated growth parameters from Scenario 2 gave poorly fitted growth curves for the Outer Porsanger Fjord. It was therefore decided to estimate total mortality rates based on growth parameters from all three scenario runs (2-4) for all fjord sites (Table 3.1), despite that Approach 2 (Scenarios 3 and 4) initially was conducted only in order to compare growth rates between the different fjord sites. As all fjord sites revealed non-linear patterns in the descending part of the catch curve, the regression line was split into two intervals, resulting in two mortality estimates.

All scenarios revealed a higher total mortality for younger shrimp ( $Z_y$ ) than for older shrimp ( $Z_o$ ) for all fjord sites (Table 3.3, Figs. 3.14, 3.15, 3.16). Total mortality rates ranged between 0.62-1.05  $y^{-1}$  and 0.57-1.01  $y^{-1}$  for younger and older shrimp, respectively (Table 3.3). For the Outer Porsanger and Tana Fjords all mortality was assumed to be due to natural causes, and total mortality estimates are thus interpreted as natural mortality (Table 3.4). For the Gullmars and Kvænangen Fjords, estimates of fishing mortality based on the cumulated catches and

biomass estimates from the surveys, revealed values of  $F$  of  $0.19 \text{ y}^{-1}$  and  $0.63 \text{ y}^{-1}$ , respectively. The estimated  $F$ s were assumed to be valid for all length groups fully recruited to the fishery and were thus subtracted from both  $Z_Y$  and  $Z_O$  (Table 3.4). The estimated natural mortality rates ranged between  $0.39\text{-}1.0 \text{ y}^{-1}$  and  $0.11\text{-}0.81 \text{ y}^{-1}$  for younger ( $M_Y$ ) and older ( $M_O$ ) shrimp, respectively (Table. 3.4).

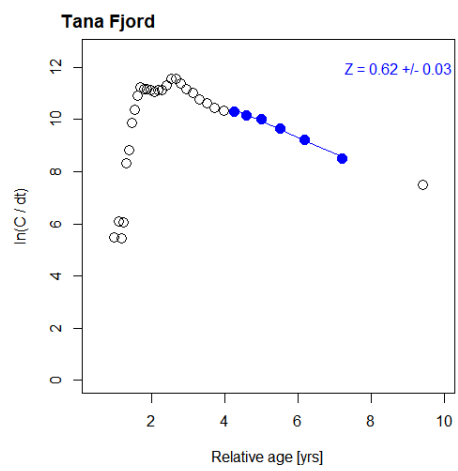
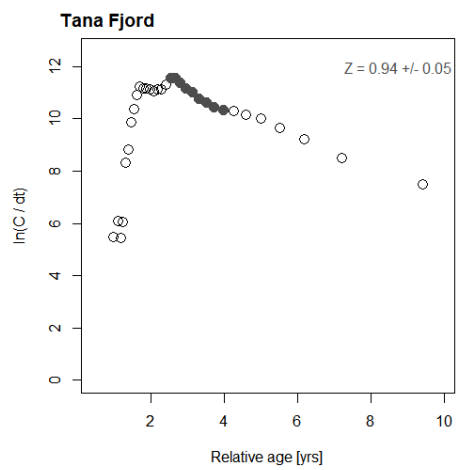
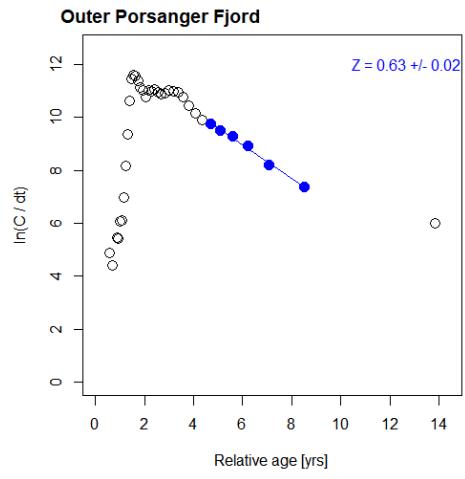
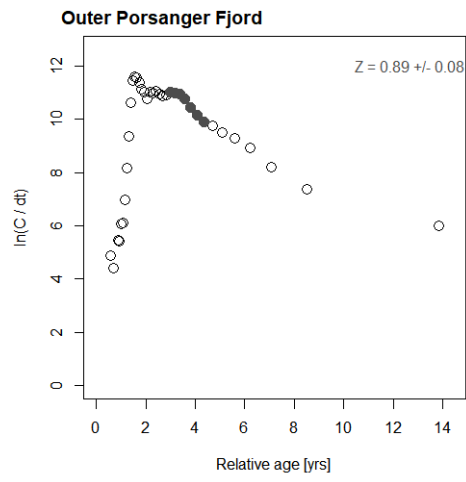
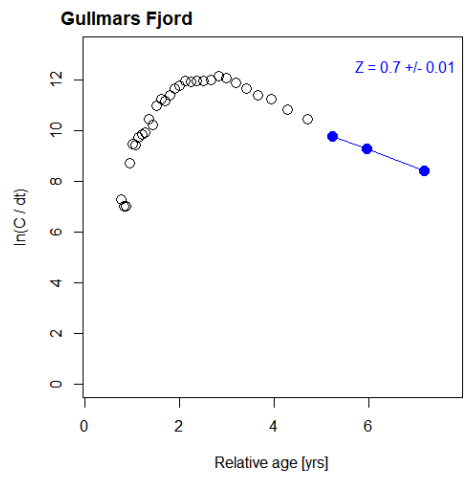
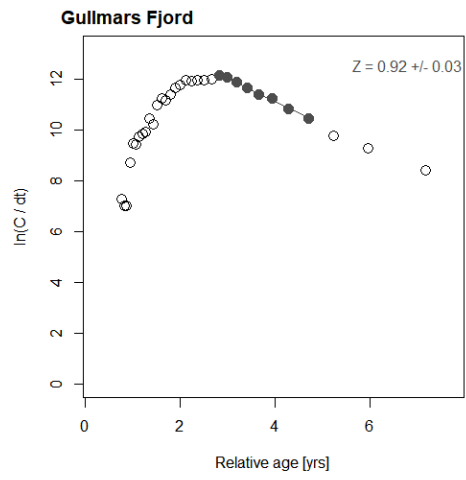
The mortality estimates which will be further addressed (Tables 3.3, 3.4) are the ones based on the most plausible growth parameters (see above, section 3.2.4). The highest total mortality rate was estimated for the fished Kvænangen Fjord for both younger and older shrimp (Table 3.3).  $M_Y$  was lowest in the Kvænangen Fjord and highest in the Tana Fjord, and  $M_O$  was lowest in the Kvænangen Fjord and highest in the Outer Porsanger Fjord (Table 3.4). Despite that there was estimated a fishing mortality in the Gullmars Fjord, initially thought to be unfished, the fjord site will still be addressed as “an unfished fjord site” in this present study, as there was not an on-going commercial shrimp trawl fishery in the fjord in the study period, such as in the Kvænangen.

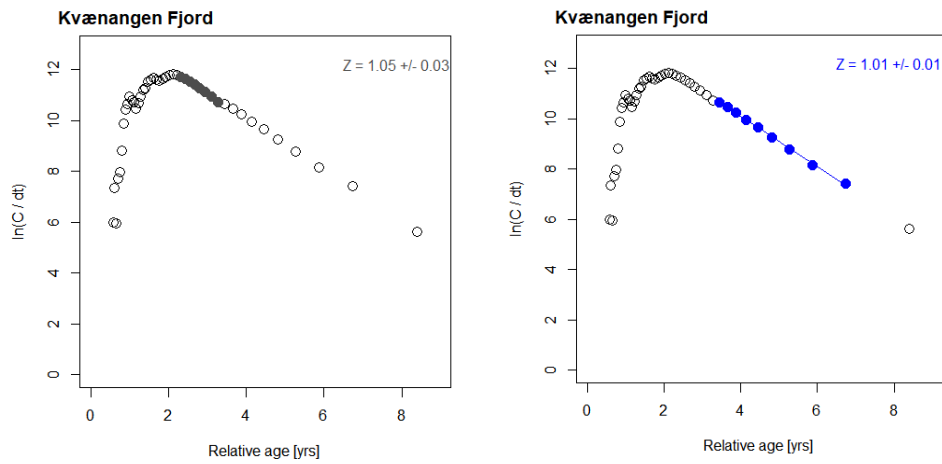
**Table 3.3** Estimated total mortality ( $Z \text{ y}^{-1} \pm 95\% \text{ CI}$ ) for the Gullmars, Tana, Outer Porsanger and Kvænangen Fjords.  $Z_Y$ : younger shrimp,  $Z_O$ : older shrimp. Bold values are those yielded from the “most plausible growth parameters” (Table 3.2).

	Scenario 2		Scenario 3		Scenario 4	
	$Z_Y$	$Z_O$	$Z_Y$	$Z_O$	$Z_Y$	$Z_O$
Gullmars Fjord	<b><math>0.92 \pm 0.03</math></b>	<b><math>0.70 \pm 0.01</math></b>	$0.78 \pm 0.04$	$0.70 \pm 0.01$	$1.04 \pm 0.06$	$0.93 \pm 0.02$
Outer Porsanger Fjord	$0.89 \pm 0.08$	$0.63 \pm 0.02$	<b><math>0.83 \pm 0.05</math></b>	<b><math>0.81 \pm 0.04</math></b>		
Tana Fjord	<b><math>0.94 \pm 0.05</math></b>	<b><math>0.62 \pm 0.03</math></b>	$1.00 \pm 0.06$	$0.57 \pm 0.03$		
Kvænangen Fjord	<b><math>1.05 \pm 0.03</math></b>	<b><math>1.01 \pm 0.01</math></b>	$1.02 \pm 0.02$	$0.74 \pm 0.04$		

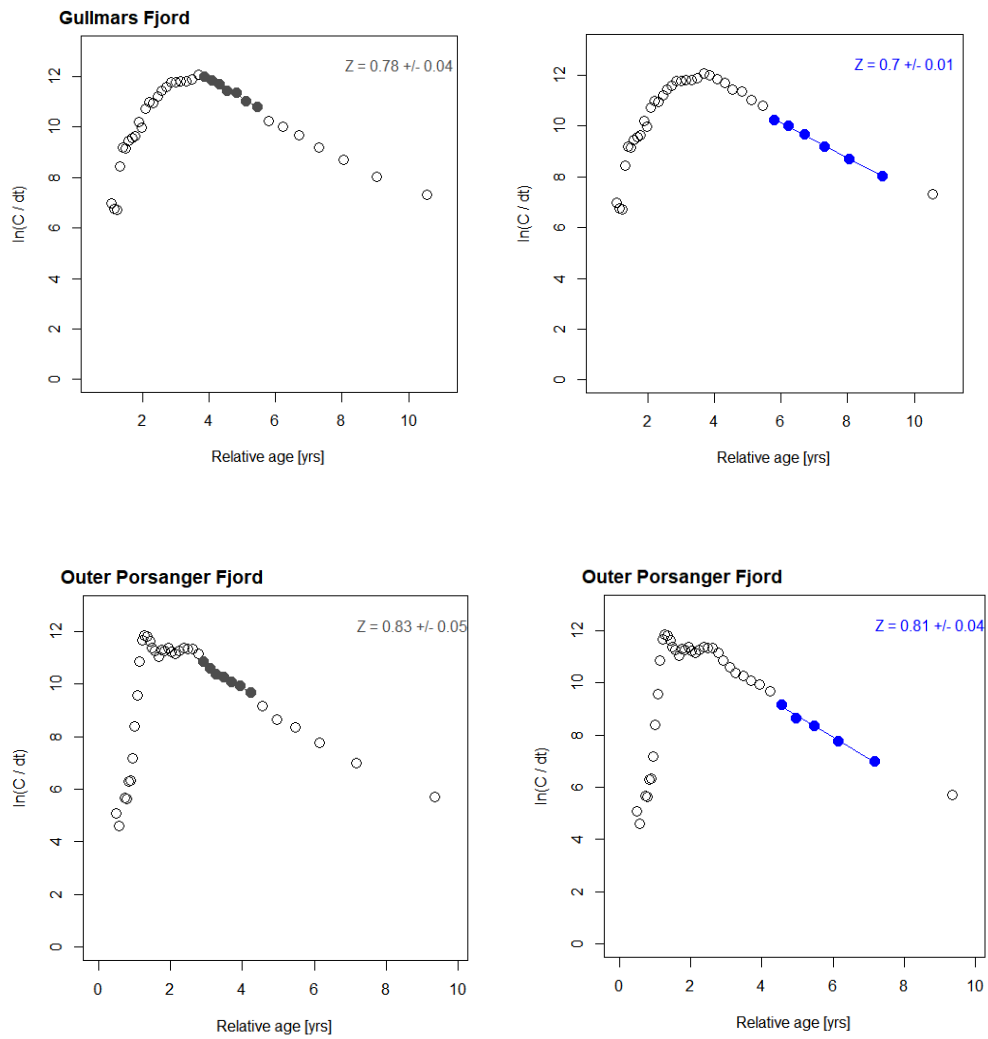
**Table 3.4.** Estimated natural mortality ( $M \text{ y}^{-1} \pm 95\% \text{ CI}$ ) for the Gullmars, Tana Outer Porsanger and Kvænangen Fjords from scenario 2, 3 and 4.  $M_Y$ : younger shrimp,  $M_O$ : older shrimp. Bold values are those based on the “most plausible growth parameters” (Table. 3.2).

	Scenario 2		Scenario 3		Scenario 4	
	$M_Y$	$M_O$	$M_Y$	$M_O$	$M_Y$	$M_O$
Gullmars Fjord	<b><math>0.73 \pm 0.03</math></b>	<b><math>0.51 \pm 0.01</math></b>	$0.59 \pm 0.04$	$0.51 \pm 0.01$	$0.85 \pm 0.06$	$0.74 \pm 0.02$
Outer Porsanger Fjord	$0.89 \pm 0.08$	$0.63 \pm 0.02$	<b><math>0.83 \pm 0.05</math></b>	<b><math>0.81 \pm 0.04</math></b>		
Tana Fjord	<b><math>0.94 \pm 0.05</math></b>	<b><math>0.62 \pm 0.03</math></b>	$1.00 \pm 0.06$	$0.57 \pm 0.03$		
Kvænangen Fjord	<b><math>0.42 \pm 0.03</math></b>	<b><math>0.38 \pm 0.01</math></b>	$0.39 \pm 0.02$	$0.11 \pm 0.04$		





**Figure 3.14.** Scenario 2: Estimated total mortality for younger ( $Z_Y$ ), grey plot and older ( $Z_O$ ), blue plot, shrimp at all fjord sites. ( $Z \pm 95\%$  CI)).



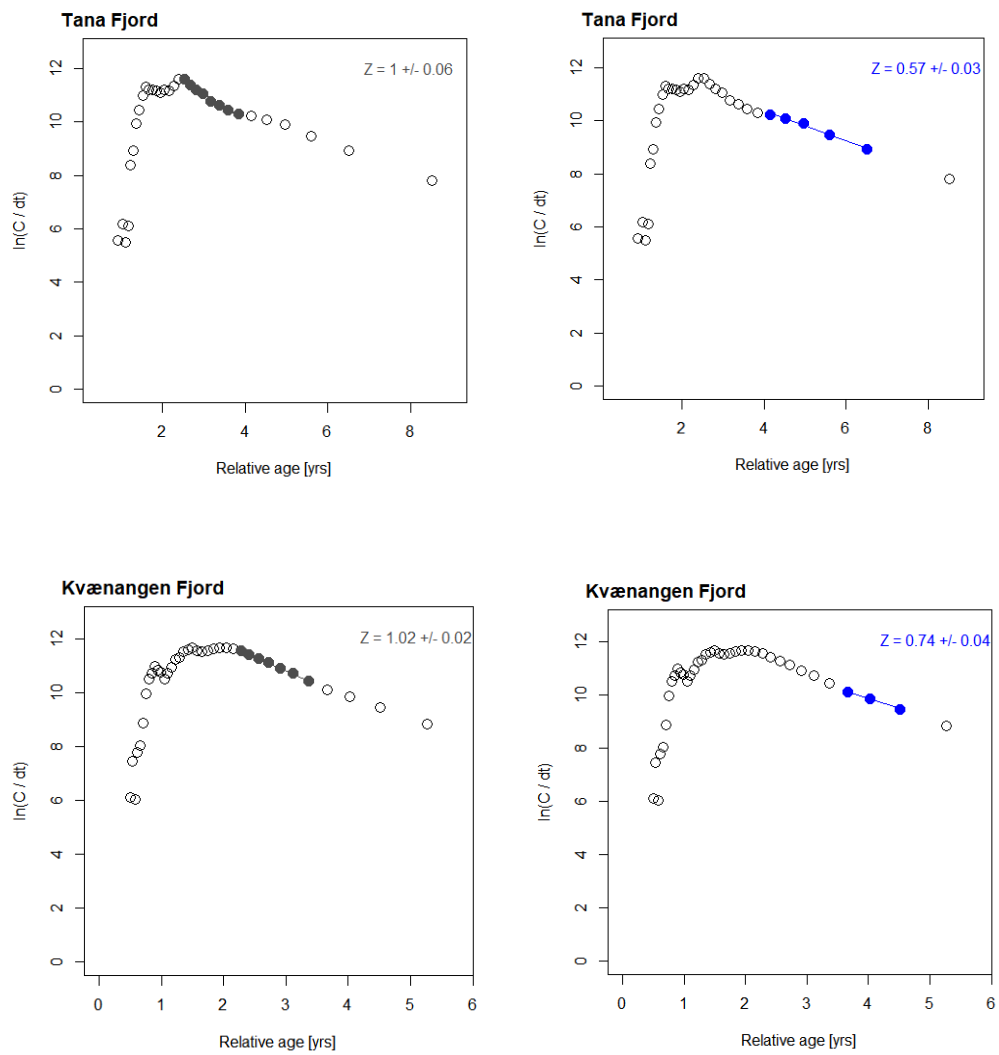


**Figure 3.15.** Scenario 3: Estimated total mortality for younger ( $Z_Y$ ), grey plot, and older ( $Z_O$ ), blue plot, shrimp at all fjord sites ( $Z \pm 95\%$  CI).

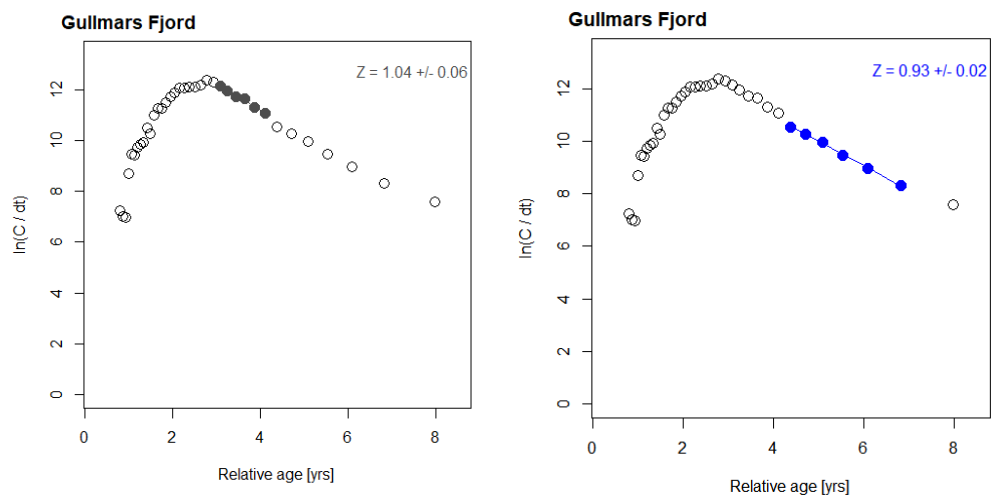


**Figure 3.16.** Scenario 4: Estimated total mortality for younger ( $Z_Y$ ), grey plot, and older ( $Z_O$ ), blue plot, shrimp ( $Z \pm 95\%$  CI) in the Gullmars Fjord.

### 3.4 BOTTOM TEMPERATURE

Monthly mean bottom temperatures in the Gullmars Fjord in 1998 ranged from 6.3 to 9.1 °C (Table 3.5) with an annual mean of 6.9 ( $\pm$  0.8) °C. Temperatures remained relatively stable between January and October, with elevated values at the end of the year. Mean bottom temperatures in the Norwegian fjord sites ranged during autumn 2018 from 4.3 °C in the Inner Porsanger Fjord to 7.5 °C in the Tana Fjord (Table 3.6). During spring 2019 temperatures ranged from -0.5 °C in the Inner Porsanger Fjord, to 5.0 °C in the Kvænangen Fjord, and from 1.5 to 6.2 °C during autumn 2019 (same fjord sites) (Table 3.6). Bottom temperatures were somewhat higher during autumn 2018 compared to autumn 2019 (Table 3.6, Fig. 3.17).

**Table 3.5.** Monthly mean bottom temperatures (°C) in the middle of the Gullmars Fjord (N58°19.40, E11°32.80) during 1998. The lacking SD for some months is due to only one conducted measurement.

Month	Temperature (°C)	
	Mean	SD
January	6.3	-
February	6.7	-
March	6.9	0.0
April	6.8	0.1
May	6.6	-
June	6.5	0.0
August	6.4	-
September	6.4	-
October	6.4	-
November	9.1	-
December	8.7	-

**Table 3.6.** Mean bottom temperatures (°C) from the Norwegian fjord sites. Bottom temperatures in autumn 2018 were measured using temperature loggers attached to only shrimp traps. For spring 2019 bottom temperatures were measured using temperature loggers attached to both shrimp traps and the trawl, whereas autumn 2019 bottom temperatures were measured using temperature loggers attached only to the trawl.

	Temperature (°C) autumn 2018		Temperature (°C) spring 2019		Temperature (°C) autumn 2019		Annual mean temperature (°C)	
	Mean	SD	Mean	SD	Mean	SD	Mean	SD
Outer Porsanger Fjord	7.0	1.2	2.5	1.4	5.5	0.8	4.0	2.2
Inner Porsanger Fjord	4.3	3.7	-0.5	0.2	1.5	0.1	2.9	3.5
Tana Fjord	7.5	0.9	4.7	1.3	5.4	0.3	5.4	1.4
Kvænangen Fjord	7.0	1.6	5.0	1.0	6.2	1.0	5.7	1.1

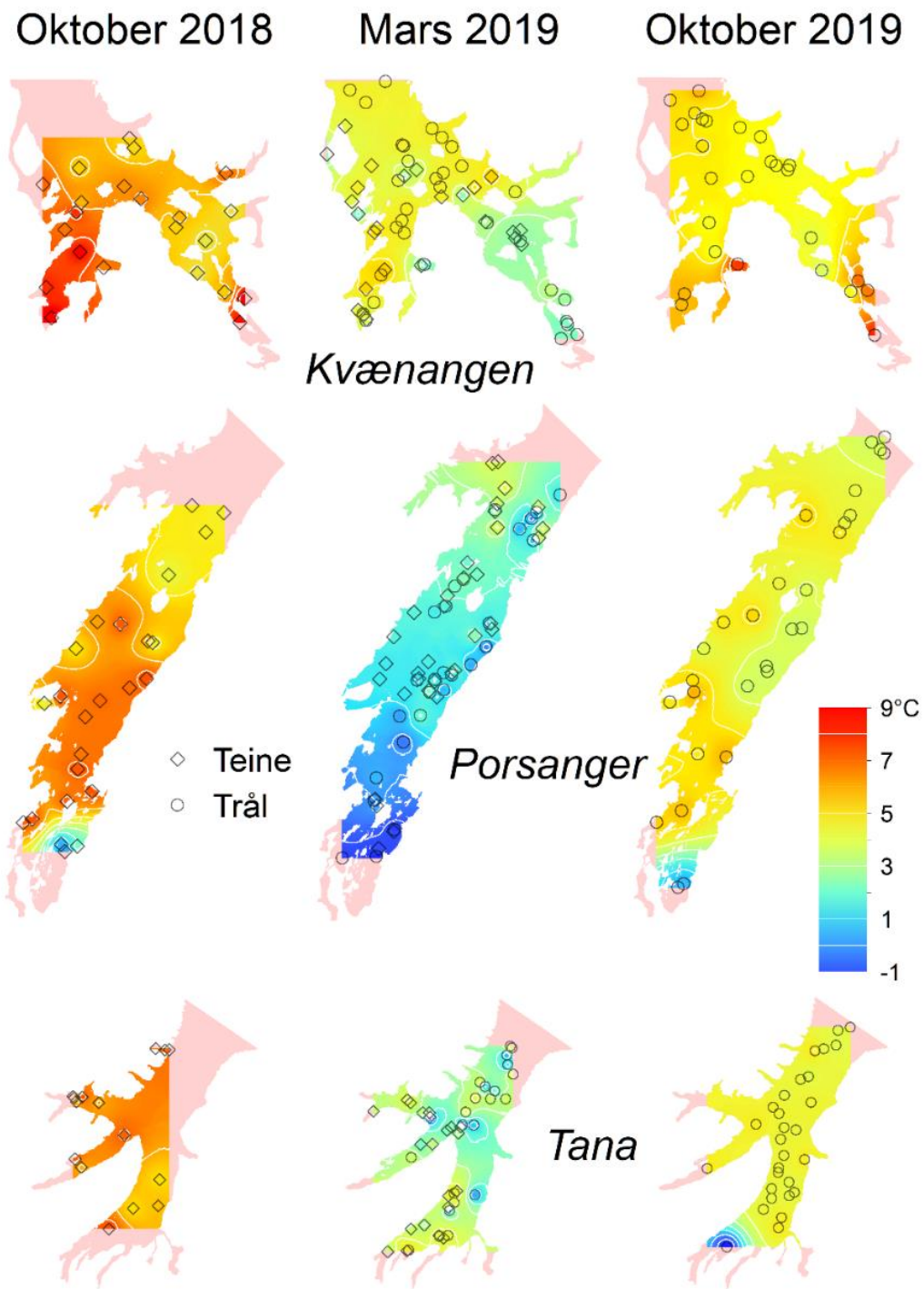


**Figure 3.17.** Bottom temperature in the Porsanger, Tana and Kvænangen Fjords of northern Norway. The circles indicate bottom temperatures measured during trawling, whereas the squares indicate temperatures measured using shrimp traps. Map made by Trude H. Thangstad, Norwegian Institute of Marine Research, 2019.

### 3.5 SHRIMP DENSITY

Shrimp density in the Inner Porsanger Fjord was remarkably higher compared to that of all the other fjord sites, with densities of approximately 22, 32 and 20 tonnes/km<sup>2</sup> for autumn 2018, spring 2019 and autumn 2019, respectively. However, as growth and mortality in the Inner Porsanger Fjord are not addressed, for the ease of comparison, values were excluded from Fig. 3.18. When comparing for the other study sites, calculated shrimp densities were highest in the Kvænangen Fjord, except during spring 2019 (Fig. 3.18). For the Gullmars Fjord, the density was remarkably lower compared to that of all the other fjord sites.

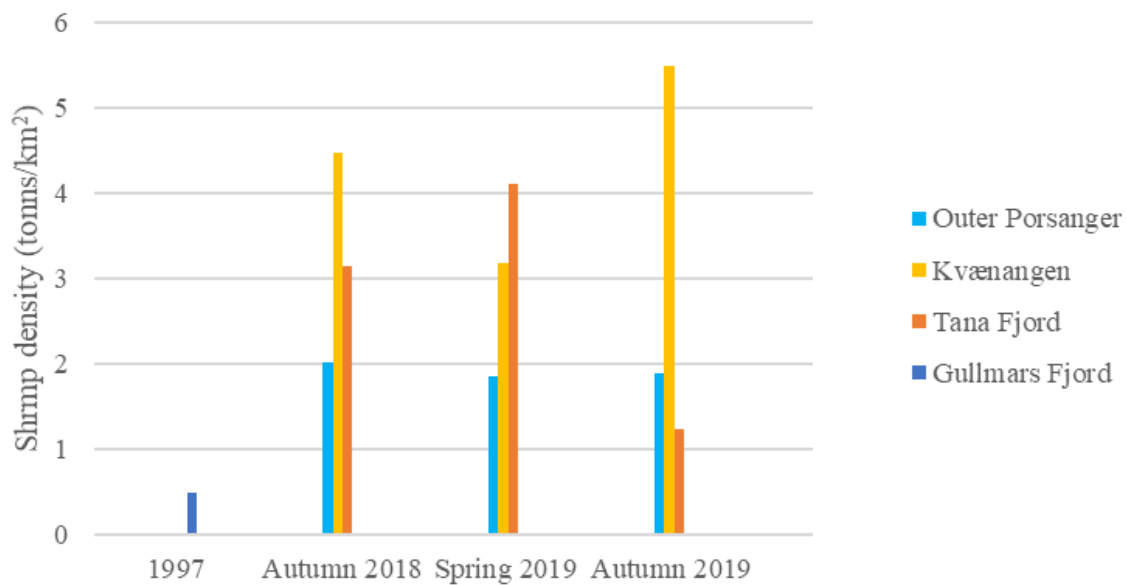


**Figure 3.18.** Shrimp density per km<sup>2</sup> per fjord study site and survey.

## 4 DISCUSSION

Estimated values for  $L_{\infty}$ ,  $K$  and  $t_{anchor}$  from the “most plausible growth parameters” ranged from 24.8-30.1 mm, 0.50-0.53  $y^{-1}$  and 0.09-0.38, respectively (Table 3.2). When comparing between fjord sites, the estimated growth was lowest in the Gullmars Fjord, followed by the Outer Porsanger, Tana and Kvænangen Fjords (Table 3.2, Fig. 3.13). A lower growth in the Gullmars Fjord compared to the fjord sites of northern Norway was unexpected, given the often observed negative relationship between growth and latitude (see section 1.3). Estimated total mortality revealed a decreasing mortality with age for all study sites (Table 3.3). The estimated natural mortality rates based on the “most plausible growth parameters” ranged between 0.42-0.94  $y^{-1}$  and 0.38-0.81  $y^{-1}$  for younger ( $M_Y$ ) and older ( $M_O$ ) shrimp, respectively (Table 3.4). Natural mortality rates were lowest in the Kvænangen Fjord, followed by the Gullmars, Outer Porsanger and Tana Fjords, for younger shrimp (Table 3.4). Given the lower bottom temperatures at higher latitudes, natural mortality was expected to be lower in northern Norway compared to that in the Gullmars Fjord, which was only the case for the Kvænangen Fjord (Table 3.4).

### 4.1 LENGTH FREQUENCY DISTRIBUTIONS

The shrimp stocks from all the study sites had size distributions with distinct modal peaks, except for the Inner Porsanger Fjord (Fig. 3.1). The number of trawl hauls conducted here, and the number of shrimps collected were much lower than for the other fjord sites (Tables 2.2, 2.3). This was probably one of the reasons why modal peaks were absent. Another explanation may be slow growth. In colder areas such as the Barents Sea, distinct modal peaks are often absent in LFQ distributions due to slow growth, and stocks are assessed based on biomass models rather than length-based models (ICES, 2019). The mean bottom temperature in the Inner Porsanger Fjord was indeed very low, resembling high arctic conditions (Fig. 3.17).

The extra modal peak in the 2018 LFQ distribution in the Outer Porsanger Fjord, compared to that of the following year can likely be explained by individual growth variation. For northern shrimp, larger males are known to undergo the transformation into females first, followed by an accelerated rate of growth in the subsequent months, while shrimp with delayed sex change may be restricted in their growth (Rasmussen, 1953; Shumway *et al.*, 1985). As such, individuals of the same cohort can consist of two distinct size groups, with one group of small males and another of larger females, which is likely the case for the Outer Porsanger Fjord.

The lack of 0-groups in the LFQ distributions (Fig. 3.1) for all fjord sites might be due to juveniles remaining on shallow grounds until the end of their first year (Hjort and Ruud, 1938; Shumway *et al.*, 1985). For all fjord sites, shrimp first appeared in the trawl catches during spring, though a distinct modal peak was only evident for the Kvænangen Fjord (Fig. 3.1). For the Gullmars Fjord, the small number of 1-group specimens caught may be explained partly by the selectivity (larger mesh size) of the trawl. For the Porsanger and Tana Fjords on the other hand, gear selectivity is not a plausible explanation for the lack of small individuals given the evident 1-group in the Kvænangen Fjord, for which the same trawl was used. This may indicate that the surveys did not cover all possible shrimp habitat in the fjords. Studies on northern shrimp in the Gulf of Maine have reported juveniles remaining on in-shore grounds for a year or more before migrating to deeper waters (Clark *et al.*, 2000). Similar observations have been made for the Norwegian Deep and Skagerrak population, where the smallest individuals (1-group) are mainly observed in Skagerrak, and only appear in the Norwegian Deep when they are larger (Søvik and Thangstad, 2020). As the location of juvenile grounds depends on local environmental conditions and bottom habitats (Shumway *et al.*, 1985), these areas' availability to trawling can be highly variable from fjord to fjord. The amount of time juveniles spend here can also vary between areas (Shumway *et al.*, 1985). Attention should also be paid to oceanographic features and possible interactions with shrimp grounds outside the fjords. Previous studies of the shrimp stock in the Gullmars Fjord detected immigration of both larvae and older shrimp, facilitated by the inflow of water masses from Skagerrak each spring (Svanesson, 1984; Bergström, 1992a). The strong outward and inward bottom and surface currents in the Tana and Porsanger Fjords (Figs. 2.3, 2.4) combined with no sill in the fjord mouths may facilitate both immigration and emigration of shrimp. Moreover, a recent study on the genetic structure of northern shrimp in fjord sites of northern Norway found that the Porsanger and Tana Fjords held a mix of coastal shrimp and Barents Sea shrimp, supporting the assumption of exchange of individuals with external areas (Hansen, 2020).

The disappearance of larger shrimp from the trawl catches in the Gullmars Fjord in February-June 97 was likely due to the migration of females to untrawlable shallow grounds, where they release their larvae (pers. com. Mats Ulmestrand, 2019). Similar observations have been made for other populations (Shumway *et al.*, 1985). However, the migration appears pro-longed, as the larger shrimp normally return to trawlable ground (and thus appear in the catches) in April (pers. com. Mats Ulmestrand, 2019).

## 4.2 GROWTH

The lower growth in the Gullmars Fjord was unexpected, given the often observed negative relationship between growth and latitude, where temperature is stated to be the main driver (Nilssen and Hopkins, 1991). As estimated mean bottom temperatures were higher in the Gullmars Fjord compared to that of the fjord sites of northern Norway (Tables 3.5, 3.6), the reasoning behind the hypothesis is supported. However, it should be noted that the bottom temperatures in the Gullmars Fjord were from 1998, the year after the study period, and as can be seen from the Norwegian study sites, temperatures can vary interannually (Table 3.6, Fig. 3.17). Nevertheless, several authors have reported on deviations from this latitudinal pattern, stating that temperature not necessarily is the main driver of life history variations in shrimp (Nilssen and Hopkins, 1991; Bergström, 1992b). Søvik and Thangstad (2020) have also reported on lower growth and smaller sized age groups in the Norwegian Deep compared to that of the Skagerrak, despite them living at more shallow and warmer grounds. Preliminary studies on growth by Hansson *et al.* (1997), based on the same data as in this present study, revealed a lower growth in the Gullmars Fjord during 1997, when the fjord had been closed for bottom trawling for six years, compared to the growth estimations conducted by (Bergström, 1992b) on the same population in the 1980s. These findings were stated to likely be due to intraspecific competition for resources as a result of the cease in bottom trawling (Hansson *et al.*, 1997). However, as estimated shrimp densities were very low compared with the other investigated fjord sites (Fig. 3.18), density dependent growth was likely not an issue.

Low levels of oxygen could have played a role in the low growth rates in the Gullmars Fjord. Decreasing growth and food conversion efficiency with declining O<sub>2</sub> content in the water have been recorded for several species of both fish and crustaceans (Green, 2009; Seidman and Lawrence, 2009; Adelman and Smith, 2011). As there was no renewal of water masses during spring 1997 (Hansson *et al.*, 1997) oxygen levels remained low throughout the year of the experiment (Fig. 2.2). Low oxygen levels during 1997 could thus have led to a poor growth season for the shrimp population this year. Whereas Svanesson (1984), cited in Hansson *et al.*, (1997), reported that no such cease in water renewal had been recorded earlier, oxygen levels during spring 95 were also lower (3-4 ml/l) compared to that of both spring 94 and 96 (5-6 ml/l) (Fig. 2.2). Repeated periods of low oxygen may serve as one explanation for the low growth in the Gullmars Fjord. Unfortunately, no oxygen measurements are available from the other investigated fjord sites for comparison. However, the strong bottom currents into the Tana and

Porsanger Fjords (Figs. 2.3, 2.4) likely facilitate renewal, and thus reoxygenation of the bottom water.

The growth patterns in the Kvænangen, Tana and Outer Porsanger Fjords seemingly follow a temperature trend, where higher temperatures correspond to higher growth, and vice versa (Fig. 3.13, Table 3.5). The growth in the fished Kvænangen Fjord stands out as much higher compared to that of the unfished Tana and Outer Porsanger Fjords. Exploited stocks may have a greater production/turnover rate, and thus growth, as the thinning of the population due to fishing can lead to less competition for food (Nilssen and Hopkins, 1991). However, the Kvænangen Fjord had a higher shrimp density than the other fjord sites, except for the Inner Porsanger Fjord, opposite of what was expected (Fig. 3.18). Interestingly, this is in accordance with statements from local fishermen that shrimp grounds need to be “plowed” in order to yield high catch rates. A possible explanation behind this observation could be that the trawling helps release nutrients from the bottom (Dounas *et al.*, 2005, 2007).

Growth estimates exist from the nearby Bals Fjord from 1976, located approximately 100 km south-west from the Kvænangen Fjord (Thomassen, 1976). At the time of the experiment from which growth was estimated, bottom temperatures remained below 3 °C throughout the year, except for briefly elevated temperatures at the end of the year (Thomassen, 1976). Plotted against the growth parameters for the investigated fjord sites of northern Norway, growth in the Bals Fjord appeared to be lower (Fig. 4.1). These findings are consistent with the expected lower growth in colder areas, and opposite (Shumway *et al.*, 1985; Nilssen and Hopkins, 1991).

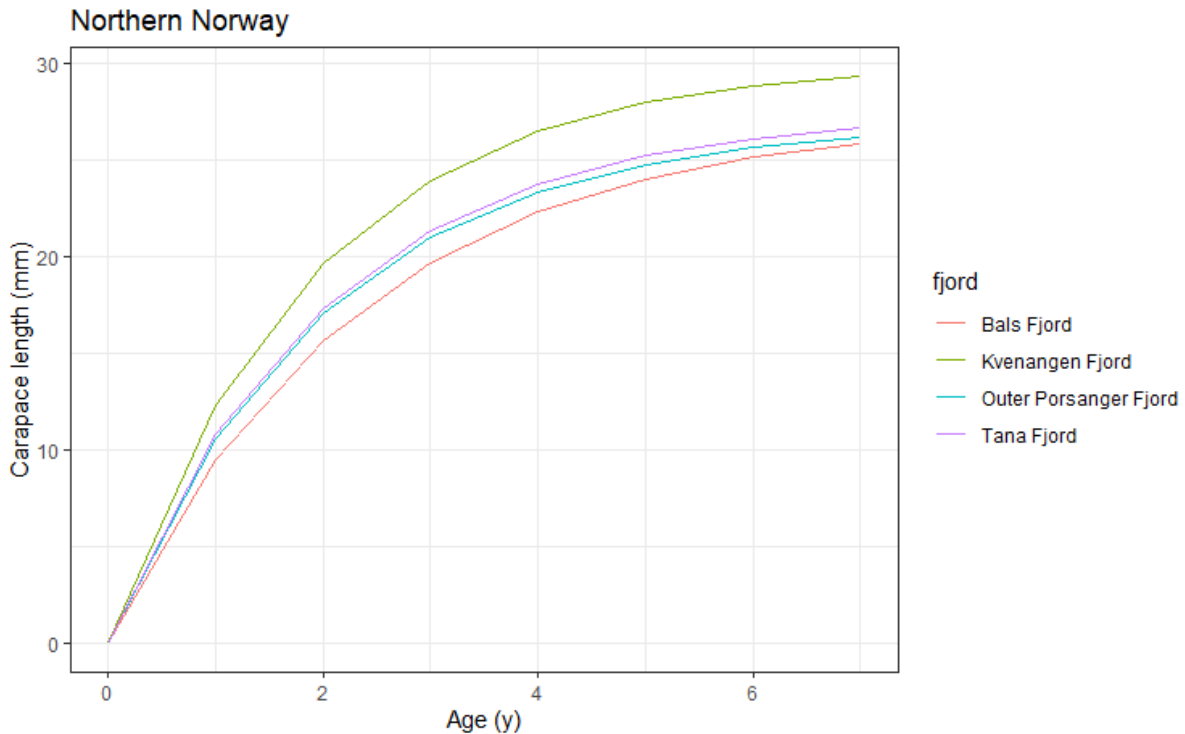


**Figure 4.1.** Growth curves (equation 4) yielded from growth parameters  $L_{\infty}$  (27.2 mm) and  $K$  (0.43) in the Bals Fjord (Thomassen, 1976) plotted against growth curves resulting from the most plausible growth parameters from the Tana, Outer Porsanger and Kvænangen Fjords (Table 3.2).

### 4.3 MORTALITY

It was hypothesized that the Gullmars Fjord would have a life history more similar to the NDSK shrimp (Nilssen and Hopkins, 1991) than the Barents Sea shrimp, and thus a more suitable  $M$  than the one presently applied (see above, section 1.3). It was thus expected that the estimated  $M$  of the Gullmars Fjord would be higher than the currently applied value in the NDSK stock assessment ( $0.75 \text{ y}^{-1}$ ). Further, it was hypothesized that values of  $M$  in the Gullmars Fjord would be higher compared to those of the other unfished fjords (see above, section 1.3). However, the results are opposite of what was expected, as both  $M_Y$  and  $M_O$  in the Gullmars Fjord are similar or lower than  $0.75 \text{ y}^{-1}$ , respectively, and as estimated natural mortality rates were higher for both younger and older shrimp in the more northern fjord sites, except for the fished Kvænangen Fjord (Table 3.4). However, given the low estimated growth for the Gullmars Fjord population, a lower natural mortality compared to the fjord sites with a higher estimated growth seems appropriate (Nilssen and Hopkins, 1991). Regardless, there are other factors than temperature and growth influencing the natural mortality of a stock, most notably predation levels (Simpfendorfer, Bonfil and Latour, 2005). Moreover, there are uncertainties related to both estimated total mortality as well as the fishing mortality, that naturally may have influenced the results (see below, section 4.4).

Natural mortality can vary, both spatially and temporarily, depending on the level of predators (Simpfendorfer, Bonfil and Latour, 2005). Consequently, the natural mortality estimates in the present study were influenced by the predation pressure at the time of sampling. In the Outer Porsanger, Tana and Kvænangen Fjords, gillnet-, longlines- and Danish seine fisheries are conducted throughout the year, targeting cod, haddock, halibut and cusk, several of which are predators of northern shrimp (Jørgensen *et al.*, 2014; Fiskeridirektoratet, 2020a). Hansson *et al.* (1997) reported on low biomasses of demersal fish (such as haddock and cod) in relation to what was expected from the fishery being closed for six years. At the time of the study period there were some fisheries using other gear types than trawling (pers. com. Mats Ulmestrand), however, no landings data exist. Whether the predation pressure was comparatively low in the Gullmars Fjord at the time of the study period is thus unfortunately not known.

The lower natural mortality for younger shrimp in the Outer Porsanger Fjord compared to that of the Tana Fjord (Table 3.4) seems appropriate given the lower growth yielded there (Table 3.2, Fig. 3.13), and the lower estimated temperature (Table 3.6). For older shrimp on the other hand, the results were opposite, where the Tana Fjord revealed a lower mortality (Table 3.4). Great uncertainties are associated with the age of large individuals, as the relationship between length and age becomes less certain as one approaches  $L_{oo}$ , where larger individuals may be bigger due to faster growth, not necessarily because they are older (Sparre and Venema, 1998). As such, estimating and comparing mortality for younger shrimp are by far more reliable compared to that for older ones. Moreover, the estimated natural mortality rates of the Porsanger Fjord were based on growth parameters yielded by Approach 2 (Scenario 3) with a fixed  $L_{oo}$ , despite that this approach initially was used for comparing growth between fjord sites only. When comparing between Scenario 2 and 3 for the Kvænangen Fjord,  $M_Y$  remained similar between the two scenarios, whereas  $M_O$  estimated from Scenario 3 growth parameters yielded a lower mortality compared to that of Scenario 2 (Table 3.4, Figs. 3.14, 3.15). Thus, fixing the  $L_{oo}$  may to some extent influence the mortality estimates, likely more so for older individuals in fjord sites with a much higher/lower estimated  $L_{oo}$ -value, such as for the Kvænangen Fjord (Table 3.1). Estimated mortality rates for the Outer Porsanger Fjord should thus be considered for further application with caution, especially for larger shrimp.

The lowest estimated natural mortality rate was found for the Kvænangen Fjord (Table 3.4), regardless of its fast growth (Table 3.2, Fig. 3.13). Whereas the total mortality estimates were relatively similar when compared to the unfished fjord sites (Table 3.3), the natural mortality estimate was much lower (Table 3.4). The results are interesting, in that it seems as  $Z$  does not

increase proportionally with an increasing  $F$ .  $F$  and  $M$  are not necessarily independent of each other, as  $F$  can lead to a thinning of the population of shrimp (Nilssen and Hopkins, 1991), and the bottom trawling itself can remove shrimp predators. However, as the commercial shrimp trawlers applied in the Kvænangen Fjord are equipped with a fish sorting grid, the commercial shrimp trawling in itself does not contribute in removing demersal fish. Fishing with other types of gear on the other hand, can contribute to lowering the predation density and thus lowering the natural mortality. There are, of course, much uncertainty related to the estimated  $F$ , which will be further discussed in section 4.4.

#### 4.4 LIMITATIONS OF STUDY

A condition for reliable length-based growth and mortality estimations is obtaining unbiased length frequency data. Bias in the collected length data can occur due to species behaviour, such as migration and schooling, or gear selectivity (Hilborn and Walters, 1992; Sparre and Venema, 1998). The length frequency data in the present study were sampled from two different experimental research surveys (see above, section 2.2), with quite different aims. The survey design in northern Norway was based on stratified random sampling, aiming to cover all trawlable shrimp grounds in the fjords. Conversely, the experimental research project in the Gullmars Fjord did not attempt to randomize the trawling in any way, as only a small part of the fjord (T1-T3) was trawled, repeatedly. As the abundance and distribution of shrimp can vary inside fjords i.e. due to migration (see above, section 4.1), the constrained trawling in the Gullmars Fjord may have resulted in data which is not representative of the whole fjord population. Additionally, the trawl gears differed, where the Norwegian survey used a trawl with 15 mm meshes in the cod end, whereas the Swedish survey used a commercial trawl with 38 mm meshes. The larger meshes of the trawl applied in the Gullmars Fjord likely introduced a higher selectivity of smaller shrimp to a larger extent than in the Norwegian fjord sites (see above, section 4.1).

Taylor (2020) highlights the importance of the data covering the smaller length classes when applying ELEFAN analyses. However, very few small individuals were sampled for all fjord sites, except for in the Kvænangen Fjord (see above, section 4.1) (Fig. 3.1). Further, Taylor (2020) suggests that the smallest bins should start at least 25 % of  $L_{\infty}$ . This was not fulfilled for any of the fjord sites, except for the Porsanger Fjord (Appendix 1, Tables A1-5). Accounting for selectivity in the data could to some extent increase the reliability of the data.

The linearized catch curve analysis assumes that the decrease in observed numbers of individuals across the age-structure of the population is the result only of mortality (Sparre and Venema, 1998; Simpfendorfer, Bonfil and Latour, 2005). Thus, the migration events in the Gullmars Fjord (see above, section 4.1) (Fig. 3.1) may to some extent have influenced the mortality estimates. Early in the work of the present study it was considered to exclude the months where migration was evident. However, as growth and mortality can be highly variable over the year (Bergström, 1992a; Sparre and Venema, 1998), estimations based on a pseudo-cohort over the whole year was thought to introduce less biases than excluding parts of the dataset. Consequently, all samples were included in the analyses.

Another main underlying assumption when estimating both growth and mortality is a constant parameter system, assuming the pseudo-cohort of which the estimates are based on are representative of the whole population (Sparre and Venema, 1998). Of course, the reality is more complex than the assumptions behind the models. Consequently, the results are highly dependent on e.g. the structure of the stock at the time of which the data were sampled (Sparre and Venema, 1998). Earlier studies on growth and recruitment in the Gullmars Fjord reported on the importance of immigration in sustaining the stock (Bergström, 1991, 1992a). Further, immigration was found to vary from year to year, supported by Hansson *et al.* (1997), reporting on no clear event of water renewal during the experiment in 1997. Thus, recruitment to the stock in the Gullmars Fjord is likely variable. Large between-year variations in recruitment have also been found for shrimp stocks in the North-Atlantic (ICES, 2019). These year-to-year variations in recruitment, which are likely true for all the studied fjord sites, influence the structure of the stocks, and consequently also the results in this present study.

Both the ELEFAN analysis and the linearized length converted catch curve analysis are based on a series of subjective choices, which naturally introduce uncertainties in the results, especially with respect to reproducibility. The moving averages (MAs) for the different fjord sites were visually determined (see above, section 2.6.2.2), where the varying width of the modal peaks left some room for interpretation (Fig. 3.1). Recent studies on bin size selection for the ELEFAN analysis in the TropFishR library found that species with large individual growth variability are sensitive to changes in bin size (Wang *et al.*, 2020), and further may increase the estimation biases of the VBGF parameters (Isaac, 1990). The hermaphroditic nature of northern shrimp and the boost in growth some individuals experience (Rasmussen, 1953; Shumway *et al.*, 1985), may cause a larger growth variability than for other species.

The greatest uncertainties related to mortality estimates from the catch curve analysis is the subjective selection of which data points should be included in the descending regression line (Sparre and Venema, 1998; Simpfendorfer, Bonfil and Latour, 2005). When selecting the data points to be included in the regression lines, it was aimed to select those forming a straight line. Whereas some of the catch curves formed an almost perfectly shaped dome, such as the Gullmars and Kvænangen Fjords, an additional peak appeared in the left part of the catch curve for the Tana and Porsanger Fjords (Figs. 3.13, 3.14, 3.15). Further, some catch curves revealed two distinct linear regression lines with different slopes, whereas for others it was not as obvious which data points should be included in each of the regression lines (Figs. 3.13, 3.14, 3.15).

No uncertainties around the separate estimates of fishing mortality were quantified. However, there are, of course, uncertainties related to these calculations (section 2.5). Whereas the total catch in the Gullmars Fjord from the study period are assumed to contain all landed shrimp, the official commercial landings in the Kvænangen Fjord has no discard estimates available and may thus be underestimated. Furthermore, there are uncertainties related to the biomass from which  $F$  is estimated. Total estimated biomass is assumed to equal all shrimp on the trawled ground. However, as the selectivity of the trawl can exclude smaller shrimp from the catches, shrimp density, and thus biomass, is probably underestimated. Shrimp conducting vertical migrations in the water column are naturally not caught by the trawl either (Hudon, Parsons and Crawford, 1992). Moreover, the estimated biomass itself depends on the estimated areas assumed to contain shrimp in each fjord. For the Gullmars Fjord, much uncertainty is related to the area estimate, as all areas below 60 m were assumed to contain shrimp. For the fjord sites of northern Norway, shrimp ground areas were decided based on known shrimp grounds as well as bathymetric maps and are thus considered more accurate in comparison. However, as the delimitations of the shrimp ground areas are still work in progress, all estimates are preliminary. Both underestimates of biomass and total catch will lead to an overestimation of  $F$ , and consequently, both  $M_Y$  and  $M_O$  might actually be higher for both fjords. Thus, the true natural mortality rates for younger and older shrimp for these specific fjord sites likely fall between  $M_Y$  and  $Z_Y$  and  $M_O$  and  $Z_O$  (Tables 3.3, 3.4), respectively.

Another aspect to consider is how applicable the analyses applied actually are. Nilssen and Hopkins (1991) states that there is a possibility that the VBGF not necessarily is fully applicable in describing discontinuous growth, such as for moulting shrimp, and that comparisons of the parameters on an inter-stock basis need to be conducted with caution. It needs to be emphasised

that the estimated values in this thesis are not tested for statistically significant differences, and comparisons have been discussed based on trends in the results only.

## 4.5 FURTHER IMPLICATIONS OF RESULTS

### 4.5.1 ECOPATH MODEL IN NORTHERN NORWAY

The Norwegian Institute of Marine Research has been asked by the Directorate of Fisheries to advice on whether the two unfished fjords in northern Norway should be re-opened for shrimp trawl fishery. Results from an ECOPATH (ecosystem) model will support the advice. The values of  $M$  estimated for the shrimp stocks in the Tana and Porsanger Fjords will serve as input in the respective ECOPATH/ECOISM models that will be built and run for the different fjord ecosystems. Natural mortality estimates from the Outer Porsanger Fjord should, however, be considered with caution, especially for larger shrimp, as these were calculated based on growth parameters estimated for a different purpose (see above, section 4.3).

### 4.5.2 NDSK STOCK ASSESSMENT

Estimating a more accurate and reliable value for  $M$  has long been on the list of topics to be explored for the NDSK shrimp stock and has been requested for the up-coming ICES benchmark of this stock in 2021. The estimated natural mortality rates from the Gullmars Fjord were lower than expected. Båtevik *et al.* (2020) who estimated an even lower  $M$  ( $0.54 \text{ y}^{-1}$ ) from the same data set, though only from the December 1996 sample, suggested that the estimated value may serve as a baseline to which a predation index can be added. Several attempts on quantifying the influence of predation pressure on  $M$  have been conducted, but have not succeeded in improving the fit of the model (Jørgensen *et al.*, 2014; Skorda, 2018). The low natural mortality was probably a result of the low growth yielded at this specific fjord site. Consequently, natural mortality rates should be considered with caution for extrapolations to other areas.

## 5 CONCLUSIONS

- Among the unfished fjord sites (the Gullmars, Outer Porsanger and Tana Fjords), estimated natural mortality rates for younger and older shrimp ranged from 0.73-0.94  $y^{-1}$  and 0.51-0.81  $y^{-1}$ , respectively.
- Latitudinal trends did not accurately predict patterns of growth and natural mortality among the studied fjord sites. Among the unfished fjord sites the slowest growth and lowest natural mortality rates were found for the Gullmars Fjord, the southernmost and warmest study site, likely explained by low levels of oxygen during the study period. However, as the fishing pressure from which the natural mortality rates in the Gullmars Fjord are estimated might be underestimated, the true natural mortality for younger and older shrimp likely fall somewhere in between the estimated values for  $M_Y$  and  $Z_Y$  and  $M_O$  and  $Z_O$  for this fjord site, respectively.
- Given the low growth yielded in the Gullmars Fjord, estimated natural mortality rates should be considered with caution for extrapolations to other areas.
- Among the unfished fjord sites of northern Norway (the Tana and Outer Porsanger Fjords), growth and natural mortality seemingly follow a temperature pattern, where the warmer Tana Fjord, relative to that of the Outer Porsanger Fjord, gave a faster growth, as well as a higher natural mortality for younger shrimp. However, as natural mortality rates in the Outer Porsanger Fjord were calculated based on growth parameters initially estimated for the purpose of comparing growth between fjord sites only, they should be considered for further assessment with caution.
- The results from the fished Kvænangen Fjord are unexpected, in that the estimated total mortality are at levels similar to those of the natural mortality of the other fjord sites, whereas the estimated natural mortality for this specific fjord site is much lower. It thus seems that total mortality does not increase proportionally with fishing pressure. However, similarly as for the Gullmars Fjord, the estimated fishing pressure in the Kvænangen Fjord might be underestimated, and the true natural mortality for younger and older shrimp likely fall somewhere in between the estimated values for  $M_Y$  and  $Z_Y$  and  $M_O$  and  $Z_O$  for this fjord site, respectively.

## 6 REFERENCES

- Aanes, S. *et al.* (2007) 'Estimation of the parameters of fish stock dynamics from catch-at-age data and indices of abundance: Can natural and fishing mortality be separated?', *Canadian Journal of Fisheries and Aquatic Sciences*, 64(8), pp. 1130–1142. doi: 10.1139/F07-074.
- Adelman, I. R. and Smith, L. L. (2011) 'Effect of Oxygen on Growth and Food Conversion Efficiency of Northern Pike', *The Progressive Fish-Culturist*. Taylor & Francis Group, 32(2), pp. 93–96. doi: 10.1577/1548-8640(1970)32[93:EOOOGA]2.0.CO;2.
- Asplin, L. *et al.* (2020) 'The hydrodynamic foundation for salmon lice dispersion modeling along the Norwegian coast', *Ocean Dynamics*. Springer Science and Business Media LLC, pp. 1–17. doi: 10.1007/s10236-020-01378-0.
- Båtevik, T. *et al.* (2020) *Estimating natural mortality and a predator pressure index of northern shrimp (Pandalus borealis)*. Lysekil, Sweden.
- Berenboim, B. I. *et al.* (1991) 'On methods of stock assessment and evaluation of TAC for shrimp *Pandalus borealis* in the Barents Sea', *ICES C.M. Murmansk*, K:15, pp. 1–22.
- Bergström, B. (1991) 'Yearly immigration of *Pandalus borealis* (Krøyer) into periodically isolated fjord populations', *Sarsia*. Bergen, 76, pp. 133–140.
- Bergström, B. (1992a) *Demography and sex change in pandalide shrimp*. Göteborg University.
- Bergström, B. (1992b) 'Growth, growth modelling and age determination of *Pandalus borealis*', *Marine ecology progress series*, 83, pp. 167–183.
- von Bertalanffy, L. (1938) 'A quantitative theory of organic growth (Inquiries on growth laws)', *Human Biology*, 76(2), pp. 181–213. doi: 10.1080/15505340.201.
- Brander, K. M. (1995) 'The effect of temperature on growth of Atlantic cod (*Gadus morhua* L.)', *ICES Journal of Marine Science*. Oxford Academic, 52(1), pp. 1–10. doi: 10.1016/1054-3139(95)80010-7.
- Caddy, J. F. (1991) 'Death rates and time intervals: is there an alternative to the constant natural mortality axiom?', *Fish Biology and Fisheries*, 1, pp. 109–138. Available at: <https://link.springer.com/content/pdf/10.1007/BF00157581.pdf> (Accessed: 14 June 2020).
- Chapman, D. G. and Robson, D. S. (1960) 'The Analysis of a Catch Curve', *Biometrics*, 16(3), p. 354. doi: 10.2307/2527687.
- Clark, S. H. *et al.* (2000) 'The Gulf of Maine northern shrimp (*Pandalus borealis*) fishery: A review of the record', *Journal of Northwest Atlantic Fishery Science*, 27, pp. 193–226. doi: 10.2960/J.v27.a18.
- Clark, W. G. (1999) 'Effects of an erroneous natural mortality rate on a simple age-structured stock

- assessment', *Canadian Journal of Fisheries and Aquatic Sciences*. National Research Council of Canada, 56(10), pp. 1721–1731. doi: 10.1139/f99-085.
- Corner, G. D., Steinsund, P. I. and Aspeli, R. (1996) 'Distribution of recent benthic foraminifera in a subarctic fjord-delta: Tana, Norway', *Marine Geology*, 134(1), pp. 113–125. doi: 10.1016/0025-3227(96)00039-4.
- Dounas, C. *et al.* (2005) 'The effect of different types of otter trawl ground rope on benthic nutrient fluxes and sediment biogeochemistry', *American Fisheries Society*, 41, pp. 539–544. Available at: <https://www.researchgate.net/publication/216187171> (Accessed: 12 June 2020).
- Dounas, C. *et al.* (2007) 'Large-scale impacts of bottom trawling on shelf primary productivity', *Continental Shelf Research*. Pergamon, 27(17), pp. 2198–2210. doi: 10.1016/j.csr.2007.05.006.
- Drengstig, A. *et al.* (2000) 'Population structure of the deep-sea shrimp (*Pandalus borealis*) in the north-east Atlantic based on allozyme variation', *Aquatic Living Resources*. ESME - Gauthier-Villars, 13(2), pp. 121–128. doi: 10.1016/S0990-7440(00)00142-X.
- Fiskeridirektoratet (2020a) *Landings data, Norwegian Directorate of Fisheries*. Available at: <https://www.fiskeridir.no/English/Fisheries> (Accessed: 25 June 2020).
- Fiskeridirektoratet (2020b) *Map, Norwegian Directorate of Fisheries*. Available at: <https://open-data-fiskeridirektoratet-fiskeridir.hub.arcgis.com/> (Accessed: 25 June 2020).
- Francis, R. (2012) 'The reliability of estimates of natural mortality from stock assessment models', *Fisheries Research*. Elsevier B.V., 119–120, pp. 133–134. doi: 10.1016/j.fishres.2011.12.005.
- Garcia, E. G. (2007) 'The Northern Shrimp (*Pandalus borealis*) Offshore Fishery in the Northeast Atlantic', *Advances in Marine Biology*. Iceland, Reykjavík: Ltd, Elsevier, 52(06), pp. 147–266. doi: 10.1016/S0065-2881(06)52002-4.
- Gayanilo, F. C. J., Sparre, P. and Pauly, D. (1996) 'FAO-ICLARM stock assessment tools Users manual'. Rome: Food and Agriculture organization of the united nations.
- Gislason, H. *et al.* (2010) 'Size, growth, temperature and the natural mortality of marine fish', *Fish and Fisheries*, 11(2), pp. 149–158. doi: 10.1111/j.1467-2979.2009.00350.x.
- Green, J. (2009) 'Growth, size and reproduction in daphnia (Crustacea: Cladocera)', *Proceedings of the Zoological Society of London*, 126(2), pp. 173–204. doi: 10.1111/j.1096-3642.1956.tb00432.x.
- Hampton, J. (2000) 'Natural mortality rates in tropical tunas: size really does matter', *Canadian Journal of Fisheries and Aquatic Sciences*. National Research Council of Canada, 57(5), pp. 1002–1010. doi: 10.1139/f99-287.

Hansen, A. (2020) *Genetic population structure of the northern shrimp (Pandalus borealis) along the Norwegian coast*. UiT The Arctic University of Norway.

Hansson, M. *et al.* (1997) *Räktrålnings effekter i Gullmarsfjorden*. Lysekil, Sweden: Fiskeriverket, Havsfiskelaboratoriet, Institute of Marine Research.

Hansson, M. *et al.* (2000) 'Effects of shrimp-trawling on abundance of benthic macrofauna in Gullmarsfjorden, Sweden', *Marine Ecology Progress Series*, 198, pp. 191–201. doi: 10.3354/meps198191.

Havforskningsinstituttet (2019) *Kyst- og fjordreke / Havforskningsinstituttet*. Available at: <https://www.hi.no/hi/temasider/arter/kyst-og-fjordreke> (Accessed: 23 June 2020).

Hightower, J. E., Jackson, J. R. and Pollock, K. H. (2001) 'Use of Telemetry Methods to Estimate Natural and Fishing Mortality of Striped Bass in Lake Gaston, North Carolina', *Transactions of the American Fisheries Society*. John Wiley & Sons, Ltd, 130(4), pp. 557–567. doi: 10.1577/1548-8659(2001)130<0557:UOTMTE>2.0.CO;2.

Hilborn, R. and Walters, C. J. (1992) *Quantitative Fisheries Stock Assessment: Choice, Dynamics and Uncertainty*, Springer, Science and Business media, B.V. Edited by R. Hilborn and C. J. Walters. Routledge, Chapman & Hall, Inc. doi: 10.1007/978-1-4615-3598-0.

Hjort, J. and Ruud, J. (1938) 'Rekefisket som naturhistorie og samfundssak', *Report on Norwegian Fishery and Marine Investigations*. Bergen, Norway: Directorate of Fisheries, 4(4), pp. 1–158.

Hoening, J. M. (2017) 'Should Natural Mortality Estimators Based on Maximum Age Also Consider Sample Size?', *Transactions of the American Fisheries Society*, 146(1), pp. 136–146. doi: 10.1080/00028487.2016.1249291.

Hopkins, C. C. E. and Nilssen, E. M. (1990) 'Population biology of the deep-water prawn (*Pandalus borealis*) in Balsfjord, northern Norway: I. Abundance, mortality, and growth, 1979–1983', *ICES Journal of Marine Science*. Oxford Academic, 47(2), pp. 148–166. doi: 10.1093/icesjms/47.2.148.

Hudon, C., Parsons, D. G. and Crawford, R. (1992) 'Diel Pelagic Foraging by a Pandalid Shrimp (*Pandalus montagui*) off Resolution Island (Eastern Hudson Strait)', *Canadian Journal of Fisheries and Aquatic Sciences*. NRC Research Press Ottawa, Canada, 49(3), pp. 565–576. doi: 10.1139/f92-066.

ICES (2016) *Report of the Benchmark Workshop on *Pandalus borealis* in Skagerrak and Norwegian Deep Sea (WKPAND), 20-22 January 2016*. Bergen, Norway.

ICES (2019) 'NAFO/ICES *Pandalus* Assessment Group Meeting, 08 to 13 November 2019', *International Council for the Exploration of the Sea*.

- Isaac, V. J. (1990) *The Accuracy of Some Length-based Methods for Fish Population Studies*, *ICLARM Tech.* Available at: <https://hdl.handle.net/20.500.12348/3196> (Accessed: 8 May 2020).
- Johnsen, E. *et al.* (2019) ‘StoX: An open source software for marine survey analyses’, *Methods in Ecology and Evolution*. British Ecological Society, 10(9), pp. 1523–1528. doi: 10.1111/2041-210X.13250.
- Jørgensen, M. *et al.* (2014) ‘Introducing time-varying natural mortality in the length-based assessment model for the *Pandalus borealis* stock in ICES Div. IIIa and IVa east - NAFO/ICES WG Pandalus assesment group - September 2014’, *Northwest Atlantic Fisheries Organization*, p. 15.
- Mankettikkara, R. (2013) *Hydrophysical characteristics of the northern Norwegian coast and fjords*. University of Tromsø.
- Mildenberger, T. K., Taylor, M. H. and Wolff, M. (2017) ‘TropFishR: an R package for fisheries analysis with length-frequency data’, *Methods in Ecology and Evolution*. British Ecological Society, pp. 1520–1527. doi: 10.1111/2041-210X.12791.
- Moreau, J., Bambino, C. and Pauly, D. (2014) *Indices of Overall Growth Performance of 100 Tilapia (Cichlidae) Populations* *Indices of Overall Growth Performance of 100 Tilapia (Cichlidae) Populations\**. Asian Fisheries Society. Available at: <https://www.researchgate.net/publication/239585807> (Accessed: 13 June 2020).
- Nilssen, E. M. and Hopkins, C. (1991) ‘Population parameters and life histories of the deep-water prawn *Pandalus borealis* from different regions’, *International Council for the Exploration of the Sea*. Tromsø, Norway, pp. 1–27.
- Pajuelo, J. G. and Lorenzo, J. M. (1996) ‘Life history of the red porgy *Pagrus pagrus* (Teleostei: Sparidae) off the Canary Islands, central east Atlantic’, *Fisheries Research*. Elsevier B.V., 28(2), pp. 163–177. doi: 10.1016/0165-7836(96)00496-1.
- Parsons, D. G. (2005) ‘Predators of northern shrimp, *Pandalus borealis* (Pandalidae), throughout the North Atlantic’, *Marine Biology Research*. Taylor & Francis, 1(1), pp. 48–58. doi: 10.1080/17451000510018944.
- Pauly, D. (1980) *On the interrelationships between natural mortality, growth parameters, and mean environmental temperature in 175 fish stocks*, *J. Cons. int. Explor. Mer.* Available at: <https://academic.oup.com/icesjms/article-abstract/39/2/175/647984> (Accessed: 16 June 2020).
- Pauly, D. (1982) ‘Studying Single-Species Dynamics in a Tropical Multispecies Context’, in Pauly, D. and Murphy, G. I. (eds) *Theory and Management of Tropical Fisheries: Proceedings of the ICLARM/CSIRO Workshop on the Theory and Management of Tropical Multispecies Stocks*. Manila, Philippines: the International Center for Living Aquatic Resources Management, pp. 33–65.

- Pauly, D. and David, N. (1981) 'ELEFAN I, a BASIC program for the objective extraction of growth parameters from length-frequency data', *Berichte der Deutschen Wissenschaftlichen Kommission für Meeresforschung*, 28(32), pp. 205–211.
- Pauly, D. and Munro, J. L. (1984) 'Once more on the comparison of growth in fish and invertebrates', *Fishbyte*. The WorldFish Center, 2(1), pp. 1–21.
- Pauly, D. and Sparre, P. (1991) 'A note on the development of a new software package, the FAO-ICLARM Stock Assessment Tools (FiSAT)', *Fishbyte, Newsletter of the Network of Tropical Fisheries Scientists*, 9(1), pp. 47–49.
- Pollock, K. H., Jiang, H. and Hightower, J. E. (2004) 'Combining Telemetry and Fisheries Tagging Models to Estimate Fishing and Natural Mortality Rates', *Transactions of the American Fisheries Society*. Wiley, 133(3), pp. 639–648. doi: 10.1577/t03-029.1.
- R-Core-Team (2013) 'R: A language and environment for Statistical Computing'. Vienna, Austria. Available at: <https://www.r-project.org/> (Accessed: 15 June 2020).
- Rasmussen, B. (1953) 'On the Geographical Variation in Growth and Sexual Development of the Deep Sea Prawn (*Pandalus borealis* Kr.)', *Reports on Norwegian Fishery and Marine Investigations*. Directorate of Fisheries, 5(3), pp. 1–160.
- Ricker, W. E. (1975) 'Computation and interpretation of biological statistics of fish populations', *Bull. Fish. Res. Bd. Can.*, 191, pp. 1–382.
- Sætra, G. (2019) *Kartlegger «før» og skal undersøke «etter» | Havforskningsinstituttet*. Available at: <https://www.hi.no/hi/nyheter/2019/april/kartlegger-for-og-skal-undersoke-etter> (Accessed: 6 March 2020).
- Savard, L., Parsons, D. G. and Carlsson, D. M. (1994) 'Estimation of Age and Growth of Northern Shrimp (*Pandalus borealis*) in Davis Strait (NAFO Subareas 0+1) Using Cluster and Modal Analyses', *Journal of Northwest Atlantic Fisheries Science*, 16, pp. 63–74. Available at: <http://journal.nafo.int> (Accessed: 13 June 2020).
- Schou Christiansen, J. and Fevolden, S.-E. (2000) 'The polar cod of Porsangerfjorden, Norway; revisited', *Sarsia*, 85(3), pp. 189–193. doi: 10.1080/00364827.2000.10414571.
- Schwamborn, R., Mildenerger, T. K. and Taylor, M. H. (2018a) 'Assessing sources of uncertainty in length-based estimates of body growth in populations of fishes and macroinvertebrates with bootstrapped ELEFAN', *Ecological Modelling*, 393, pp. 37–51. doi: <https://doi.org/10.1016/j.ecolmodel.2018.12.001>.
- Schwamborn, R., Mildenerger, T. K. and Taylor, M. H. (2018b) 'fishboot: Bootstrapped-based

methods for the study of fish stocks and aquatic populations. R package version 0.1’.

Seidman, E. R. and Lawrence, A. L. (2009) ‘Growth, feed, digestibility, and proximate body composition of juvenile *Penaeus vannamei* and *Penaeus monodon* grown at a different dissolved oxygen level’, *Journal of the World Mariculture Society*. John Wiley & Sons, Ltd, 16(1–4), pp. 333–346. doi: 10.1111/j.1749-7345.1985.tb00214.x.

Shumway, S. E. *et al.* (1985) ‘Synopsis of Biological Data on the Pink Shrimp, *Pandalus borealis* Krøyer, 1838’, *NOAA Technical Report NMFS 30*, 28(144), p. 57.

Siddeek, M. S. M. (1991) ‘Estimation of natural mortality of Kuwait’s grooved tiger prawn *Penaeus semisulcatus* (de Haan) using tag-recapture and commercial fisheries data’, *Fisheries Research*. Elsevier, 11(2), pp. 109–125. doi: 10.1016/0165-7836(91)90102-L.

Simpfendorfer, C. A., Bonfil, R. and Latour, R. J. (2005) ‘Mortality estimation.’, in *Management techniques for elasmobranch fisheries*. Rome: Food and Agriculture organization of the united nations, pp. 127–142.

Skorda, E. T. (2018) *Stomach sampling and analyses of shrimp predators in Skagerrak*. Technical University of Denmark.

Skúladóttir, U. (1985) ‘Tagging and recapture results of *Pandalus borealis* (Krøyer) in Icelandic waters’, *ICES C.M.*, K:42, pp. 1–12.

Skúladóttir, U. (1999) ‘Size at Sexual Maturity of Female Northern Shrimp (*Pandalus borealis* Krøyer) in the Denmark Strait 1985-93 and a Comparison with the nearest Icelandic Shrimp Populations’, *Journal of Northwest Atlantic Fishery Science*, 24, pp. 27–37. Available at: <http://journal.nafo.int> (Accessed: 13 June 2020).

Søvik, G., Strand, H. K. and Nedreaas, K. (2019) *Kartlegging av fjordøkosystemene i Tana- og Porsangerfjorden før en eventuell åpning for reketrålffiske*. Bergen, Norway: Havforskningsinstituttet.

Søvik, G. and Thangstad, T. H. (2020) ‘NAFO/ICES PANDALUS ASSESSMENT GROUP MEETING - FEBRUARY AND OCTOBER/NOVEMBER 2020. Results of the Norwegian Bottom Trawl Survey for Northern Shrimp (*Pandalus borealis*) in Skagerrak and the Norwegian Deep (ICES Divisions 3.a and 4.a East) in 2020.’, *Reproductive Biology*, 2004(June), pp. 1–16.

Sparre, P. and Venema, S. C. (1998) *Introduction to tropical fish stock assessment. Part 1. Manual*. 2nd edn, *FAO Fisheries Technical Paper*. 2nd edn. Rome: FAO.

Svanesson, A. (1984) *Hydrography of the Gullmar Fjord (Gullmarsfjordens hydrografi)*. Lysekil, Sweden: Havsfiskelaboratoriet Lysekil, Institute of Hydrographic Research.

Taylor, M. H. (2020) *Using the TropFishR ELEFAN functions, Cran r-project*. Available at:

[https://cran.r-project.org/web/packages/TropFishR/vignettes/Using\\_TropFishR\\_ELEFAN\\_functions.html](https://cran.r-project.org/web/packages/TropFishR/vignettes/Using_TropFishR_ELEFAN_functions.html)  
(Accessed: 20 May 2020).

Taylor, M. H. and Mildenerger, T. K. (2017) 'Extending electronic length frequency analysis in R', *Fisheries Management and Ecology*, 24(4), pp. 330–338. doi: 10.1111/fme.12232.

Thomassen, T. (1976) 'Growth, recruitment and mortality of *Pandalus borealis* (Krøyer) in Balsfjord, northern Norway', *International Council for the Exploration of the Sea*, K:31, pp. 1–10.

Tserpes, G. and Tsimenides, N. (2001) 'Age, growth and mortality of *serranus cabrilla* (linnaeus, 1758) on the cretan shelf', *Fisheries Research*. Elsevier, 51(1), pp. 27–34. doi: 10.1016/S0165-7836(00)00237-X.

Vetter, E. F. (1988) 'Estimation of natural mortality in fish stocks: a review', in *Collected reprints*. California: National marine fisheries service, Southwest fisheries science centre, pp. 25–40. doi: 10.1016/S0140-6736(00)85147-8.

Wang, K. *et al.* (2020) 'Selecting optimal bin size to account for growth variability in Electronic Length Frequency ANalysis (ELEFAN)', *Fisheries Research*. Elsevier B.V., 225, p. 105474. doi: 10.1016/j.fishres.2019.105474.

Williams, E. H. (2011) 'The Effects of Unaccounted Discards and Misspecified Natural Mortality on Harvest Policies Based on Estimates of Spawners per Recruit', *Changed publisher: Wiley*. Taylor & Francis Group . doi: 10.1577/1548-8675(2002)022<0311:TEOUDA>2.0.CO;2.

Xiao, Y. and McShane, P. (2000) 'Estimation of Instantaneous Rates of Fishing and Natural Mortalities from Mark–Recapture Data on the Western King Prawn *Penaeus latisulcatus* in the Gulf St. Vincent, Australia, by Conditional Likelihood', *Transactions of the American Fisheries Society*, 129(4), pp. 1005–1017. doi: 10.1577/1548-8659(2000)129<1005:eoirof>2.3.co;2.

# 7 APPENDICES

## APPENDIX 1 CATCH DATA

A)

**Table A1.** Average catch data in each mid-length interval per average sampling date from The Gullmars Fjord. All values are timed by 100.

Mid lengths	09.12.1996	19.02.1997	12.03.1997	16.04.1997	09.05.1997	18.06.1997	25.08.1997	13.09.1997	20.10.1997	11.11.1997
8.25	0	0	0	0	0	0	0	0	34	50
8.75	0	34	34	0	0	0	0	0	0	0
9.25	0	0	34	0	34	0	0	0	0	0
9.75	0	67	300	20	0	0	0	0	0	0
10.25	0	400	334	60	67	0	0	0	0	0
10.75	0	167	234	140	200	100	0	0	0	0
11.25	0	100	300	160	300	300	0	34	0	0
11.75	0	100	0	180	667	300	100	0	34	0
12.25	0	0	34	180	700	200	400	34	0	0
12.75	167	0	100	80	667	600	600	100	334	150
13.25	34	34	67	40	200	500	400	367	500	150
13.75	200	0	100	0	167	200	1000	800	1800	750
14.25	367	134	67	40	34	0	1200	1300	2567	1150
14.75	467	300	334	160	200	0	700	1134	2400	1200
15.25	800	667	800	540	367	300	600	734	2400	1850
15.75	1534	1700	2334	1640	1300	900	500	500	967	900
16.25	1767	2067	2900	2680	2334	900	500	234	634	750
16.75	1300	2134	3834	3200	2767	2600	800	500	834	400
17.25	1234	1400	1667	2280	2767	3200	2600	1067	1400	1950
17.75	1000	967	1200	1400	1967	3300	3000	1767	3300	3350
18.25	1634	1367	1634	2160	1534	2400	3100	2334	2700	3750
18.75	2767	2034	3134	3800	2134	1500	2900	1734	2700	3050
19.25	3600	4167	5134	5900	3367	4100	1300	1600	1567	2650
19.75	3100	3834	5967	5740	3767	4400	1600	1167	1700	1900
20.25	2100	2934	4434	4240	3700	5500	1200	2067	2134	2400
20.75	2134	2700	3000	3180	3300	3800	2400	2167	2867	2250
21.25	1767	1534	1567	1500	2100	2500	3000	3734	2767	3200
21.75	1934	2067	1267	981	1600	1800	3900	4034	2867	3900
22.25	2500	1434	1334	540	1000	1000	2100	3167	1500	4450
22.75	2234	1500	800	600	1134	800	2100	2134	1500	3800
23.25	1900	1500	734	420	700	800	1000	1700	467	1850
23.75	1867	1267	734	400	634	1200	600	1334	434	1500
24.25	1500	1600	734	560	467	300	800	1167	467	900
24.75	1867	1134	667	300	300	200	300	634	267	700
25.25	1534	967	467	320	334	0	500	267	300	350
25.75	1400	834	234	160	34	200	300	134	134	200
26.25	734	500	234	160	67	600	600	100	34	50
26.75	467	200	134	80	167	0	200	200	0	0
27.25	334	200	134	20	100	0	0	0	34	0
27.75	200	200	67	20	0	0	100	34	0	50
28.25	0	67	0	0	0	0	0	0	0	0
28.75	34	0	0	0	34	0	0	0	0	0

**B)**

**Table A2.** Average catch data in each mid-length interval per average sampling date from the Outer Porsanger Fjord. All values are timed by 100.

Mid lengths	04.10.2018	06.04.2019	12.10.2019
5.75	0	15	0
6.25	0	0	0
6.75	0	15	0
7.25	0	0	0
7.75	0	0	0
8.25	0	15	0
8.75	0	15	0
9.25	0	15	15
9.75	17	15	0
10.25	34	15	29
10.75	167	15	86
11.25	667	15	200
11.75	2650	0	658
12.25	6267	0	1472
12.75	7234	29	2186
13.25	6600	58	2715
13.75	4767	172	3272
14.25	3167	629	2872
14.75	2267	1258	2615
15.25	1700	1800	1658
15.75	2050	3558	1286
16.25	2484	3700	858
16.75	3134	3443	1486
17.25	2534	2772	2115
17.75	1984	2386	2986
18.25	2067	2158	4200
18.75	2884	2243	4943
19.25	3200	2715	4543
19.75	3500	3100	4243
20.25	2567	3358	3858
20.75	1850	3272	2643
21.25	1584	2743	2358
21.75	2034	2343	1486
22.25	2034	1958	1815
22.75	2017	1629	1629
23.25	1517	1872	1758
23.75	1267	1472	1829
24.25	900	872	1358
24.75	450	658	1186
25.25	550	500	1086
25.75	300	415	858
26.25	317	243	558
26.75	167	143	358
27.25	117	43	243
27.75	67	29	215
28.25	34	15	72
28.75	0	29	29
29.25	0	0	15

C)

**Table A3.** Average catch data in each mid-length interval per average sampling date from the Inner Porsanger Fjord. All values are timed by 100.

Mid lengths	04.10.2018	09.04.2019	14.10.2019
11.75	0	100	100
12.25	0	0	0
12.75	0	0	0
13.25	0	0	0
13.75	0	100	0
14.25	50	0	100
14.75	100	400	100
15.25	250	100	500
15.75	400	500	200
16.25	600	1000	100
16.75	2250	1100	300
17.25	2950	2400	1200
17.75	4800	5000	1600
18.25	4500	5400	4600
18.75	3350	7500	6600
19.25	1950	6500	6500
19.75	1450	5700	6400
20.25	1950	3000	3700
20.75	2950	4800	3700
21.25	3250	2400	2100
21.75	3700	3200	2500
22.25	3000	1800	1400
22.75	1500	1900	2000
23.25	1300	900	1100
23.75	1150	1200	900
24.25	1150	800	1700
24.75	500	700	2100
25.25	300	700	1400
25.75	600	500	1100
26.25	350	300	1800
26.75	300	300	1200
27.25	150	500	400
27.75	300	200	200
28.25	150	100	0
28.75	50	100	100
29.25	0	0	100

D)

**Table A4.** Average catch data in each mid-length interval per average sampling date from the Tana Fjord. All values are timed by 100.

Mid lengths	29.10.2018	30.03.2019	19.10.2019
10.75	0	29	0
11.25	0	0	0
11.75	0	15	13
12.25	0	15	0
12.75	15	0	13
13.25	200	0	88
13.75	343	15	138
14.25	1100	29	313
14.75	1886	86	538
15.25	3029	15	1338
15.75	4172	315	1838
16.25	2900	586	2600
16.75	2229	1515	2650
17.25	1329	3100	2038
17.75	415	4572	1288
18.25	700	5229	1350
18.75	1415	3915	2250
19.25	2915	2615	4038
19.75	3858	2386	6975
20.25	4029	1672	8250
20.75	2972	2386	7038
21.25	1729	3900	5225
21.75	1786	4786	3650
22.25	1729	4529	2338
22.75	1943	4072	2113
23.25	2086	3300	2288
23.75	2515	2800	2288
24.25	2829	3286	2288
24.75	2943	3500	2313
25.25	2758	4058	2088
25.75	2643	3386	1938
26.25	2500	2786	1638
26.75	1458	2115	1400
27.25	986	1915	1100
27.75	900	1115	825
28.25	629	458	613
28.75	300	300	250
29.25	143	158	150
29.75	29	58	50
30.25	29	58	75
30.75	0	15	13
31.25	0	15	13
31.75	29	0	0

E)

**Table A5.** Average catch data in each mid-length interval per average sampling date from the Kvænangen Fjord. All values are timed by 100.

Mid lengths	20.10.2018	20.03.2019	03.10.2019
7.75	0	17	0
7.75	0	0	0
8.25	0	67	0
8.75	0	17	0
9.25	0	100	0
9.75	0	134	0
10.25	0	300	17
10.75	0	967	0
11.25	0	1717	0
11.75	15	2184	0
12.25	72	2850	34
12.75	115	2367	150
13.25	315	1650	600
13.75	486	717	834
14.25	843	384	1367
14.75	1386	150	1917
15.25	1986	67	2650
15.75	2200	50	3000
16.25	3229	234	3350
16.75	3200	267	4367
17.25	2486	817	5400
17.75	2129	1650	4467
18.25	1958	3250	3234
18.75	2515	4567	2267
19.25	3400	5417	1900
19.75	3743	6150	2034
20.25	4672	5434	2817
20.75	5186	4434	3467
21.25	5000	4634	3600
21.75	4100	4150	4417
22.25	3743	4900	3667
22.75	3443	4667	3600
23.25	3172	4334	3150
23.75	3029	3684	3434
24.25	2772	2584	3817
24.75	2386	1700	3950
25.25	2258	1884	4000
25.75	2286	1484	3934
26.25	2000	1600	3350
26.75	1800	1234	2950
27.25	1315	1417	2434
27.75	843	1000	2384
28.25	615	800	1967
28.75	258	734	1467
29.25	100	467	1350
29.75	29	300	617
30.25	15	150	484
30.75	0	0	300
31.25	15	34	84
31.75	0	0	134
32.25	0	0	84
32.75	0	0	17
33.25	0	0	0
33.75	0	0	0
34.25	0	0	0
34.75	0	0	17

## APPENDIX 2 SCENARIO 1

A)

The best fitted growth parameters yielded by the bootstrapped ELEFAN\_SA with Scenario 1 settings (Table 2.4) were visualized for each fjord site by a von Bertalanffy growth curve with associated CIs (Fig A1). Growth curves for the Inner and Outer Porsanger Fjord and the Kvænangen Fjord yielded wider CIs than the ones of the Tana and Gullmars Fjord (Fig A1). The estimated values for  $L_{\infty}$ ,  $K$ , and  $t_{anchor}$  varied between the five fjord sites (Table 3.1). The distributions of the bootstrapped growth parameters, visualized by the univariate density estimate plots (Fig. A2), were, for all fjord sites bimodal for several of the parameters. The von Bertalanffy growth curves, yielded from the best fitted growth parameters, superimposed on the LFQ distributions are presented in Fig. A3. The growth curves tracing through the modal peaks revealed from five to seven age groups (including the 0-group) (Fig. A3). The second and third growth curves, representing the 1- and 2- groups, respectively, hit all 1- and 2- group modal peaks for all sampling events at all fjord sites, except for the Inner Porsanger Fjord where only the 2- and 3- groups in autumn 2018 are traced through. For the Outer Porsanger Fjord, the fourth growth curve traced through the 4-group instead of the 3-group for the autumn 2018 sample (Fig. A3).

B)

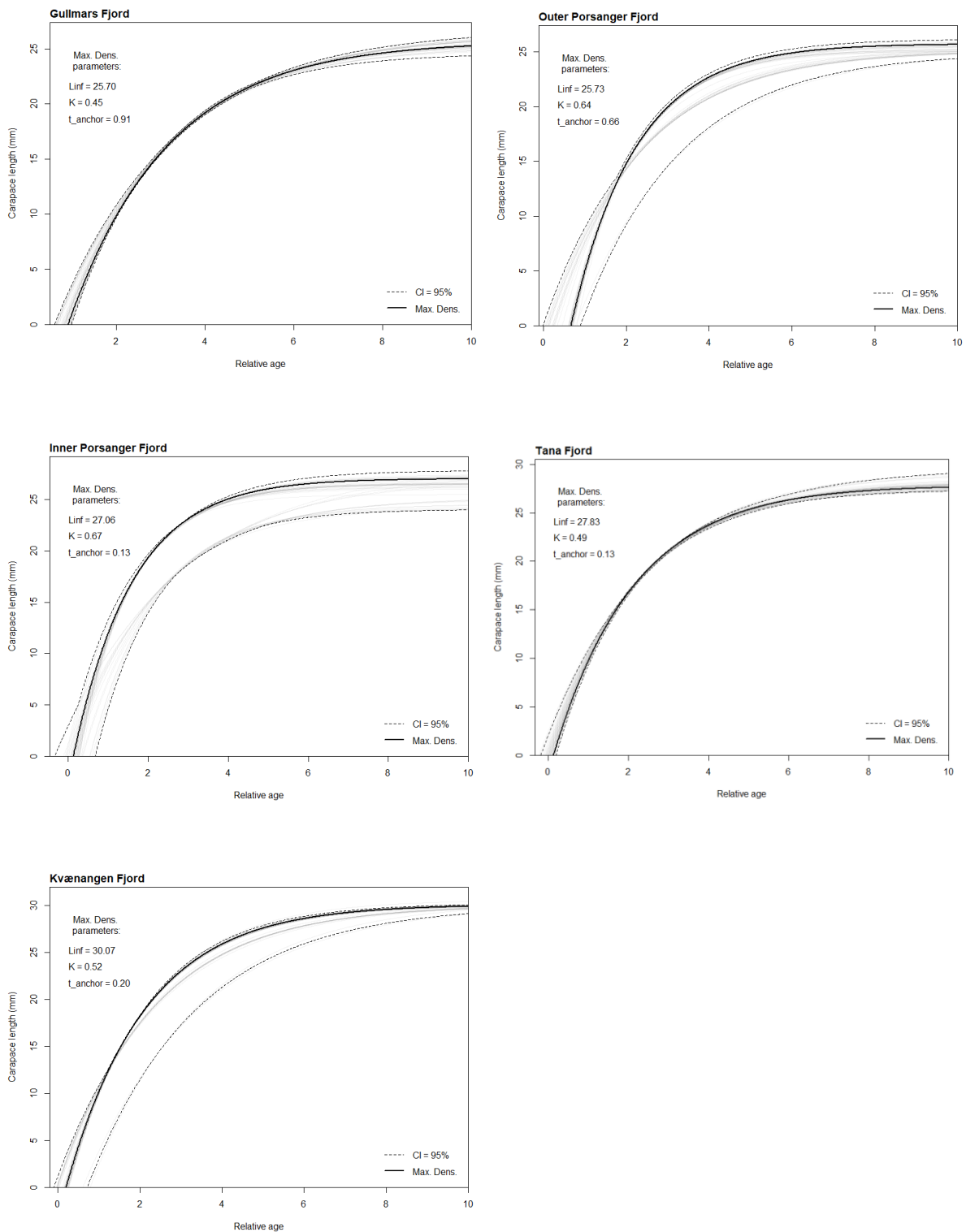


**Figure A1.** Scenario 1: Output from the bootstrapped ELEFAN analysis with simulated annealing from all fjord sites. The best fitted von Bertalanffy growth curve (Max. Dens) is plotted from the best fitted growth parameters (Max. Dens. Parameters) with confidence intervals (CI=0.95 %) (dotted lines). Grey lines indicate other iterations from the same run in the analysis.

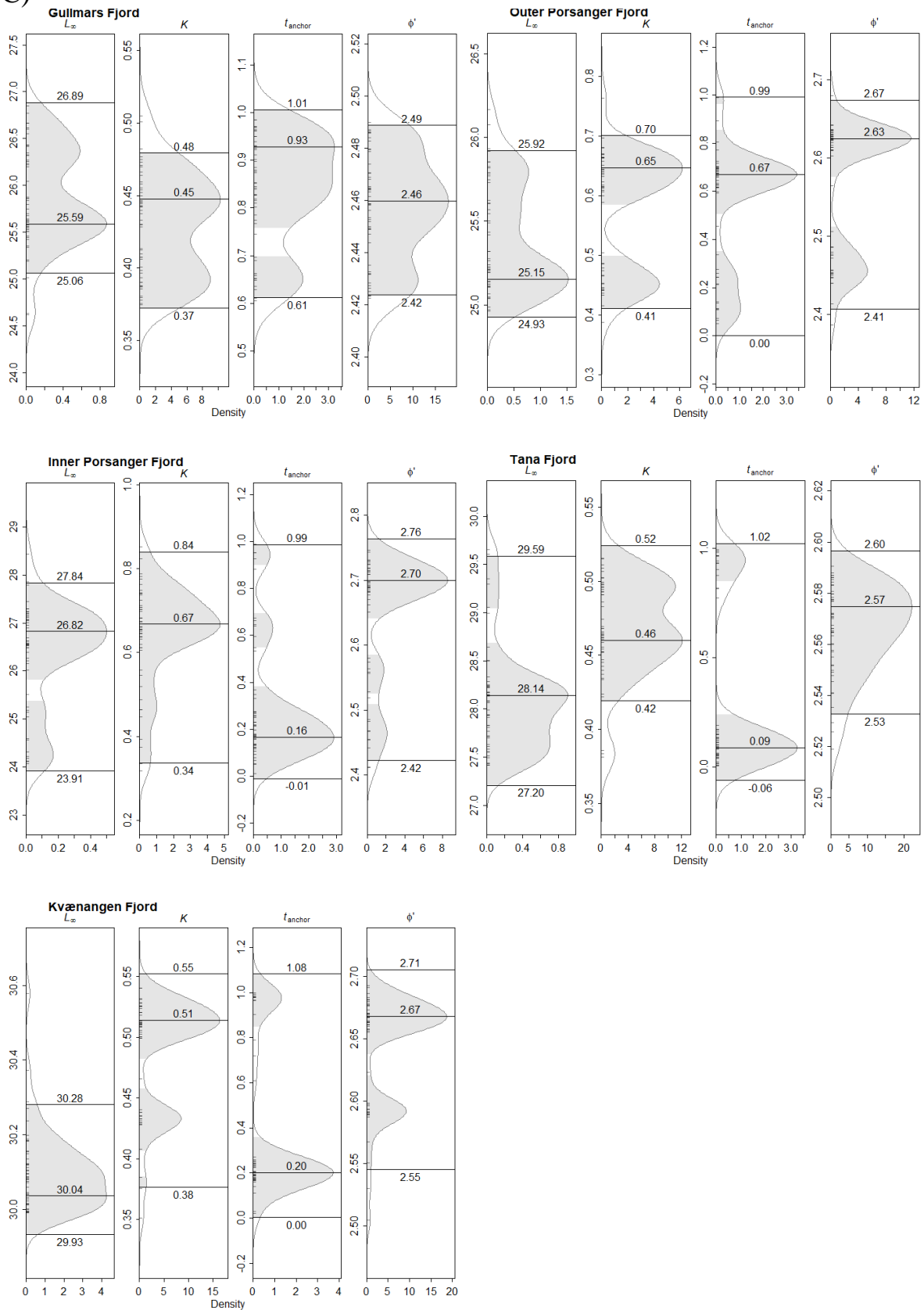


**Figure A2.** Scenario 1: Univariate density estimate plots for the von Bertalanffy growth parameters from the bootstrapped ELEFAN analysis with simulated annealing, for all fjord sites.

D)

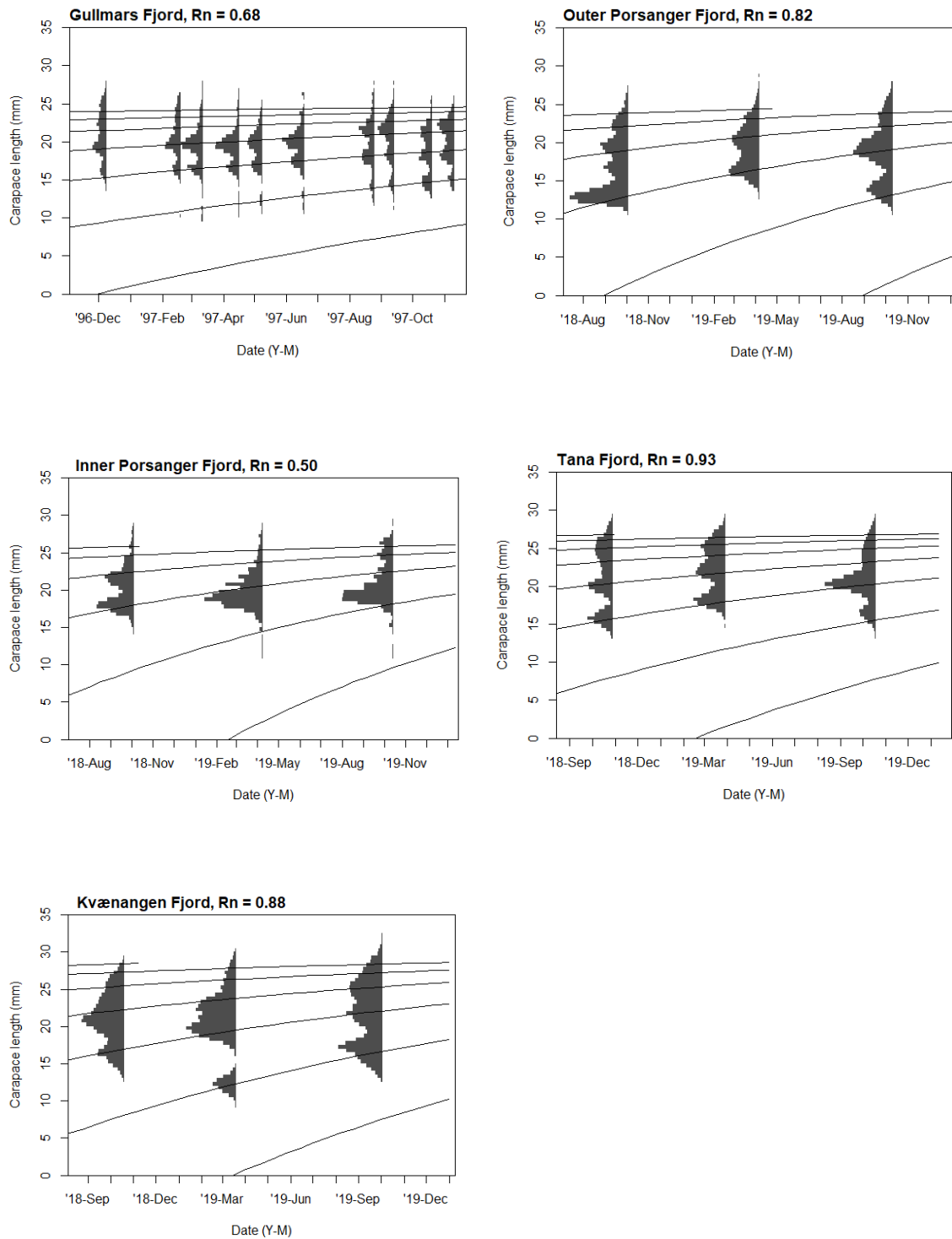


**Figure A3.** Scenario 1: The estimated von Bertalanffy growth curve superimposed on length frequency distributions of northern shrimp for all fjord sites.

## APPENDIX 3 SCENARIO 4

A)

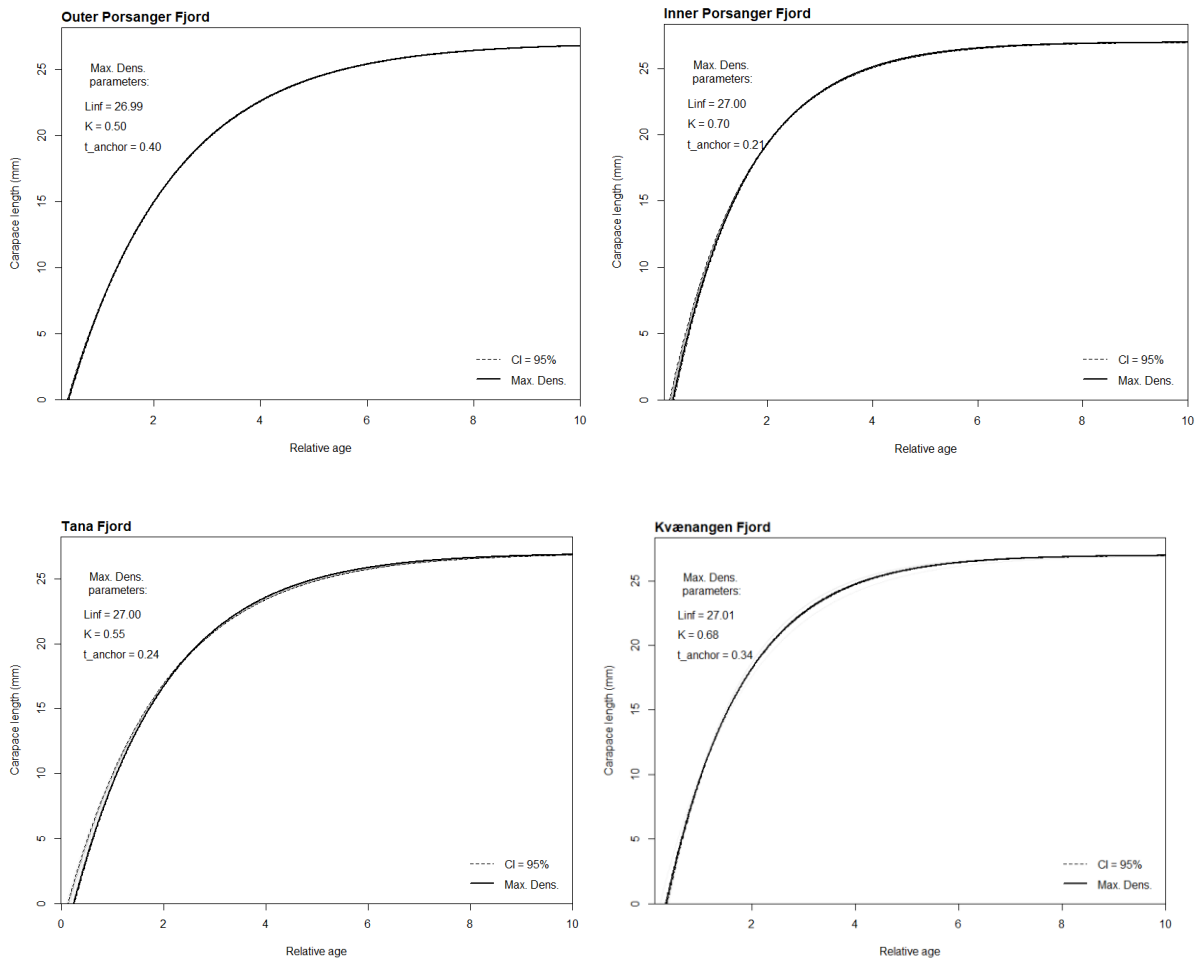


**Figure A4.** Scenario 4: Output from the bootstrapped ELEFAN analysis with simulated annealing from all fjord sites except for the Gullmars Fjord. The best fitted von Bertalanffy growth curve (Max. Dens = dotted line) is plotted from the best fitted growth parameters (Max. Dens. Parameters) with confidence intervals (CI=0.95 %). Grey lines indicate other iterations from the same run in the analysis.

B)

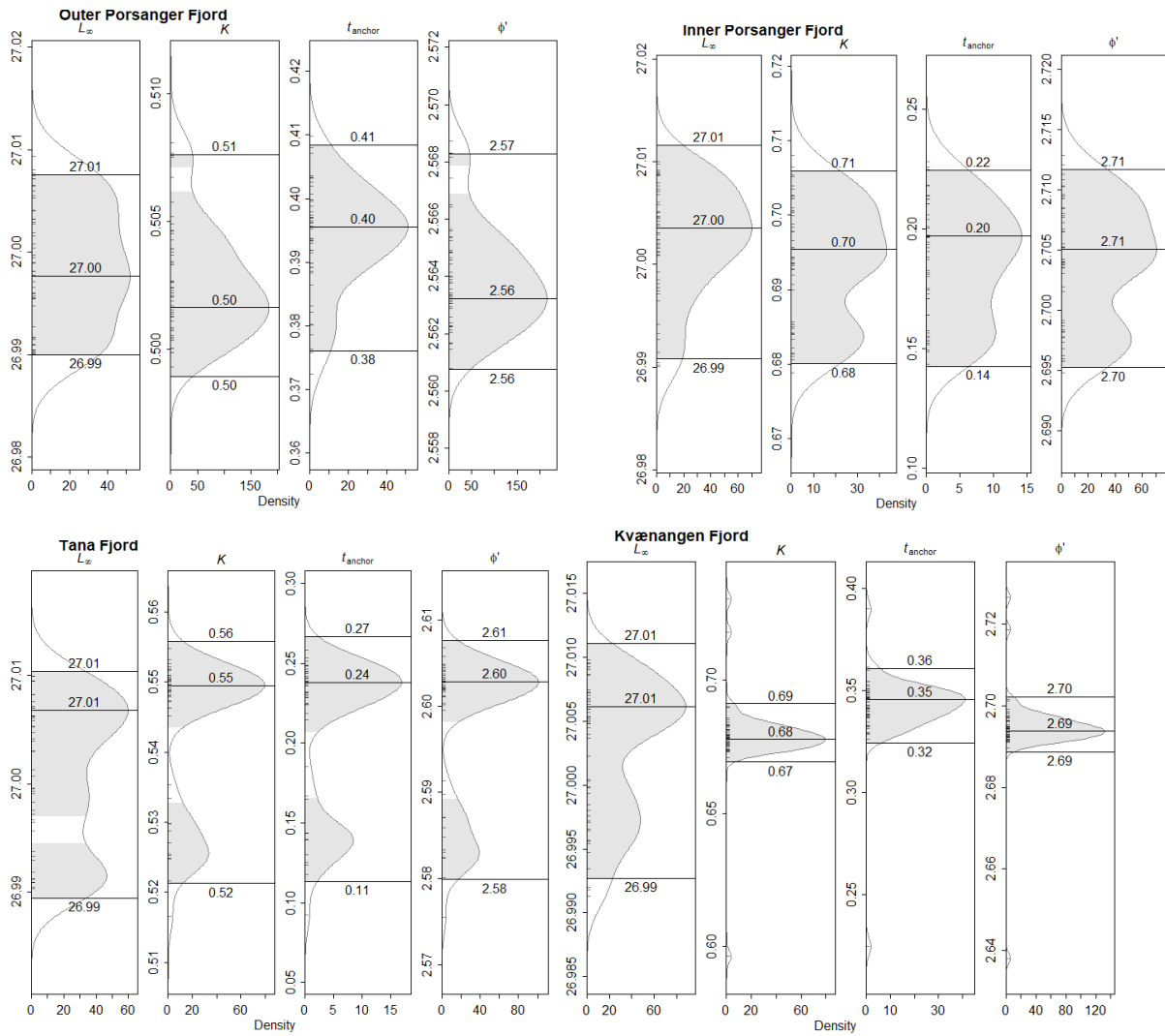


**Figure A5.** Scenario 4: Univariate density estimate plots for the von Bertalanffy growth parameters from the bootstrapped ELEFAN analysis with simulated annealing, for all fjord sites except for the Gullmars Fjord.

C)

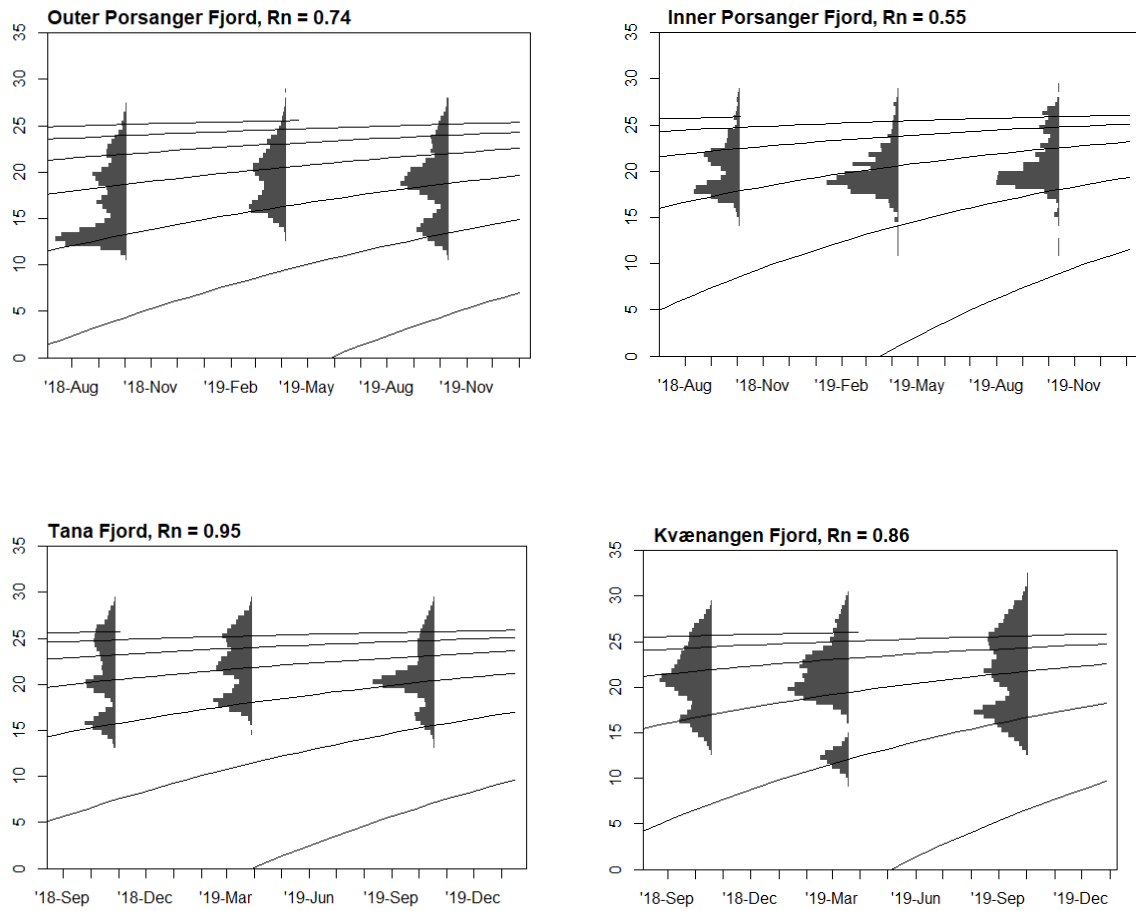


**Figure A6.** Scenario 4: The estimated von Bertalanffy growth curve superimposed on length frequency distributions of northern shrimp for all fjord sites except for the Gullmars Fjord.